NASA CONTRACTOR
REPORT

Report No. 61309

DESIGN AND DEVELOPMENT OF TECHNIQUES FOR FABRICATION OF CRYOGENIC TANK SUPPORT STRUCTURES FOR LONG TERM STORAGE IN SPACE FLIGHTS

By D. H. Bartlett and J. C. McGinnis

The Boeing Company
Aerospace Systems Division
Seattle, Washington

June 1969

Final Report

Prepared for

NASA-GEORGE C. MARSHALL SPACE FLIGHT CENTER
Marshall Space Flight Center, Alabama 35812

TECHNICAL REPORT STANDARD TITLE PAGE

1. REPORT NO.	2. GOVERNMENT ACCESSION NO.	3. RECIPIENT'S CATALOG NO.
NASA CR-61309		

4. TITLE AND SUBTITLE Design and Development of Techniques for Fabrication of Cryogenic Tank Support Structures for Long Term Storage in Space Flights	5. REPORT DATE June 1969 6. PERFORMING ORGANIZATION CODE
7. AUTHOR(S) D. H. Bartlett and J. C. McGinnis	8. PERFORMING ORGANIZATION REPORT # D2-121073-1
9. PERFORMING ORGANIZATION NAME AND ADDRESS The Boeing Company Aerospace Systems Division Seattle, Washington	10. WORK UNIT NO. 11. CONTRACT OR GRANT NO. NAS 8-20901
12. SPONSORING AGENCY NAME AND ADDRESS NASA-George C. Marshall Space Flight Center Marshall Space Flight Center, Alabama 35812	13. TYPE OF REPORT & PERIOD COVERED NASA Contractor Report Final 14. SPONSORING AGENCY CODE

15. SUPPLEMENTARY NOTES

16. ABSTRACT

The investigation described in this report was conducted in two phases. Phase I consisted of design and analytical optimization of several conical support structural concepts for the 32 ft. diameter Modular Nuclear Vehicle (MNV) LH_2 tank. The concepts were compared on a weight and heat flow basis, and the most promising configuration selected for subscale fabrication in Phase II. The period of performance for Phase I was April through October 1968.

In Phase II a 117-inch diameter conical support was fabricated for the MSFC 105-inch LH_2 test tank. The part was intended for thermal performance evaluation, therefore the cross section was a full size representation of the MNV conical support design. A trial assembly of the subscale part was made prior to shipment to MSFC. The period of performance for Phase II was November 1968 through June 1969.

17. KEY WORDS	18. DISTRIBUTION STATEMENT
	STAR Announcement (See DRF)

19. SECURITY CLASSIF. (of this report)	20. SECURITY CLASSIF. (of this page)	21. NO. OF PAGES	22. PRICE
U	U	108	

MSFC - Form 3292 (May 1969)

FOREWORD

This report describes a 15-month effort to define and fabricate a low heat leak conical support typical of Modular Nuclear Vehicle LH_2 Tankage. The work was conducted on Contract NAS 8-20901 during the period April 1968 through June 1969, for the NASA/George C. Marshall Space Flight Center. Mr. H. M. Walker of the Manufacturing Engineering Laboratories was the NASA Contracting Officers Representative.

The program was performed by the Structural Development organization of Structures Technology, Aerospace Systems Division of The Boeing Company. Mr. C. F. Tiffany was Program Manager and Mr. D. H. Bartlett was technical leader. Mr. J. C. McGinnis was responsible for structural analysis and optimization. Mr. A. D. Jones and L. H. Rogers performed detailed design and stress analysis functions respectively. Mr. K. W. Osborne prepared the drawings and performed shop liaison.

The manufacturing effort was under the direction of Mr. C. L. Lofgren, Manufacturing Development. Mr. D. E. Gieseking was responsible for fabrication of the conical support and Mr. F. W. Dunn was the principal contributor. Mr. D. G. Good prepared the technical illustrations and art work.

TABLE OF CONTENTS

LIST OF ILLUSTRATIONS

LIST OF ILLUSTRATIONS (Continued)

LIST OF ILLUSTRATIONS (Continued)

LIST OF ILLUSTRATIONS (Continued)

1.0 INTRODUCTION

The investigation described in this report was conducted in two phases. Phase I consisted of design and analytical optimization of several conical support structural concepts for the 32 ft. diameter Modular Nuclear Vehicle (MNV) LH_2 tank. The concepts were compared on a weight and heat flow basis, and the most promising configuration selected for subscale fabrication in Phase II. The period of performance for Phase I was April through October 1968.

In Phase II a 117-inch diameter conical support was fabricated for the MSFC 105-inch LH_2 test tank. The part was intended for thermal performance evaluation, therefore the cross section was a full size representation of the MNV conical support design. A trial assembly of the subscale part was made prior to shipment to MSFC. The period of performance for Phase II was November 1968 through June 1969.

2.0 SUMMARY

In phase I, various compression structure concepts were optimized to determine the minimum cross sectional area configuration. The loads and design envelope were supplied by MSFC. The structural arrangements studied were honeycomb sandwich, corrugated skin and skin stiffened with zees, bars and hat sections. Fiberglass reinforced plastic and titanium alloy were the materials selected for the investigation.

Detail designs were developed for each optimized structural concept. The end attachments, as well as the number and details of longitudinal joints, were considered. Analysis of the effects of thermally induced strains was also conducted. A weight summary was prepared for each concept. The summary was sufficiently detailed to identify the effect of end attachments and longitudinal joints on total weight. The idealized one dimensional heat flow was calculated for each concept. A 256 day mission was assumed and LH_2 boil-off losses plus support concept weight provided the means of determining the most promising approach.

In the study phase, it was concluded that fiberglass honeycomb sandwich was the most efficient when both support and LH_2 boil-off weights were considered. The corrugated titanium support had the least structural weight and the fiberglass honeycomb sandwich was second lightest. It was found that edge attachment details had a significant effect on total weight. These details represented as much as 50% of the support weight in the case of fiberglass sandwich and over 40% for corrugated titanium.

A design of a subscale fiberglass honeycomb sandwich conical support was prepared. The core thickness, skin gages, longitudinal splice details and length were the same as the full size (32 ft. tank) cone design so that heat flow per inch of circumference would be the same.

In Phase II, the conical support was fabricated and delivered to MSFC. The entire support was made of fiberglass reinforced plastic with the exception of fasteners and

the splice plates at inboard and outboard ends.

The configuration of the tapered laminate ends of the fiberglass cone proved difficult to manufacture. Additionally, the low density core required elaborate processing to avoid collapse. Techniques were developed to stabilize the core and several intermediate steps were introduced in building up the laminate ends to produce the required configuration. Some residual stress was apparent in removing the quarter segment assemblies from the mold. In the free state these parts had a slightly smaller radius than the mold, however analysis indicated that they could be forced into contour incurring only a nominal bending stress.

3.0 PHASE I - STUDY PROGRAM

3.1 GROUND RULES

The design envelope, loads, and load factors to be used in the study were selected by MSFC. The envelope is depicted in Figure 1.

Methods of construction to be considered were honeycomb sandwich, zee stiffened skin, bar stiffened skin, hat stiffened skin, and corrugations. Both metallic and nonmetallic materials would be assumed for each construction concept.

Vertical splice joint and top and bottom edge attachment details would be developed for each structural concept. The optimum number of cone segments was to be determined based on parameters such as heat leak, weight, fabrication ease, and simplicity of assembly.

Thermally induced stresses would be considered in the designs. There was no design stiffness requirement.

MSFC was interested principally in obtaining a test part that would typify the heat leak and insulation assembly problems of the 32 ft diameter conical support. Therefore, the subscale support would be identical in length and cross sectional geometry to provide a heat leak per inch of circumference typical of the full size cone.

3.2 MATERIALS

Titanium alloys 6Al-4V and 5Al-2.5Sn were the candidate metallic materials considered in the study. 6Al-4V was used in the annealed condition to simplify fabrication and because the higher strength of heat treated material was not needed.

Fiberglass reinforced epoxy plastic was the nonmetallic material selected. This material had been shown to be suitable for cryogenic applications in previous studies (References 1 and 2). The material form was style 181-"S" glass cloth. Honeycomb sandwich designs utilized fiberglass core impregnated with phenolic resin (HRP).

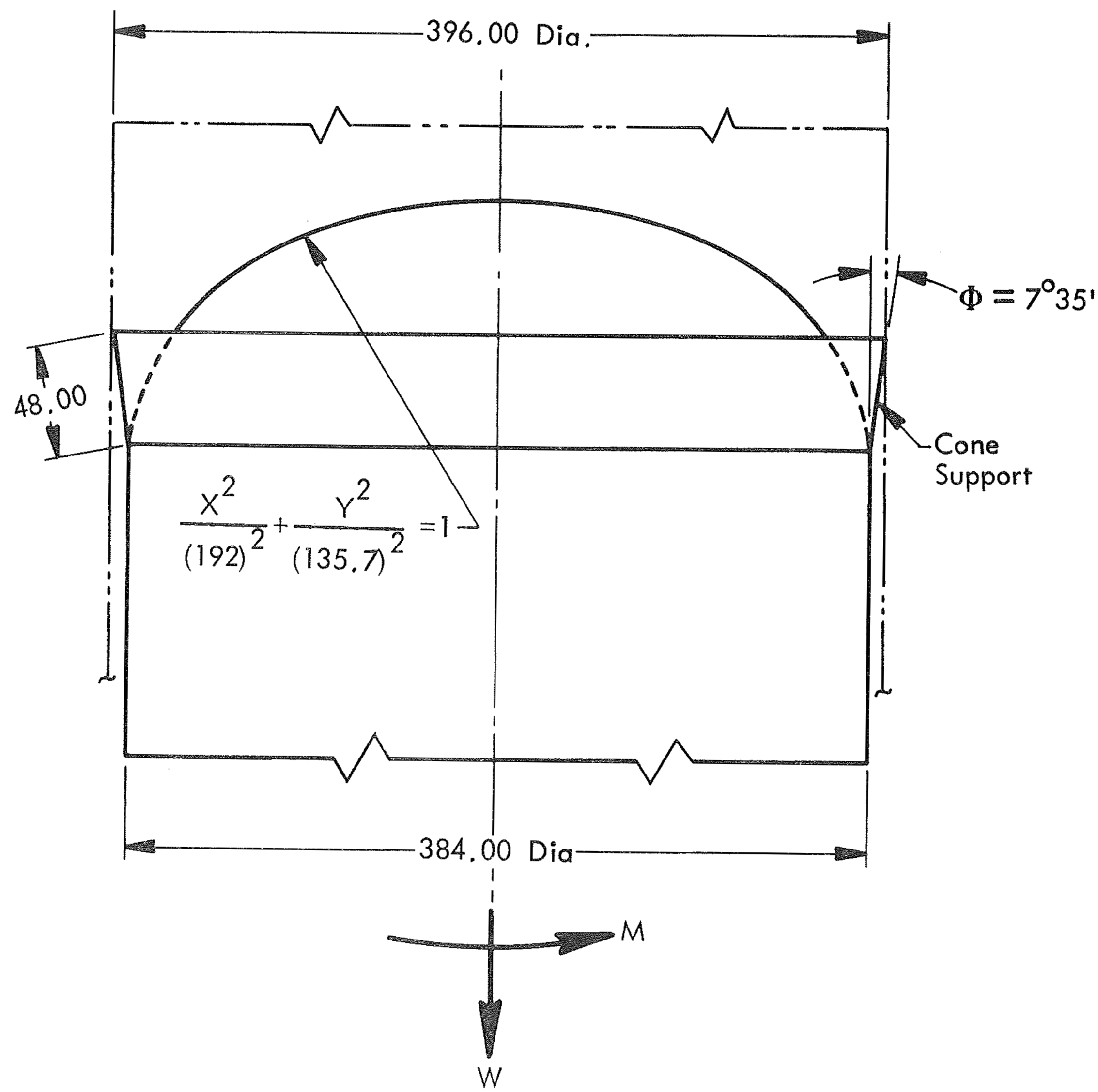

Figure 1: CONE SUPPORT CONFIGURATION

The allowable design properties of the materials used in the program were as follows:

Style 181-S/901 Fiberglass Cloth Preimpregnated with U.S. Polymeric E-787 Epoxy Resin or Equivalent (Ref. 1)

ITEM	PARALLEL lbs/in^2	45° lbs/in^2	NORMAL lbs/in^2
F_{tu}	65,000*	14,196	65,000
F_{cu}	58,225	26,782	53,118
F_{bry}	31,810	--	--
E	3,062,848	1,552,301	2,837,151
G	1,500,000	400,000	1,500,000
F_{su}	11,000	27,000	11,000
Interlaminar Shear	6,455	--	--
Thermal Conductivity $\frac{BTU\text{-}in}{In^2\text{-}Hr\text{-}^{\circ}F}$	0.013	--	--

$\mu = 0.125$ Density = 0.066 lbs/in^3 * Adjusted by Boeing

6Al-4V Titanium - Annealed

F_{tu} = 134,000 lbs/in^2

F_{cy} = 132,000 lbs/in^2

F_{su} = 79,000 lbs/in^2

E = 16.4×10^6 lbs/in^2

G = 6.2×10^6 lbs/in^2

F_{bru} = 252,000 (e/D = 2.0) lbs/in^2

F_{bry} = 208,000 (e/D = 2.0) lbs/in^2

μ = .30

Density = .16 lbs/in^3

Thermal Conductivity = 0.24 $\frac{BTU\text{-}In}{in^2\text{-}Hr\text{-}^{\circ}F}$

3.3 LOADS

Three loading conditions were considered. These were:

<u>Load Condition 1 (maximum q) limit</u>

$W = 300,000$ lbs

$M = 106.1 \times 10^6$ in-lbs

$\left.\begin{array}{l}\text{Axial Acceleration} = 2.0\text{ G} \\ \text{Lateral Acceleration} = 0.5\text{ G}\end{array}\right\}$ Combined

<u>Load Condition 2 (S-IC Burnout) limit est.</u>

$W = 300,000$ lbs.

Axial Acceleration = 5.0 G

<u>Load Condition 3 (S-IC cutoff) limit</u>

$W = 300,000$ lbs.

Axial Acceleration = -2.5 G

Factors of Safety were:

Ultimate = 1.4

Yield = 1.1

Shell loads were determined from the following expressions:

$$N_x = \frac{P}{\pi D \cos \Phi} \pm \frac{4M}{\pi D^2 \cos \Phi}$$ Tension or Compression Loading-lbs/in

$$N_{xy} = \frac{V}{\pi R}$$ Shear Flow - lbs/in.

where P = total axial load (W x G)

V = shear load due to lateral acceleration.

Φ = cone angle ($7^\circ 35'$)

The shell loads for the three conditions are tabulated on the following page.

CONDITION	IN SHELL PLANE LOADING LBS/IN.	LIMIT		ULTIMATE	
		396"D TOP	384"D BOTTOM	396"D TOP	384"D BOTTOM
1 (Max. q)	Compression	-382	-364	-535	-509
	Tension	1355	1367	1897	1914*
	Shear	241	249	338	348*
2 (Burnout)	Compression	--	--	--	--
	Tension	1216	1254	1703	1756
	Shear	--	--	--	--
3 (Cutoff)	Compression	-608	-627	-851	-878*
	Tension	--	--	--	--
	Shear	--	--	--	--

* Critical Ultimate Design Conditions

3.4 STRUCTURAL CONCEPT OPTIMIZATION

3.4.1 Corrugated Structure

The 60° corrugation studied in the program consisted of a constant thickness sheet formed into a repeating series of equilateral corrugations. There were no face sheets on the corrugation surfaces and circumferential rings were used at each end of the conical frustum. This type of design appeared well suited to cryogenic applications where large thermal gradients between support structure and the tank could produce significant thermal stresses. The corrugated structure would permit an "accordion action" of the panel and thus relieve stresses due to thermal gradients.

In the tank support areas pressure loads did not exist and the primary loading was axial plus lateral shear. A corrugated sheet without face panels is essentially uni-directional. The closely spaced "stiffeners" can provide high compressive strength and it was assumed that all the material was acting in both compression and shear.

Analysis Criteria

The following assumptions were made in the analysis:

1. Whenever "Optimization" was mentioned directly or in any of its forms, it meant that a minimum cross sectional area (weight, heat flow) was effected for a given material.

2. The conical frustum was designed as an equivalent cylinder and R was the radius of curvature of the small end normal to the surface and L was the slant height of the conical frustum. Test data (Ref. 3) indicated that buckling occurred when the maximum meridional stress (at the small end of the cone) reached the critical value for a cylinder having curvature of the cone and a thickness equal to that of the cone.

3. The maximum compression loading that would occur in the shell due to combined bending plus axial load was treated as acting uniformly around the circumference of the shell for general instability analysis. (This was conservative as shown in Ref. 4).)

4. The critical shear instability load was equivalent to a long corrugated flat panel with simply supported edges subjected to the maximum sheat stress existing in the conical frustum.

5. The interaction of shear and compression was negligible. (The maximum shear stress occurred at 90° from the maximum axial stress and was zero at point of maximum compression load.)

6. The equilateral corrugation shape was optimum (all elements had the same critical stress) and the angle of corrugation $\theta = 60^\circ$ was near optimum (Ref. 5).

7. General or panel instability would occur as column instability.

8. Stresses would remain elastic.

9. Distortion effects due to curvature were negligible.

10. The optimum cross sectional geometry had been achieved when the column stress and the crippling stress were equal.

11. The structure existing on the tank at the support interface would act as a ring to support the corrugation along with the corrugation edge member.

12. The overall height from the tank-cone intersections at the 396 inch and 384 inch diameters were conservatively used as the effective height of the conical frustum.

Equilateral Corrugation Section Properties

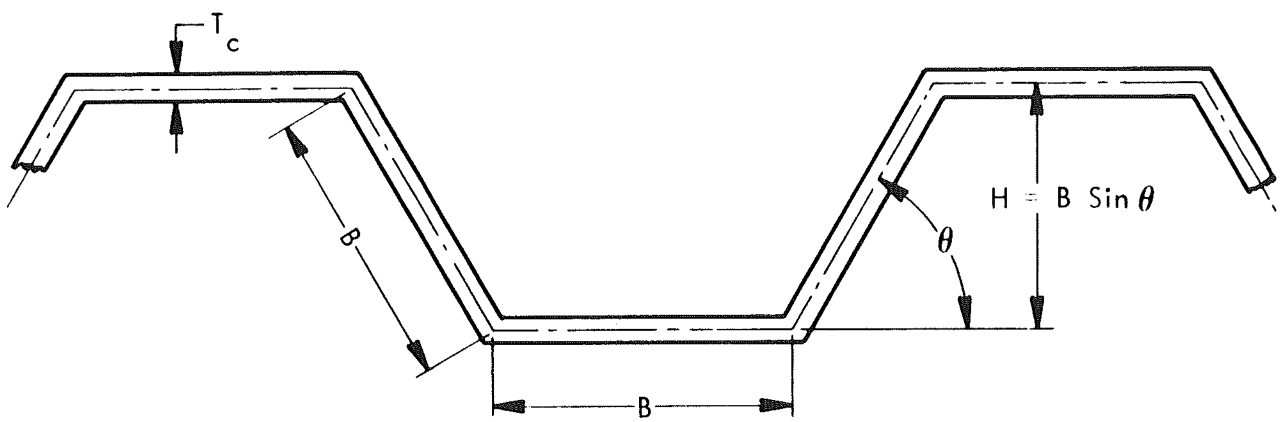

General Section Properties

$$I = \frac{T_c B^2}{3} \left(\frac{\sin^2 \theta}{1 + \cos \theta}\right) = \text{Moment of inertia per inch}$$

$$A = 2 \left(\frac{T_c}{1 + \cos \theta}\right) = \text{Cross sectional area per inch}$$

$$\rho = \sqrt{I/A} = \frac{B \sin \theta}{\sqrt{6}} = .408 \text{ B} \sin \theta = \text{Radius of Gyration per inch}$$

60° Corrugation Properties

$$\rho = \frac{1}{2\sqrt{2}} B = .354 \text{ B}$$

$$A = 4/3\ T_c = 1.333\ T_c$$

$$I = 1/6\ T_c\ B^2 = .1666\ T_c\ B^2$$

Failure Modes

Local Instability - Crippling

In order to predict the local crippling of the corrugation skin, it was assumed that the edges were simply supported and the flats of the corrugations were long plates. The critical local crippling stresses were:

Compression: $$F_{ccr} = \frac{4.0\ \pi^2\ E}{12\ (1 - \mu^2)} \left(\frac{T_c}{B}\right)^2$$ Ref. 6

Shear: $$F_{sccr} = \frac{5.35\ \pi^2\ E}{12\ (1 - \mu^2)} \left(\frac{T_c}{B}\right)^2$$ Ref. 6

General Instability - Panel Buckling

General instability or panel buckling consists of Euler column buckling between the end ring supports for compression loads. The panel can also fail in shear general buckling. Assuming simply supported end conditions the following was used to predict the buckling stress:

Compression: $$F_{col} = \frac{\pi^2\ E}{(L/\rho)^2}$$ Ref. 7

Reference 8 was used for the analysis of corrugated shear webs. This analysis was verified with experimental data. In the design of corrugated shear webs, it was necessary to consider the flexural stiffness of the web in the vertical and horizontal directions. The formula for critical shear load per inch is:

$$N_{xy} = \frac{4\ K_s \sqrt[4]{D_1\ D_2^{\ 3}}}{L^2}$$ Ref. 8

where:

D_1 = plate flexural stiffness in circumferential direction = $E\,T_c^3 \times (1 + \cos\theta)/24$

D_2 = plate flexural stiffness in depthwise direction = $E\,A\,\rho^2$ =

$$\frac{E\,B^2 \sin^2\theta\,T_c}{3\,(1 + \cos\theta)}$$

T_c = corrugation skin thickness - in.

B = corrugation width of flat - in.

L = corrugation length between fasteners - in.

K_s is the shear buckling coefficient which is dependent upon the radius of gyration $- \rho$ and the edge restraint ε. Assuming simply supported edges, K_s was found from Figure 2. The parameter, $\lambda/L\ \sqrt[4]{D_2/D_1}$, was conservatively taken as near unity.

This gave K_s = 8.15 for a simply supported edge condition. Substitution of the corrugation parameters gave:

$$N_{xy} = \frac{.7928\,K_s\,E\,T_c^{1.5}\,B^{1.5}\,\sin\theta^{1.5}}{L^2\,(1 + \cos\theta)^{.5}}$$

$$F_{scr} = \frac{.7928\,K_s\,E\,T_c^{.5}\,B^{1.5}\,\sin\theta^{1.5}}{L^2\,(1 + \cos\theta)^{.5}}$$

For 60° Corrugation

$$F_{scr} = \frac{.5217\,K_s\,E\,T_c^{.5}\,B^{1.5}}{L^2}$$

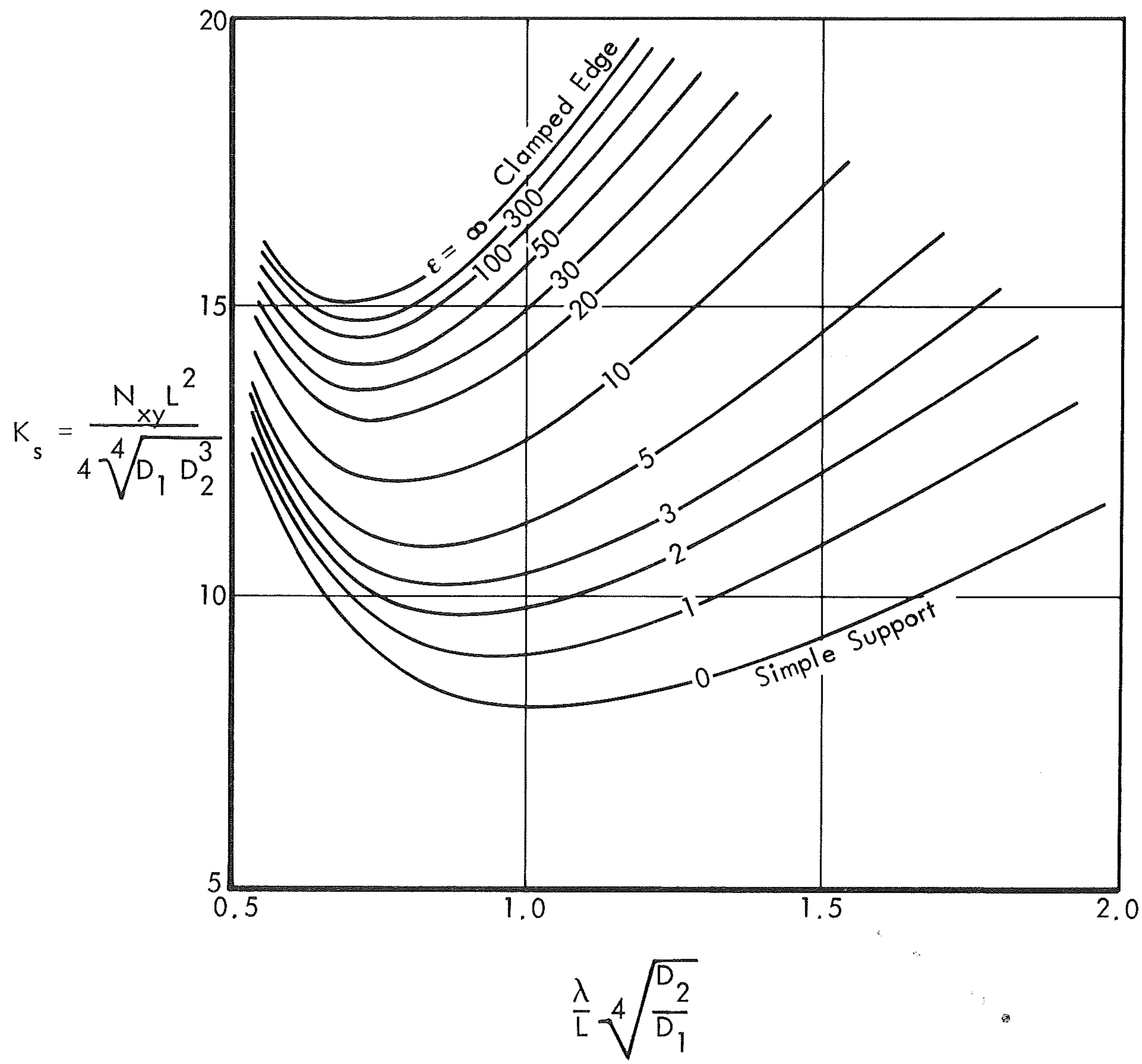

Figure 2: SHEAR BUCKLING COEFFICIENTS OF LONG CORRUGATED PLATES WITH NONDEFLECTING EDGE SUPPORTS

For Simply Supported Edges $K_s = 8.15$

$$F_{scr} = \frac{4.25\ E\ T_c^{.5}\ B^{1.5}}{L^2}$$

Optimization Procedure

In order to arrive at an optimum corrugation configuration, the critical stress levels for Euler and local crippling were equated to one another. The constraints that the corrugations must not fail by local shear crippling or general shear buckling were imposed; however, these did not become active in this design. This is because the shear loading was of a low enough magnitude. The shear and compression loading was not coupled since the maximum value occurred at different locations.

Equating $F_{ccr} = F_{col}$

$$\frac{4.0\ \pi^2\ E\ T_c^2}{12\ (1 - \mu^2)\ B^2} = \frac{\pi^2\ E\ \rho^2}{L^2}$$

Since $\rho = \frac{1}{2\sqrt{2}} B$ for the 60° corrugation being considered here, the above equation was reduced to

$$B^2 = T_c\ L \sqrt{\frac{32}{12\ (1 - \mu^2)}}$$

Equating actual stress level with the local crippling stress:

$$f_c = \frac{N_x}{4/3\ T_c} = \frac{3\ N_x}{4\ T_c} = \text{actual stress level lbs/in}^2$$

$$\frac{3\ N_x}{4\ T_c} = \frac{4.0\ \pi^2\ E\ T_c^2}{12\ (1 - \mu^2)\ B^2}$$

$$B^2 = \frac{16\pi^2 E T_c^{\ 3}}{36 N_x (1 - \mu^2)}$$

Equating the B^2 terms:

$$T_c L \sqrt{\frac{32}{12 (1 - \mu^2)}} = \frac{16 \pi^2 E T_c^{\ 2}}{36 N_x (1 - \mu^2)}$$

$$T_c^{\ 2} = \frac{36 L N_x (1 - \mu^2) 32}{16 \pi^2 E \sqrt{12 (1 - \mu^2)}}$$

$$T_c = .6102 (1 - \mu^2)^{1/4} \sqrt{\frac{N_x L}{E}}$$

Therefore, with the ring spacing given, the optimum corrugation skin thickness was calculated from the above equation. Knowing T_c, the other corrugation geometry was calculated by:

$$B = \frac{1.278 \sqrt{T_c L}}{(1 - \mu^2)^{1/4}}$$

Corrugation Ring Requirements

An investigation of ring requirements was made, employing analytical methods for optimizing ring quantities. The study results are discussed in the following paragraphs.

Experimental evidence had indicated that a certain ring stiffness was required to force an inflection point of the buckling pattern at the ring support. This required ring stiffness was:

$$E_r I_r = 3 \times 10^{-5} \frac{\pi \cdot N_x D^4}{L} \qquad \text{(Reference 9)}$$

This was two times the requirement recommended by Shanley (Reference 10) for the monocoque shells that have hoop stiffness.

To optimize the 60° corrugation, using the Reference 9 approach, the following procedure was used:

a. Design the corrugation without any intermediate rings to reduce the unsupported length and calculate the resulting weight.

b. Add one ring and design the corrugation based on the reduced value of unsupported length and calculate the resulting weight of the corrugation plus the ring.

c. Continue adding the rings until an increase in total weight is noted. At this point, the optimum ring spacing has been found.

This analysis showed that it was not efficient to add rings to the tank support. The ring requirements appeared to be too extreme for this particular application of large diameters. The ring requirements were investigated by another method (Reference 11). This method treated the corrugation as a beam on an elastic foundation. The ring spring stiffness required to force an inflection point of the buckling pattern at the point of support was taken as $K = 23\ E\ I_R/R^3$ where I_R was the moment of inertia of the ring frame and

$$P_{cr} = 2\sqrt{\frac{EIK}{a}}$$

where EI was the corrugation flexural stiffness and "a" was the ring spacing. This method yielded realistic ring requirements but, as before, it was more weight efficient to delete the reinforcing rings.

Results

The final optimized sizing of corrugated titanium and fiberglass structure is shown in Figures 3 and 4 for:

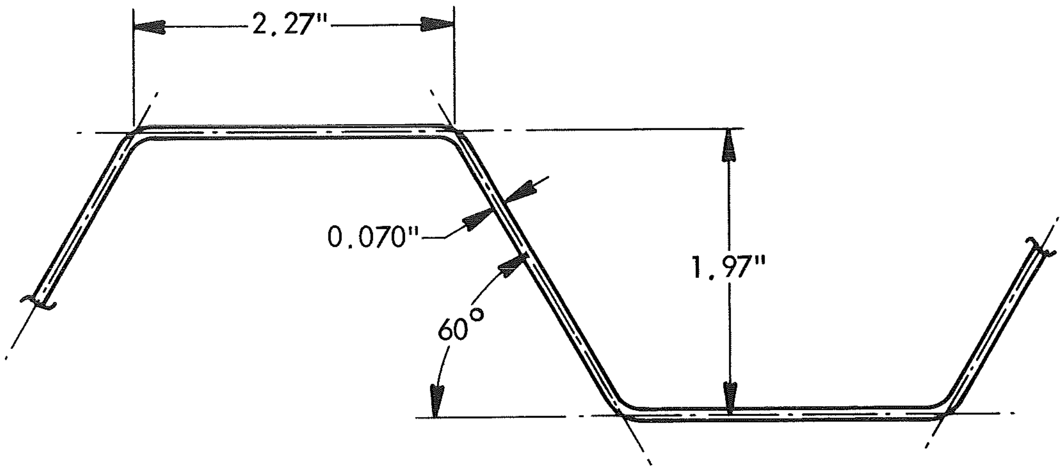

Applied Ult Load Compression = 851.45 Lbs/In
Shear = 338.0 Lbs/In

Eff Area = .0921 In^2/In

Weight = .0061 Lbs/In Circum & Length

Applied Ult. Compression Stress	=	9,249 Lbs/In^2
Allowable Compression Crippling Stress	=	9,249 Lbs/In^2
Allowable Compression Buckling Stress	=	9,249 Lbs/In^2
Applied Ult. Shear Stress	=	4,890 Lbs/In^2
Allowable Shear Crippling Stress	=	12,371 Lbs/In^2
Allowable Shear Buckling Stress	=	5,553 Lbs/In^2
Applied Ult. Tension Stress	=	27,500 Lbs/In^2
Allowable Ult. Tension Stress	=	65,000 Lbs/In^2

Figure 3: FIBERGLASS CORRUGATION

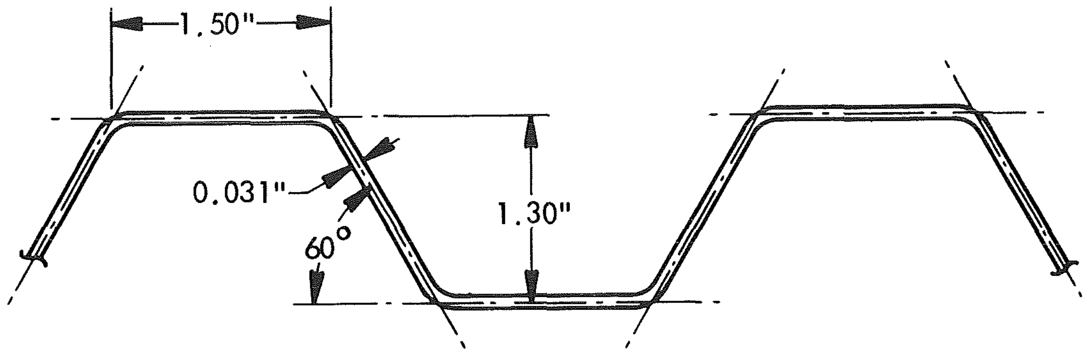

Applied Ult Load	Compression	=	851.45 Lbs/In
	Shear	=	338.0 Lbs/In

Eff Area = .0413 In^2/In Weight = .0066 Lbs/In Circum & Length

Applied Ult. Compression Stress	=	20,063 Lbs/In^2
Allowable Compression Crippling Stress	=	25,207 Lbs/In^2
Allowable Compression Buckling Stress	=	22,055 Lbs/In^2
Applied Ult. Shear Stress	=	10,906 Lbs/In^2
Allowable Shear Crippling Stress	=	33,715 Lbs/In^2
Allowable Shear Buckling Stress	=	10,910 Lbs/In^2
Applied Ult. Tension Stress	=	61,000 Lbs/In^2
Allowable Ult. Tensile Stress	=	134,000 Lbs/In2

Figure 4: TITANIUM CORRUGATION

N_x = -851 lbs/in applied ultimate compression loading
+1897 lbs/in applied ultimate tension loading

N_{xy} = 338 lbs/in applied ultimate shear loading

R_{eff} = 193.69 in. normal to surface at small end

L = 45.47 in. slant height

The fiberglass support had more than twice the cross sectional area; however, the weight was less.

3.4.2 Stiffened Construction

Analysis

It has been established that the most efficient structure is that in which every type of instability which could cause failure occurs simultaneously.

The stringer-skin combination can develop several separate types of instability, which may be coupled to a greater or lesser degree (Reference 12).

(a) Skin buckling (or initial buckling). This generally involves waving of the skin between stringers in a half-wavelength comparable with the stringer pitch. There will also be a certain amount of waving of the stringer web and lateral displacement of the free flange. For some proportions the latter may become larger than the skin displacements, and the mode becomes more torsional or local in nature (see (b) and (c)).

(b) Local instability. Secondary short-wavelength buckling may take place in which the stringer web and flange are displaced out of their own planes in a half-wavelength comparable with the stringer depth. There will be smaller associated movements of the skin and lateral displacements of the stringer free flange.

(c) Torsional instability. The stringer rotates as a solid body about a longitudinal axis in the plane of the skin, with associated smaller displacements of the skin normal to its plane and distortions of the stringer cross-section. The half-wavelength is usually of the order of three times the stringer pitch.

(d) Flexural instability. Simple strut instability of the skin-stringer combination in a direction normal to the plane of the skin. There may be small associated twisting of the stringers. The half-wavelength is generally equal to the frame spacing.

(e) Inter-rivet buckling. Buckling of the skin as a short strut between rivets; this can be avoided by using a sufficiently close rivet pitch along the stringer.

(f) Wrinkling. A mode of instability similar to inter-rivet buckling, but analogous to wrinkling of a sandwich structure, in which the skin develops short-wavelength buckling as an elastically supported strut. For all practical skin-stringer combinations it can be avoided by keeping the line of attachment very close to the stringer web.

Failure of Stringers

When the skin stringer combination approaches its Euler instability stress, development of instabilities (a), (b), (c), (e), or (f) will so reduce the flexural stiffness as to cause premature collapse.

Buckled Skin Versus Unbuckled Skin Designs

If the Euler instability stress is reasonably remote, instability (a) (skin buckling) will not precipitate failure, and the structure will carry increased load, with the skin buckled until failure occurs by the onset of instability (b), (c), (e), or (f). In general an excessive margin of flexural stiffness is needed to prevent failure due to any of these latter four modes.

By letting failure occur at more than about three times the skin buckling stress, stringers are relatively sturdy and coupling between skin buckling and stringer local distortion is negligible. It has also been established that coupling of modes reduces the lower instability stress and raises the higher, and thus leads to a less efficient design. Efficient designs can be obtained, however, by either not allowing the skin to buckle at all, or letting the skin buckle at a comparatively low stress.

The unbuckled skin design was used throughout this study. While this type of structure was not quite as efficient as the buckled skin design for load magnitudes that were low, this structure did offer increased shear stiffness over the buckled design. The structure was analyzed thoroughly to prevent any instabilities from occurring which would cause premature failure.

Optimization Procedures

The optimization used to determine the minimum cross sectional area made use of:

1. Multiple load conditions of compression plus shear
2. Local and general instability analysis
3. Imposed constraints such as:
    a. Minimum gage requirements
    b. Minimum stiffener moment of inertia required to break up panels for shear instability
    c. Minimum stiffener gage requirements to restrain shear buckles
    d. Torsional instability requirements for zee sections
    e. Minimum size of outstanding legs of zee sections to offer support to vertical legs.

All elements of the stiffened construction were checked for local crippling by the following formulas:

(Compression) $$F_{ccr} = \frac{K\,E}{12\,(1-\mu^2)}\,(t/b)^2$$

and

(Shear) $$F_{scr} = \frac{K_s\,E}{12\,(1-\mu^2)}\,(t/D)^2$$

where

$K_s = 5.35 + 4(D/L)^2$

D = stiffener spacing

L = length of panel

b = width of element

t = thickness of element

The panel general instability was checked using the Euler column formula with simply supported ends.

$$F_{col} = \frac{\pi^2 E}{(L/\rho)^2}$$

The optimization was performed with a digital computer using an iterative procedure. Iterations were performed on the geometrical variables over the range of interest. The configuration which provided the minimum area while satisfying all constraints was saved as the final optimum configuration.

The restraints imposed and associated formulas follow:

Outer Flange Minimum Length Restraint

The outer lip of the zee stiffner should not be shorter than necessary to offer stability to the flange as shown below:

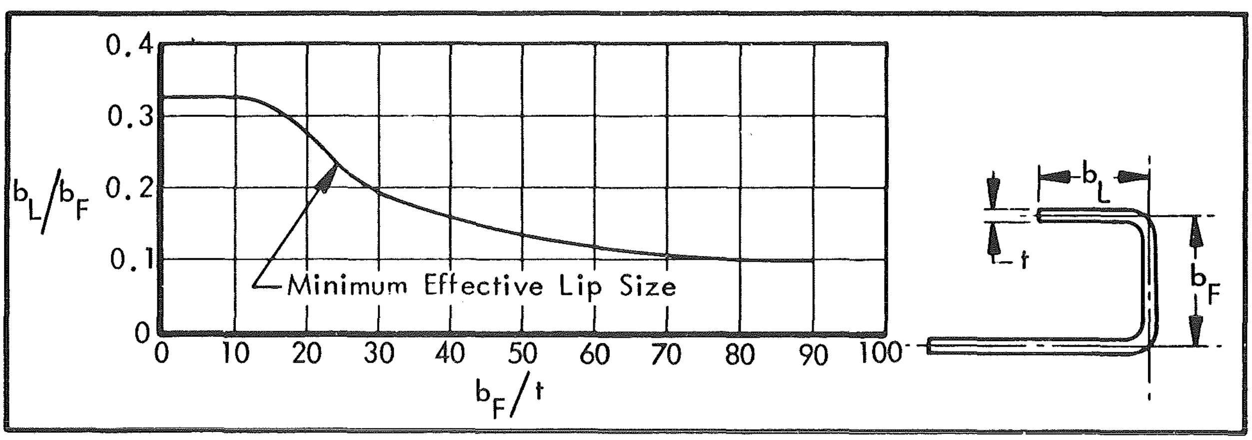

Above Minimum Effective Curve: Consider lip as a flat segment with 1 edge free. Consider adjacent flange as having 0 edges free.

Below Minimum Effective Lip Curve: Consider the flange adjacent to lip as segment with 1 edge free. The length of the flange becomes $b = b_F + b_L$. Use this b in analyzing the flange.

Shear Restraints

(A) Local Shear Instability

The sheet material was not allowed to buckle between stiffening members. The allowable shear local instability stress was obtained by

$$F_{sccr} = \frac{5.35\,\pi^2 E}{12\,(1 - \mu^2)}\,(t/D)^2$$

(B) Stiffener Moment of Inertia Requirement with Non-buckling Web

The minimum required value of stiffener moment of inertia to prevent failure due to shear loads was computed using the following formula:

$$I_{s\ req'd} = D/t \left[\frac{L^2\ t\ fs}{16E}\right]^{4/3}$$

where fs was the shear stress in the web.

(C) Stiffener Flange Thickness Required Next to Web

The web stiffeners were required to decrease the size of the web panels to prevent (1) buckles from forming across the stiffener, and (2) the web from buckling as a whole section. The allowable shear instability stress was determined from

$$F_{scr} = \frac{\pi^2 k_s E}{12\,(1 - \mu^2)}\,(t/D)^2$$

where $k_s = 1.1064\ K_s$

K_s was the plate shear buckling coefficient derived from the following graph:

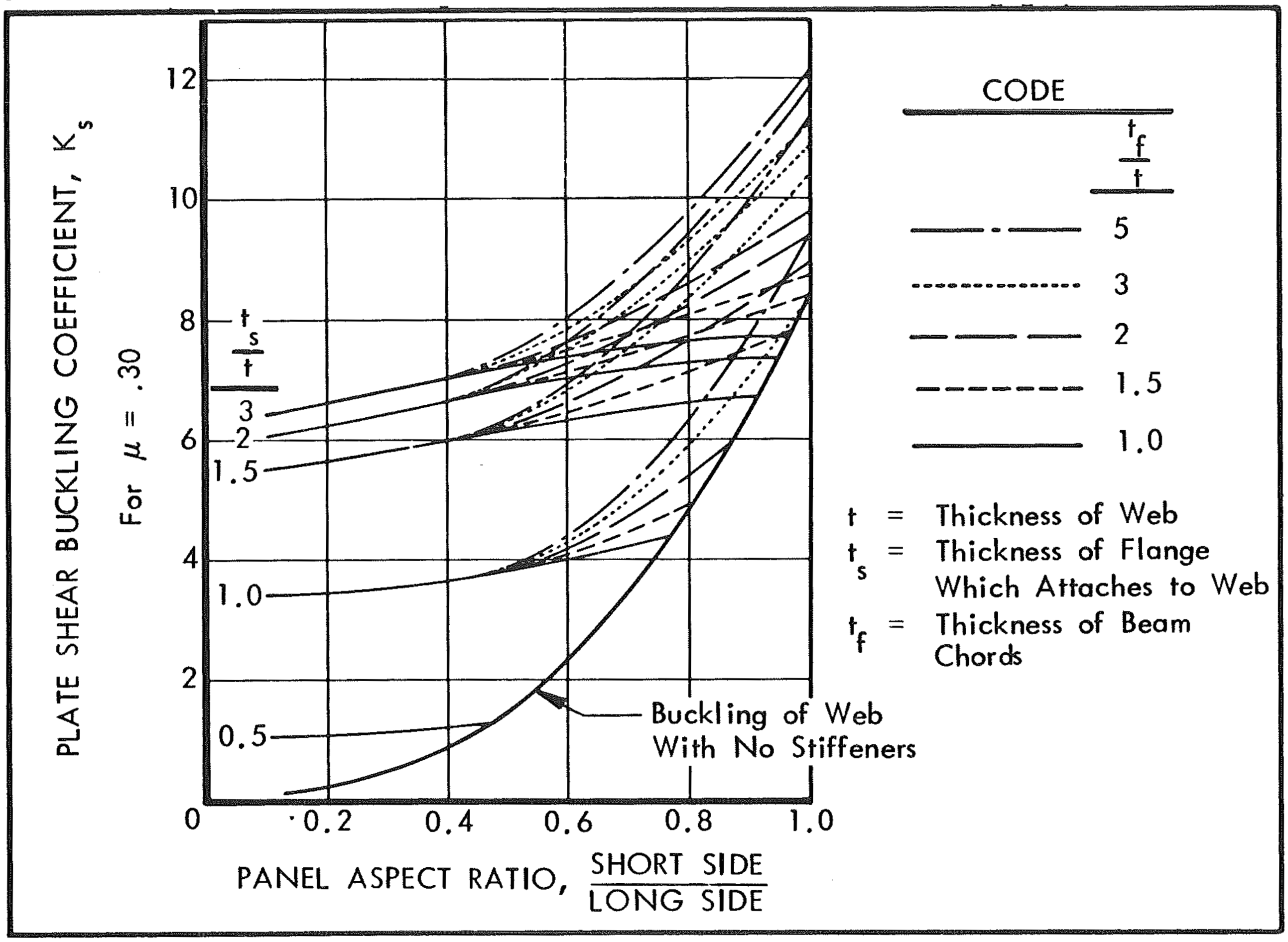

Torsional Instability Restraint

The torsional instability restraint was applied to the stiffened construction. The hat section and bar section stiffened structure did not require this restraint.

Torsional failure of stiffened panels was investigated by making the assumption that the stiffener with some adjacent skin acted as a column. This was done to simplify a difficult problem. A rigorous solution (Reference 13) to the problem of a stiffened panel failing torsionally was obtained by assuming the stiffener to be forced to rotate about a point in the plane of the skin along the line of attachment. The solution obtained by the rigorous treatment yielded a higher allowable critical load.

The J–section shown below was used to approximate sections from stiffened panels of zee sections attached to skin. The length "c" was replaced by an effective width of plate. The attached flange of the zee section was distributed along the effective length so that the thickness t_2 became:

$$t_2 = t_{skin} + \frac{A_{flange}}{\text{eff. width}}$$

The constants x_o, y_o, and Γ for the sheet and stiffener were computed from the equations given below. The critical stress was then computed by calculating the equivalent slenderness ratio and substituting into the Euler column formula. The equations for x_o and y_o yielded exact solutions, whereas, the equation for Γ was an approximation.

J - Section

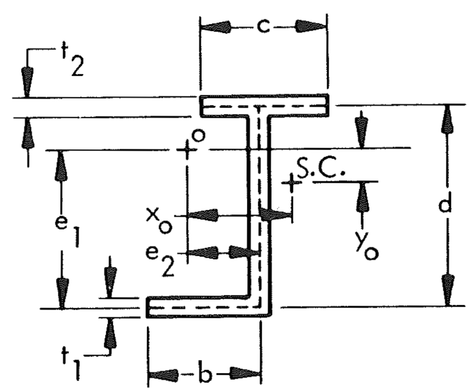

$$x_o = e_2 + \frac{b^2 d t_1}{I_x I_y - I_{xy}^2}\left[\frac{I_y e_1}{2} - I_{xy}\left(\frac{e_2}{2} - \frac{b}{3}\right)\right]$$

$$y_o = e_1 - d + \frac{b^2 d t_1}{I_x I_y - I_{xy}^2}\left[\frac{I_{xy} e_1}{2} - I_x\left(\frac{e_2}{2} - \frac{b}{3}\right)\right]$$

where:

$$I_1 = \frac{t_1 b^3}{12}, \quad I_2 = \frac{t_2 c^3}{12}$$

$$\Gamma = \frac{d^2 I_1 I_2}{I_1 + I_2} \quad \text{(Approximate solution)}$$

It was assumed that centrally loaded columns would buckle in the plane of a principal axis without rotation of the cross section, but experience revealed that columns having open cross sections showed a tendency to bend and twist simultaneously under axial load. The actual critical load of such columns, due to their small torsional rigidity, could be less than the critical load predicted by the generalized Euler formula.

To check the torsion failure mode it was necessary to compute a radius of gyration which yielded the greatest slenderness ratio which could then be used to predict a strength. The radii of gyration which were checked were the usual ρ_{xx} and ρ_{yy} and an equivalent radius of gyration. To compute the equivalent radius of gyration the following was needed:

$$\rho_{\theta} = \sqrt{\frac{c_w \Gamma}{I_o} + \frac{c_{\theta} L^2 GJ}{\pi^2 E_c I_o}} \quad \text{in.}$$

where J and I_o were cross sectional properties defined below:

J was the torsion constant of St. Venant (For open thin walled sections $J = \frac{1}{3}\sum mt^3$ where m was the middle line length of each flange or web and t the thickness).

$$I_o = I_{xx} + I_{yy} + A\,(y_o^2 + x_o^2) \quad \text{in.}^4$$

where y_o, x_o were components of distance from the shear center to the centroid.

The c's were fixity coefficients defined as follows:

c_w = Coefficient indicating amount of fixity against warping

c_{θ} = Coefficient indicating amount of fixity against twisting.

The coefficients c_w and c_{θ} are usually assumed as equal to one.

If $\mu = 0.3$ and $\frac{G}{E_c} = \frac{1}{2(1+\mu)}$ then

$$\rho_\theta = \sqrt{\frac{c_w \Gamma}{I_o} + .039 \frac{c_\theta L^2 J}{I_o}}$$

If the cross section of the column had no axis of symmetry, the modes of failure were dependent on one another. The slenderness ratio was obtained as follows:

$$\frac{L}{\rho_e}$$

where $(\rho_e)^2$ was the smallest root of a cubic equation given in Reference 14.

Results

Figures 5, 6, 7, 8, 9 and 10 show the optimized configurations of hat, bar, and zee stiffened panels of both titanium and fiberglass construction. In all cases the cross sectional area of fiberglass was greater than in the titanium counterparts; however, the fiberglass parts weighed less.

3.4.3 Honeycomb Construction

Analysis

A study of the effects of orientation of the honeycomb core ribbon was made on allowable buckling strength and heat flow. The shear modulus of the core was approximately twice as great in the direction of the ribbon as in a direction perpendicular to the ribbon. If the ribbon were oriented in the circumferential direction of the cone, the heat flow was substantially reduced whereas, the allowable longitudinal buckling load was only slightly reduced.

If the heat flow of the core was calculated for the cross sectional area of the foil material and developed length, it was found that the core had a heat flow 1.5 times greater when the ribbon was oriented in the longitudinal direction than in the circumferential direction. If the core ribbon developed length was not used in the heat flow

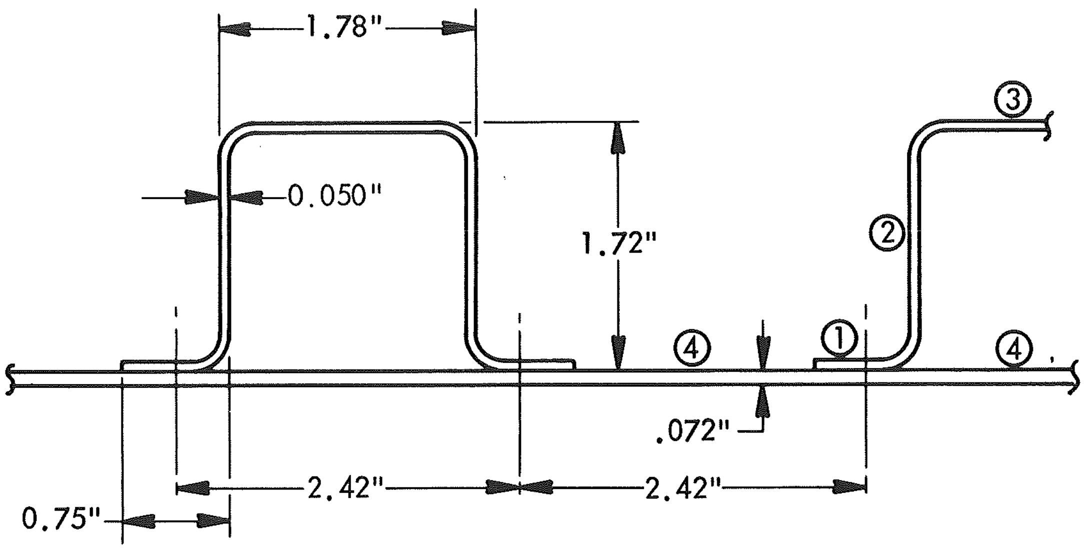

Applied Ult. Load Compression = 851.45 Lbs/In
Shear = 338.0 Lbs/In

Eff Area = .1400 In^2/In Weight = .00924 Lbs/In Circum. & Length

Applied Ult. Compression Stress 6,016 Lbs/In^2

Allowable	①	21,969 Lbs/In^2
Compression	②	9,539 " "
Crippling	③	9,000 " "
Stresses	④	9,000 " "

Allowable Column Buckling Stress 6,256 Lbs/In^2

Applied Ult. Shear Stress 4,674 Lbs/In^2

Critical Shear Stress 4,698 Lbs/In^2 (Stiffener Critical)

Figure 5: FIBERGLASS HAT SECTION

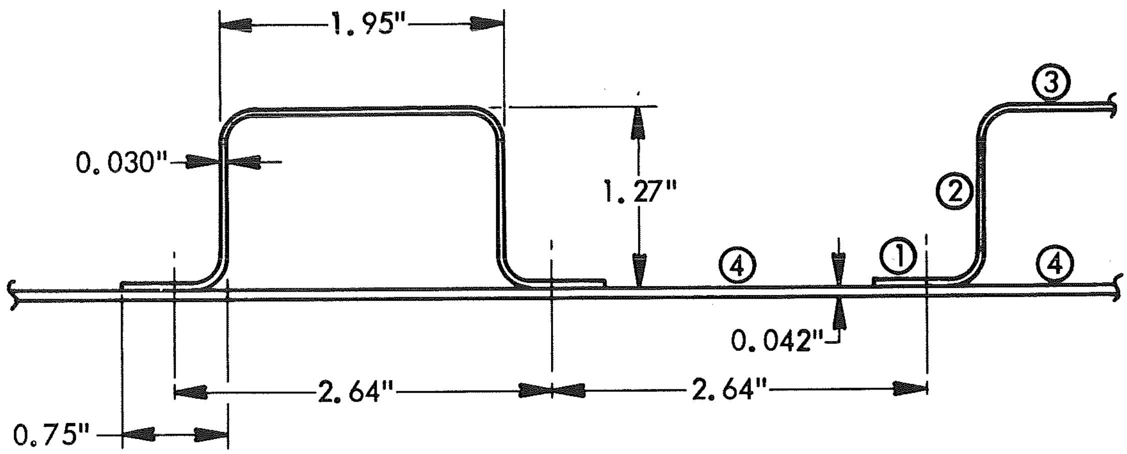

Applied Ult. Load Compression = 851.45 Lbs/In
Shear = 338.0 Lbs/In

Eff. Area = .0725 In^2/In Weight = .0116 Lbs/In Circum. & Length

Applied Ult. Compression Stress = 11,306 Lbs/In^2

Allowable Compression Crippling Stresses	① 44,262 Lbs/In^2
	② 36,446 Lbs/In^2
	③ 15,000 Lbs/In^2
	④ 15,000 Lbs/In^2
Allowable Column Buckling Stress	= 19,063 Lbs/In^2
Applied Ult. Shear Stress	= 11,270 Lbs/In^2
Critical Shear Stress	= 11,721 Lbs/In^2 (Stiffener Critical)

Figure 6: TITANIUM HAT SECTION

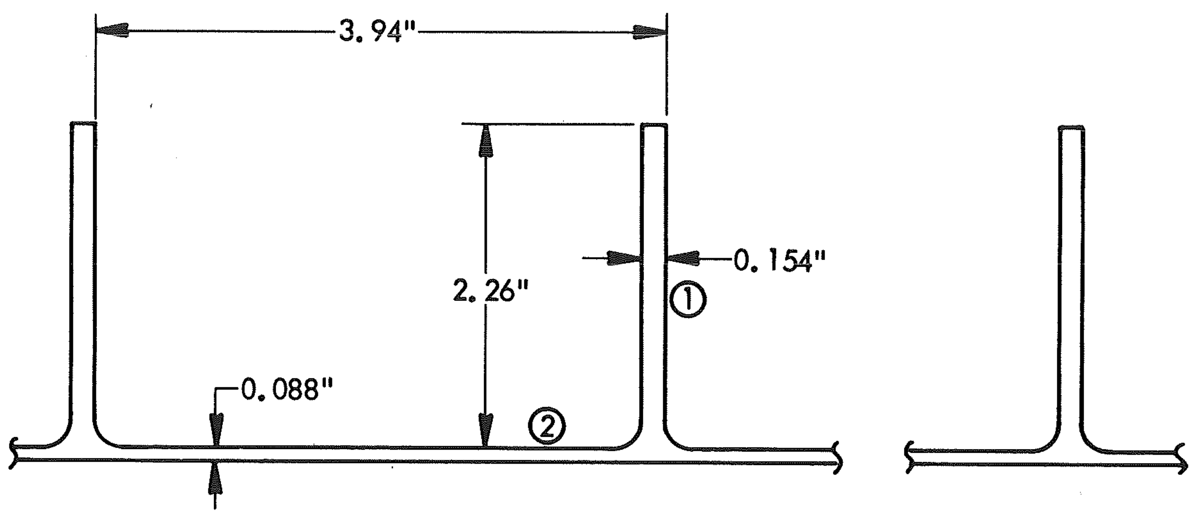

Applied Ult. Loads:	Compression = 851.45 Lbs/In Shear = 338.00 Lbs/In
Eff Area = .176 In^2/In	Weight = .0116 Lbs/In Circum & Length
Applied Ult. Compression Stress	= 4,829 Lbs/In^2
Allowable Crippling Compression Stress 1 & 2	= 5,000 Lbs/In^2
Allowable Column Buckling Stress	= 4,933 Lbs/In^2
Applied Ult. Shear Stress	= 2,195 Lbs/In^2
Critical Shear Stress	= 4,482 Lbs/In^2

Figure 7: FIBERGLASS BAR STIFFENED PANEL

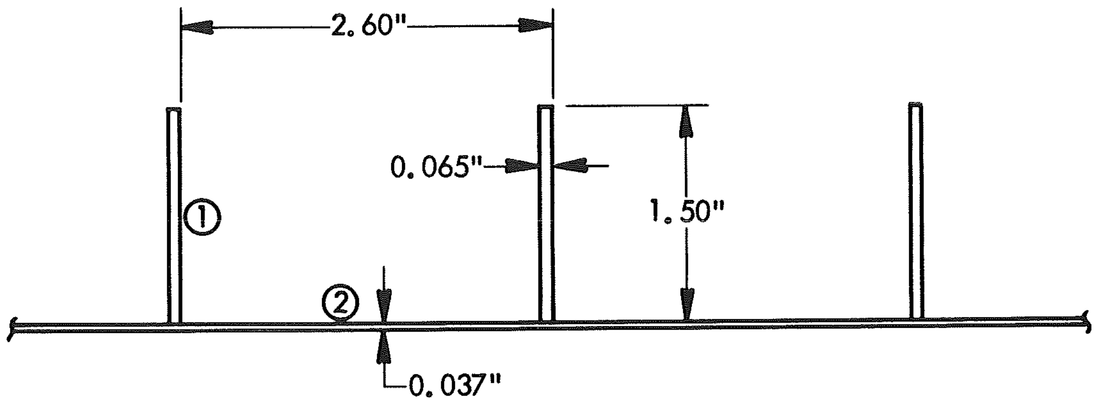

Applied Ult. Loads:	Compression = 851.45 Lbs/In Shear = 338.00 Lbs/In	
Eff. Area = .0744 In^2/In	Weight = .0119 Lbs/In Circum & Length	

Applied Ult. Compression Stress	=	11,438 Lbs/In^2
Allowable Crippling Compression Stress ① & ②	=	12,000 Lbs/In^2
Allowable Column Buckling Stress	=	11,529 Lbs/In^2
Applied Ult. Shear Stress	=	4,543 Lbs/In^2
Critical Shear Stress	=	7,042 Lbs/In^2

Figure 8: TITANIUM BAR STIFFENED PANEL

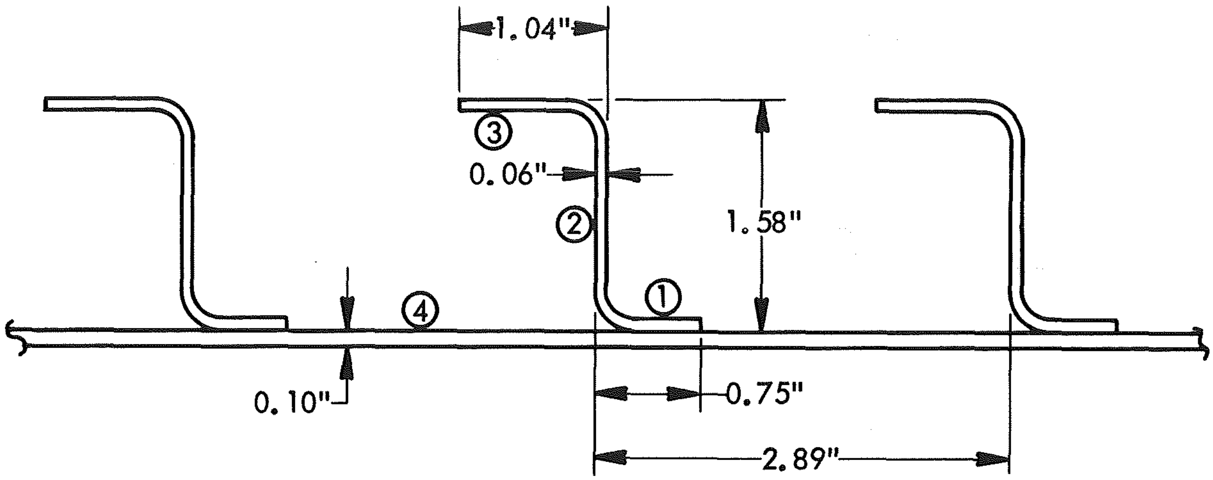

Applied Ult. Load — Compression = 851.45 Lbs/In
Shear = 338.0 Lbs/In

Eff. Area = .1675 In^2/In   Weight = .0111 Lbs/In Circum. & Length

Applied Ult. Compression Stress = 5,083 Lbs/In^2

Allowable Compression Crippling Stresses	①	31,000 Lbs/In^2
	②	16,912 Lbs/In^2
	③	12,000 Lbs/In^2
	④	12,000 Lbs/In^2

Allowable Column Buckling Stress = 5,118 Lbs/In^2

Applied Ult. Shear Stress = 5,633 Lbs/In^2

Critical Shear Stress = 8,132 Lbs/In^2
(Stiffener Critical)

Figure 9: FIBERGLASS ZEE SECTION

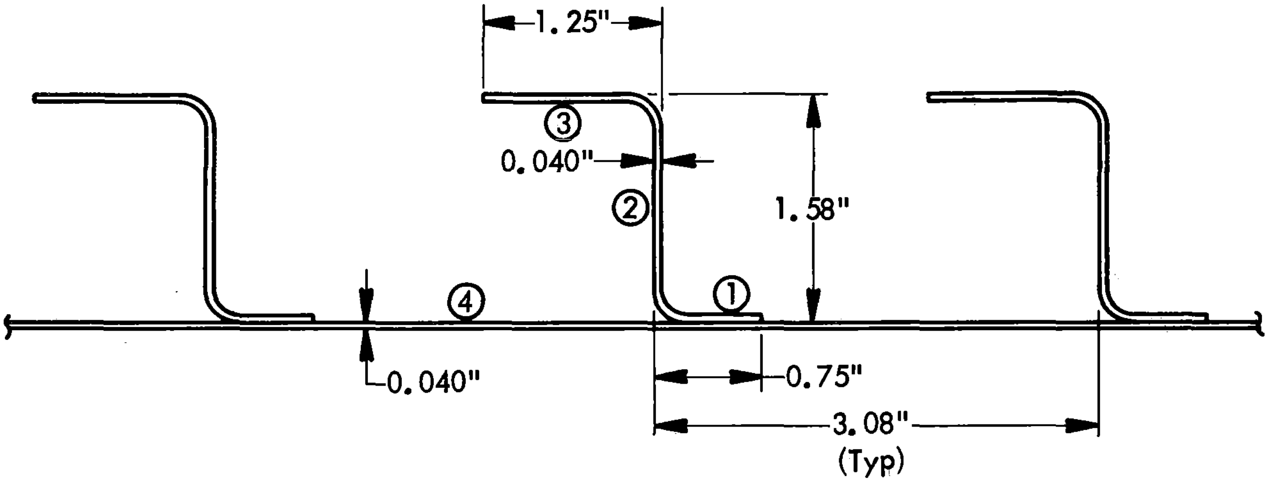

Applied Ult. Load	Compression = 851.45 Lbs/In	
	Shear = 338.0 Lbs/In	

Eff. Area = .0855 In^2/In Weight = .0137 Lbs/In Circum & Length

Applied Ult. Compression Stress = 9,958 Lbs/In^2

Allowable Compression Crippling Stresses	①	80,920 Lbs/In^2
	②	42,162 Lbs/In^2
	③	21,200 Lbs/In^2
	④	10,000 Lbs/In^2
Allowable Column Buckling Stress		= 9,958 Lbs/In^2 (Torsional Instability)
Applied Ult. Shear Stress		= 8,450 Lbs/In^2
Critical Shear Stress		= 9,258 Lbs/In^2 (Stiffener Critical)

Figure 10: TITANIUM ZEE SECTION

calculations, the heat flow difference between core direction became 1.732 instead of 1.5. Therefore, the designs were made with the ribbon oriented in the circumferential direction. Figure 11 shows core dimensional relationships. The equations used for calculating core heat flow were:

Using direct length

$$\text{Effective cross sectional core area perpendicular to ribbon direction} = \frac{\rho_c \times T_c}{3991 \times \rho_f}$$

$$\text{Core heat flow} = \frac{K_c \times \rho_c \times T_c}{3991 \times \rho_f}$$

Using developed length

$$\text{Core heat flow} = \frac{K_c \times \rho_c \times T_c}{4608\ \rho_f}$$

where K_c = mean thermal conductivity of the core

ρ_c = density of the core

T_c = core thickness

ρ_f = density of the foil

Several different methods utilizing different theories were available for the design of sandwich cylinders subjected to axial compression or bending loads which could cause buckling. One method, MIL-HDBK-23 (Reference 15), used a large deflection theory and established the minimum postbuckling load of the theoretical load-shortening curve of sandwich cylinders as the design load of the cylinders; thus, it could not be expected to predict the buckling load. This had been the most commonly used method in design but the method was found to be quite conservative, e.g., Reference 16.

A second method made use of small-deflection classical buckling theory which differed from ordinary curved-plate theory principally by the inclusion of the effects of deflections due to transverse shear. This theory was modified, when necessary, to account for the fact that cylinders do not always sustain the classical buckling load prior to

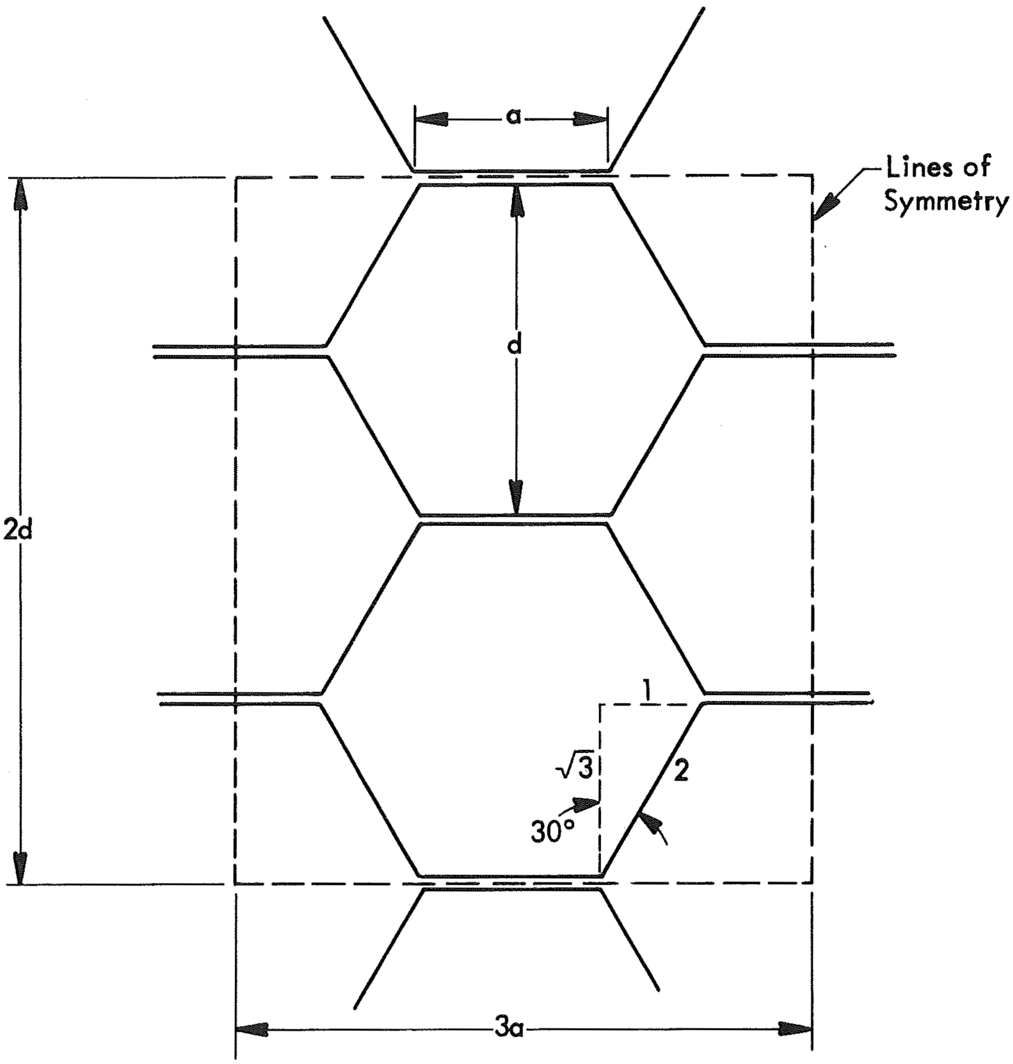

Ribbon
Direction

d = Cell Size

a = Side of Cell

$a = d/2 \cos 30° = d/\sqrt{3}$

Figure 11: HONEYCOMB CELL CONFIGURATION

buckling. However, the modification was slight when compared to monocoque shells. This method yielded buckling loads that could be as high as 2 1/2 times that of the first method. The principal problem encountered in applying this method to design was the lack of sufficient experimental data to substantiate the method. Equations for the application of this method were taken from Reference 17.

A third method made use of an effective moduli of elasticity and thickness of the sandwich shell as described in Reference 18. The values of E_e and T_e can be substituted into the formulas for solid isotropic shells or plates. These effective values are:

$$E_e = \frac{H}{2\sqrt{3(1-\mu^2)D/H}} = \text{Effective modulus of elasticity}$$

$$T_e = 2\sqrt{3(1-\mu^2)D/H} = \text{Effective thickness}$$

where μ = Poisson's ratio of the face material

$H = E_f(t - t_c)$ (Extensional Stiffness)

t is the overall thickness of the honeycomb panel and t_c is the core thickness and E_f = modulus of elasticity of face material.

$$D = E_f(t^3 - t_c^3)/12(1-\mu^2) \quad \text{(Bending Stiffness)}$$

The values obtained for critical buckling loads and deflections by this substitution are always unconservative, due to shear deflections.

Conservative values of critical buckling loads per inch of panel edge were obtained by:

$$P_{cr} = \frac{1}{\frac{1}{P_{cre}} + \frac{1}{U}}$$

$U = 1/2\,(t + t_c)\quad G_c$ = transverse shear stiffness

G_c = core shear modulus – lbs/in^2

in which P_{cr} is a conservative value of the critical load per inch of panel edge, P_{cre} is the unconservative value obtained by substituting E_e and T_e in a formula for solid isotropic plates.

For this method the equations for isotropic monocoque shells that are based on considerable experimental data and presented in Reference 19 were used. These were:

$$P_{cr} = C\, 2 \pi E T^2$$

$$F_{cr} = C \; E \; \frac{T}{R}$$

$$C = \text{Buckling Coefficient}$$

$$C = .606 - .546 \left\{ 1.0 - \exp. \left[- \frac{1}{16} \; (R/T)^{1/2} \right] \right\} + .9 \, (R/L)^2 \; (T/R)$$

where T and E can be replaced by T_e and E_e.

A fourth method also made use of the effective moduli of elasticity and thickness of the honeycomb sandwich shell wall as described in Reference 18. A one inch strip of the shell was treated as an Euler column.

It was shown that the buckling of this conical support would always occur in only 1/2 of a longitudinal wave (axisymmetric mode), therefore, this method of analysis was applicable. This approach was considered to be quite conservative since no effect of curvature or hoop stiffness was included. The Euler column load was reduced for the effect of shear deflection of the core material. This method yielded allowable loads which were intermediate to the other methods and was chosen for final design.

The final design equation became:

$$P_{cr} = \frac{\pi^2 D}{L^2 + \dfrac{\pi^2 D}{U}}$$

where D was the bending stiffness and U was the shear stiffness as previously defined.

A comparison of the various analysis methods is shown in Figure 12. This comparison is for a representative fiberglass honeycomb cylinder tank support using .036 inch face skins and 2 inch core for a length of 45.47 inches. It is shown that the analysis method chosen is conservative.

Optimization Procedure

The optimization was performed with a digital computer using an iterative procedure.

The honeycomb sandwich was checked for intracell buckling, face wrinkling, and shear crimping in addition to the overall shell buckling that was discussed in the previous section. The equations for the first three failure modes listed are as follows:

Intracell compression buckling stress (Reference 18)

$$F_{cib} = 2E\,(t_f/\text{cell})^2$$

where t_f = face skin thickness - in.

cell = cell size - in.

Face wrinkling stress (Reference 17)

$$F_{cw} = .43\,(E \times E_{core} \times G_{core})^{1/3}$$

where E_{core} = Core compression modulus of elasticity - lbs/in^2

G_{core} = Core shear modulus of elasticity - lbs/in^2

Face shear crimping stress due to compression loads (Reference 17)

$$F_{csc} = \frac{G_{core}\,(t_c + 2\,t_f)}{2\,t_f}$$

where t_c = core thickness - in.

t_f = face skin thickness - in.

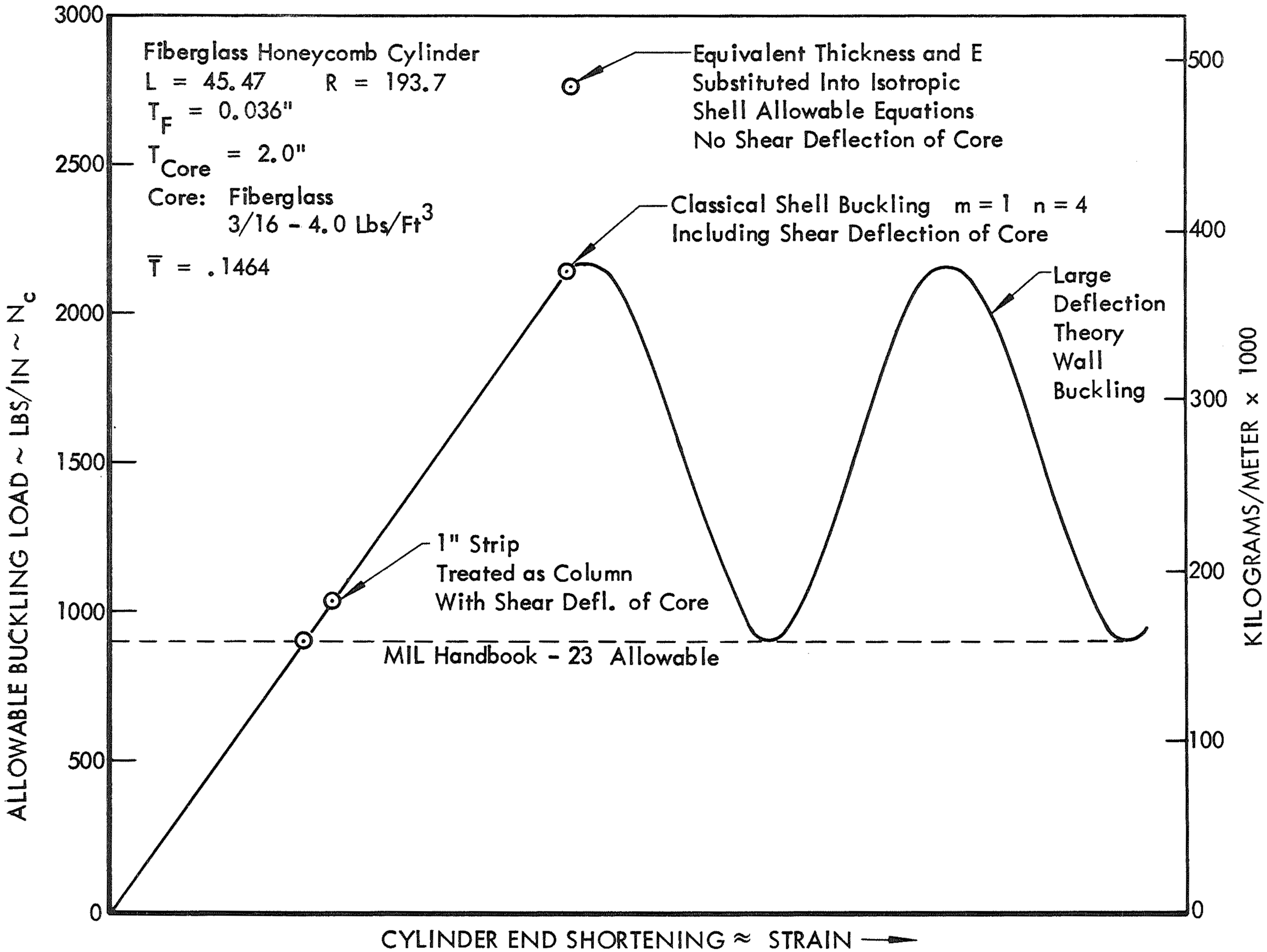

Figure 12: COMPARISON OF METHODS TO PREDICT ALLOWABLE BUCKLING OF HONEYCOMB CYLINDERS

The configuration which fulfilled these requirements and provided minimum cross sectional area was considered optimum.

Face thicknesses in increments of .009 inches were considered for fiberglass. Minimum gage for the titanium was .005 inches and increments of .001 inches were considered. Standard sizes of fiberglass honeycomb core were used.

The design loading was 878 lbs/inch which occurred at the bottom of the support and was the critical condition since tapering of the honeycomb construction was not considered.

Results

The optimization results for both fiberglass and titanium sandwich cone supports are tabulated in Figures 13 and 14. It can be seen that optimum weight and heat flow did not occur with one configuration, thus a compromise was necessary. Figures 15 and 16 show the configurations selected. The all fiberglass configuration was only slightly "off optimum" in heat flow and was narrower, which minimized clearance problems between cone support and tank head. The titanium configuration selected was the one with minimum heat flow. This was necessary to make the concept competitive with fiberglass construction. The weight difference between fiberglass and titanium construction was negligible; however, the cross sectional area of the titanium member was significantly less.

3.4.4 Weight-Heat Flow Comparisons

Figure 17 lists the results of the study. It should be noted that the values are for one inch of cone circumference and, therefore, do not represent total heat flow or weight. Also the weight and heat flow additions due to edge attachments are not included. A comparison of results shows fiberglass construction to be superior for like configurations both on a weight and heat flow basis. The weight-heat flow parameter differences were largely the effect of the fiberglass thermal conductivity, pointing out the main advantage of this material.

	FACE SKIN THICKNESS IN.	FIBERGLASS CORE			$\bar{T}$ EFFECTIVE THICKNESS	KA/IN $\frac{BTU-IN}{HR-^{\circ}F}$ $\times 10^{-3}$ *	WEIGHT LBS/IN^2
		THICKNESS IN.	HEX CELL SIZE	DENSITY LBS/FT^3			
	.036	2.0	3/8	2.2	.1232	1.15 (1.12)	.0081
	.036	2.1	3/8	2.2	.1251	1.16 (1.13)	.0083
	.027	2.2	1/4	3.5	.1341	1.08 (1.03)	.0089
OPT. WT.	.027	2.3	3/8	2.2	.1109	0.95 (.92)	.0073
	.027	2.4	3/8	2.2	.1129	0.96 (.93)	.0075
	.027	2.5	3/8	2.2	.1148	0.97 (.94)	.0076
	.027	2.6	3/8	2.2	.1168	0.98 (.95)	.0077
OPT. Q	.018	2.7	1/4	3.5	.1315	0.93 (.87)	.0087
	.018	2.8	1/4	3.5	.1345	0.95 (.89)	.0087
	.018	2.9	1/4	3.5	.1376	0.97 (.90)	.0091
	.018	3.0	1/4	3.5	.1407	0.99 (.92)	.0093
	.018	3.1	1/4	3.5	.1437	1.00 (.93)	.0095
	.018	3.2	1/4	3.5	.1468	1.02 (.95)	.0097
	.018	3.3	1/4	3.5	.1499	1.04 (.96)	.0099
	.018	3.4	1/4	3.5	.1530	1.06 (.98)	.0101
	.018	3.5	1/4	3.5	.1560	1.07 (.99)	.0103
	.018	3.6	1/4	3.5	.1591	1.09 (1.01)	.0103
	.027	3.7	3/8	2.2	.1380	1.10 (1.02)	.0091
	.018	3.7	1/4	3.5	.1622		
	.027	3.8	3/8	2.2	.1399	1.11 (1.04)	.0092
	.018	3.8	1/4	3.5	.1652		
	.027	3.9	3/8	2.2	.1418	1.13 (1.05)	.0094
	.018	3.9	1/4	3.5	.1683		

* Numbers In Parenthesis Are For Developed Core Length

Figure 13: HONEYCOMB CONSTRUCTION - FIBERGLASS

	FACE SKIN THICKNESS IN.	FIBERGLASS CORE THICKNESS IN.	FIBERGLASS CORE HEX CELL SIZE	FIBERGLASS CORE DENSITY LBS/FT^3	$\bar{T}$ EFFECTIVE THICKNESS	KA/IN $\frac{BTU-IN}{HR-^{\circ}F}$ $\times 10^{-3}$ *	WEIGHT LBS/IN^2
	.022	1.0	3/16	4.0	.0637	10.76 (10.73)	.0102
	.018	1.1	3/16	4.0	.0571	8.86 (8.83)	.0091
	.015	1.2	3/16	4.0	.0526	7.44 (7.41)	.0084
	.013	1.3	3/16	4.0	.0500	6.50 (6.46)	.0080
	.011	1.4	3/16	4.0	.0475	5.56 (5.52)	.0076
OPT WT	.010	1.5	1/4	3.5	.0442	5.06 (5.02)	.0071
	.009	1.6	3/16	4.0	.0464	4.64 (4.59)	.0074
OPT Q	.008	1.7	3/16	4.0	.0458	4.18 (4.13)	.0073
	.008	1.8	3/16	4.0	.0472	4.20 (4.15)	.0076
	.008	1.9	3/16	4.0	.0487	4.21 (4.16)	.0078
	.008	2.0	3/16	4.0	.0501	4.23 (4.18)	.0080
	.008	2.1	3/16	4.0	.0515	4.25 (4.20)	.0082
	.008	2.2	3/16	4.0	.0530	4.27 (4.22)	.0085
	.008	2.3	3/16	4.0	.0545	4.29 (4.23)	.0087
	.008	2.4	3/16	4.0	.0559	4.31 (4.25)	.0089
	.008	2.5	3/16	4.0	.0574	4.33 (4.27)	.0092
	.008	2.6	3/16	4.0	.0588	4.35 (4.28)	.0094
	.008	2.7	3/16	4.0	.0603	4.37 (4.30)	.0096
	.008	2.8	3/16	4.0	.0617	4.39 (4.32)	.0099
	.008	2.9	3/16	4.0	.0632	4.41 (4.34)	.0100

* Numbers in Parenthesis Are For Developed Core Length

Figure 14: HONEYCOMB CONSTRUCTION - TITANIUM

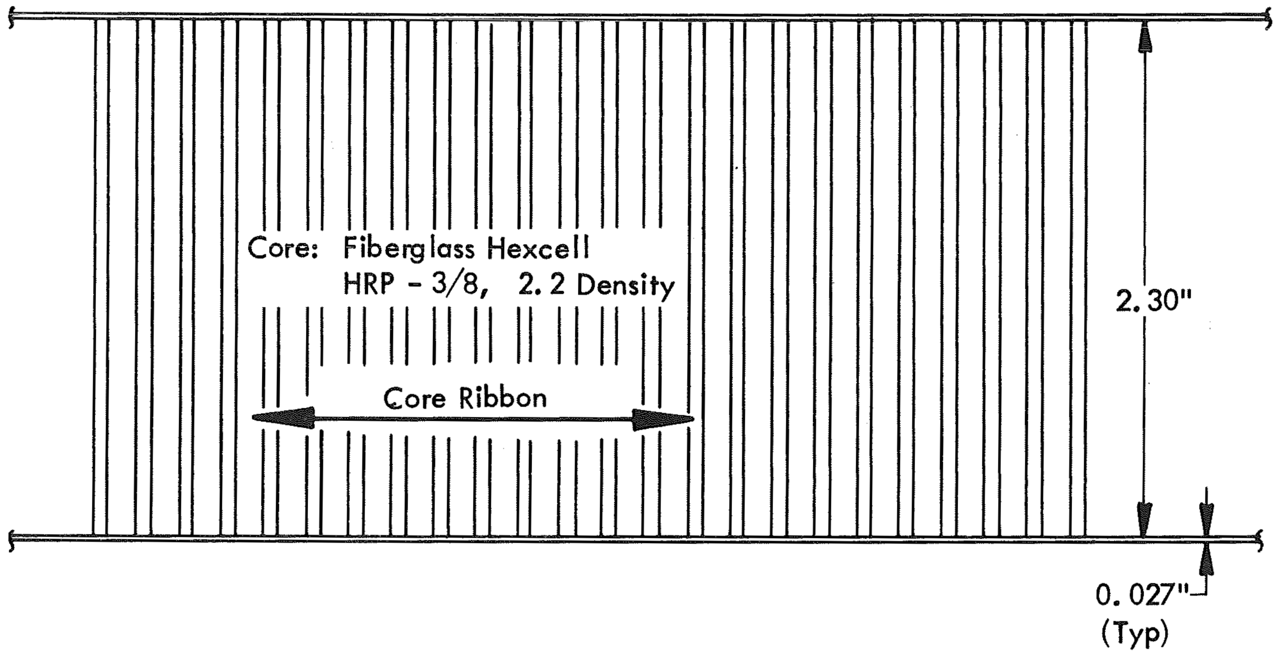

Applied Ult. Load Compression = 878.06 Lbs/In
Shear = 338.00 Lbs/In

Eff Area = .1109 In^2/In Weight = .0073 Lbs/In Circum & Length

Applied Ult Compression Stress	= 24,391 Lbs/In^2
Allowable Compression Buckling Stress	= 25,503 Lbs/In^2
Allowable Compression Intracell Buckling Stress	= 31,104 Lbs/In^2
Allowable Compression Face Wrinkling Stress	= 52,435 Lbs/In^2
Allowable Compression Shear Crimping Stress	= 516,800 Lbs/In^2

Figure 15: HONEYCOMB, FIBERGLASS FACES

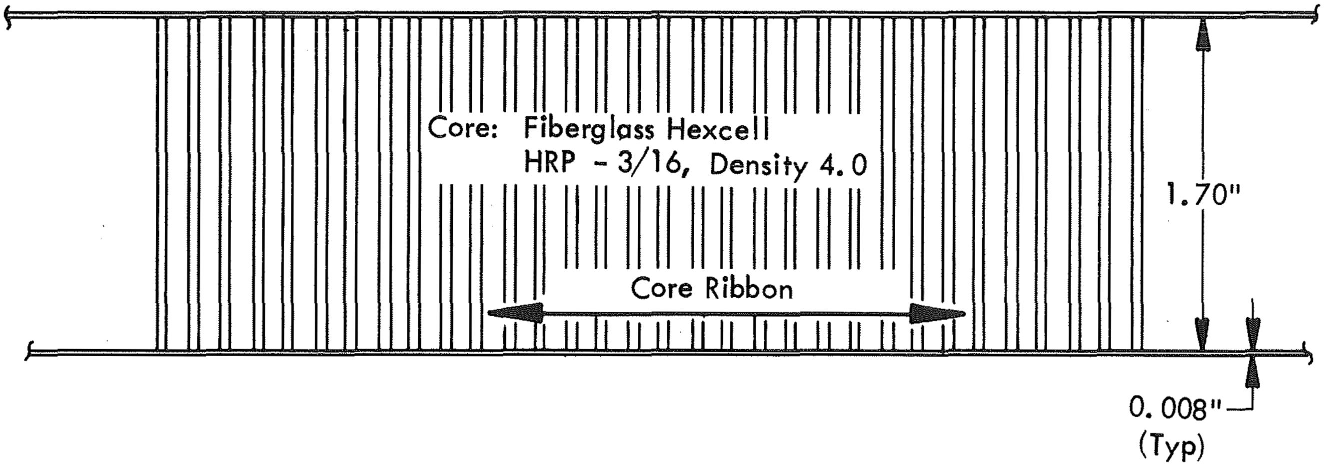

Applied Ult. Load	Compression	= 878.06 Lbs/In
	Shear	= 338.00 " "

Eff. Area = .0458 In^2/In, Weight = .0073 Lbs/In Circum & Length

Applied Ult Compression Stress	=	54,879 Lbs/In^2
Allowable Compression Buckling Stress	=	59,641 " "
Allowable Compression Intracell Buckling Stress	=	59,711 " "
Allowable Compression Face Wrinkling Stress	=	201,240 " "
Allowable Compression Shear Crimping Stress	=	1,211,925 " "

Figure 16: HONEYCOMB, TITANIUM FACES

CONSTRUCTION	FIBERGLASS				TITANIUM			
	EQUIV. AREA / INCH-CIRCUM (IN^2/IN)	WEIGHT / INCH-CIRCUM & INCH-LENGTH (LBS/IN^2)	HEAT FLOW / INCH-CIRCUM & INCH-LENGTH (BTU/HR)	WEIGHT HEAT FLOW PRODUCT $\times 10^{-3}$	EQUIV. AREA / INCH-CIRCUM (IN^2/IN)	WEIGHT / INCH-CIRCUM & INCH-LENGTH (LBS/IN^2)	HEAT FLOW / INCH-CIRCUM & INCH LENGTH (BTU/HR)	WEIGHT HEAT FLOW PRODUCT $\times 10^{-3}$
CORRUGATION	.092	.0061	.60	3.7	.041	.0066	4.96	32.7
HONEYCOMB	.111	.0073	.48	3.5	.046	.0073	2.09	15.3
HAT STIFFENER	.140	.0092	.91	8.4	.073	.0116	8.75	101.5
ZEE STIFFENER	.168	.0111	1.09	12.1	.086	.0137	10.31	141.5
BAR STIFFENER	.176	.0116	1.15	13.4	.074	.0119	8.87	105.5

Heat Flow Values Assume That Part is Sufficiently Long to Yield Equilibrium Temperatures of $-423°$ F and $-80°$ F at Cold and Warm Ends Respectively and Heat Flow is One Dimensional Without Insulation Interaction.

Load Nc = 851 LBS/IN

Titanium Mean Thermal Conductivity = 0.24 $\frac{BTU - IN}{IN^2 - HR - °F}$

Fiberglass Mean Thermal Conductivity = 0.013 "

Figure 17: WEIGHT - HEAT FLOW RESULTS

Fiberglass honeycomb sandwich was the best choice of materials in this comparison chart with fiberglass corrugations a close second choice. The most promising titanium construction method yielded a heat flow 4 times greater for approximately equivalent weight.

Figure 18 shows weight trends for various construction methods as the compression loading was increased. The figure shows that the zee and bar stiffened panels were the heaviest. This was due largely to the conservative torsional instability analysis employed. The titanium zee was less efficient than the fiberglass zee because of the same lack of torsional stiffness in thin gages. The other forms of construction were not subject to this mode of failure. The requirements of (1) critical local shear stability of the skin, and (2) stiffener moment of inertia for modes of general instability in shear, showed major effects on all the stiffened types of construction. These effects gave fiberglass a weight advantage over titanium because local shear buckling of the skin is a function of ET^2 in the elastic range, e.g., for the equal weight stiffeners of fiberglass and titanium shown in the sketch below, the moment of inertia of the fiberglass is greatest as is ET^2.

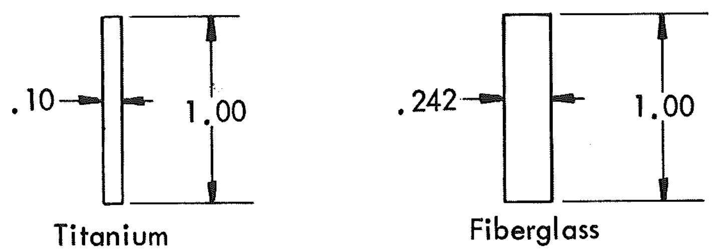

$$ET^2 \text{ (fiberglass)} = 3.0 \times 10^6 \, (.242)^2 = 17.6 \times 10^4$$

$$ET^2 \text{ (titanium)} = 16.4 \times 10^6 \, (.10)^2 = 16.4 \times 10^4$$

For the honeycomb sandwich analysis, the fiberglass face skins were restricted to .009 inches or increments thereof, while the titanium skins were allowed to vary in increments of .001 inch. This caused the cross over of the weight curves. The corrugated construction did not employ any gage limitations and is more indicative of actual material capabilities, i.e., fiberglass has weight advantages for lower loads and titanium for higher loads.

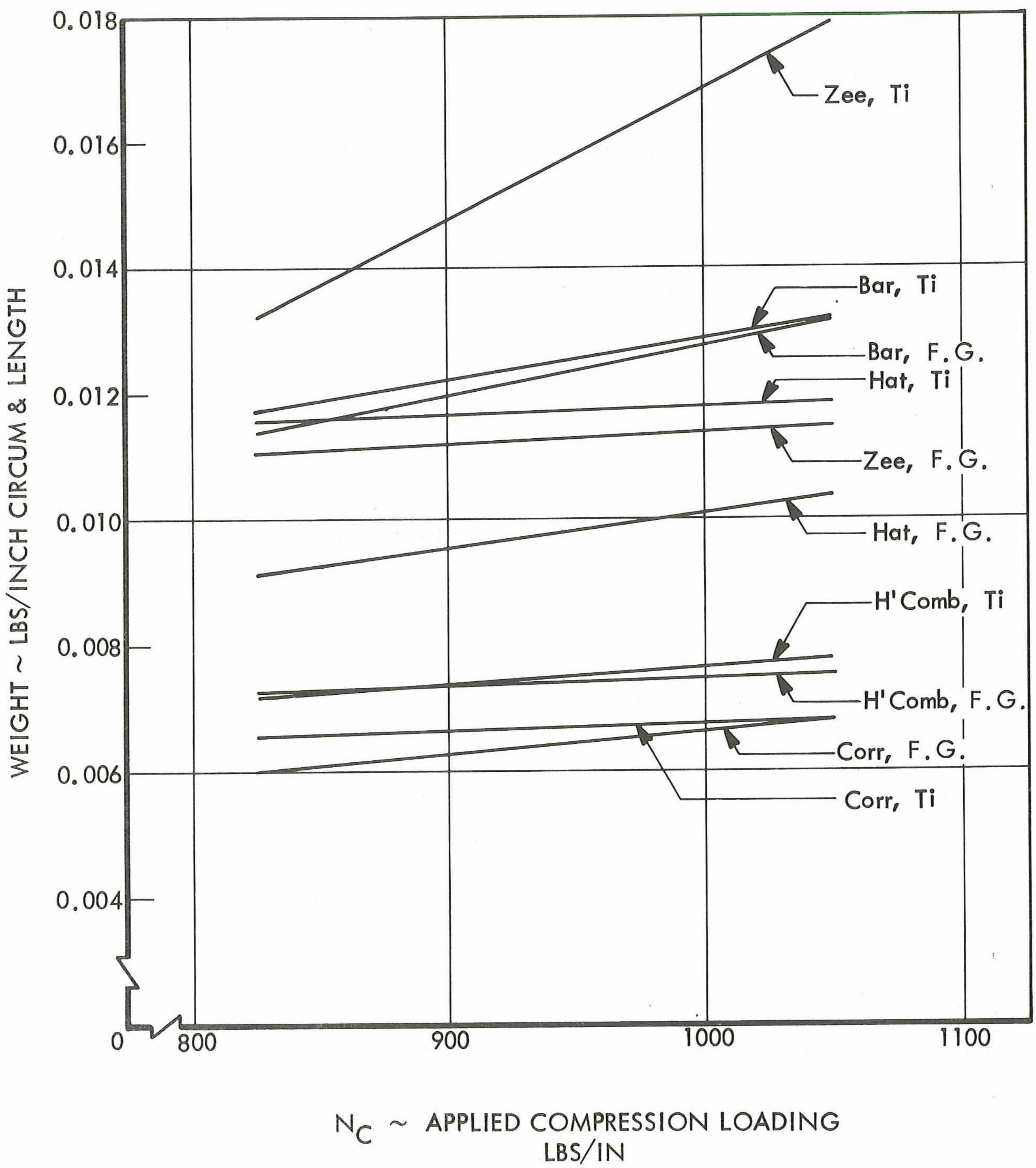

Figure 18: WEIGHT TRENDS

3.5 STRUCTURAL CONCEPT DESIGNS

Detail designs were developed for each structural concept studied. The designs were prepared and analyzed in sufficient detail to allow realistic weight estimation. The designs are presented in Figure 19 through 26.

It was assumed that the cone would become a semi-permanent part of the tank assembly and, therefore, blind fasteners could be used in limited access areas such as the cone to tank joint. However, it was believed necessary to maintain disassembly capability at the forward attachment to stage structure.

The skin stiffened designs of Figures 24, 25, and 26 all involved the use of somewhat complex end attachment fittings. The fittings were necessary to assure a uniform stress distribution across skin and stiffener, which was assumed to be the case in the computer structural optimization studies. The method of fabricating the bar stiffened titanium construction was not explored in detail and instead the welded concept proposed by other investigators was assumed. The welded configuration may in reality be difficult to manufacture and maintain straightness in the thin gages.

The corrugated designs show two approaches to end attachment. The inner and outer ring designs of Figures 19 and 21 require that the load concentration at the fasteners be dissipated into all surfaces of the corrugation. An improvement of this approach is shown in Figures 20 and 22 where all surfaces of the corrugation are attached providing a more uniform load transfer across the joint. This latter configuration requires fabrication of a large quantity of complex plates.

The honeycomb sandwich with the "in plane" attachment leg provides the simplest attachment scheme since complex formed metal parts are eliminated. This concept can also be manufactured in a minimum number of segments because the bonded structure is lightweight and rigid providing ease of handling for subsequent assembly stages.

An analysis of thermal stresses was made. The approach taken was to consider the area ratios of "hot" and "cold" members, A_h and A_c. These ratios, in conjunction

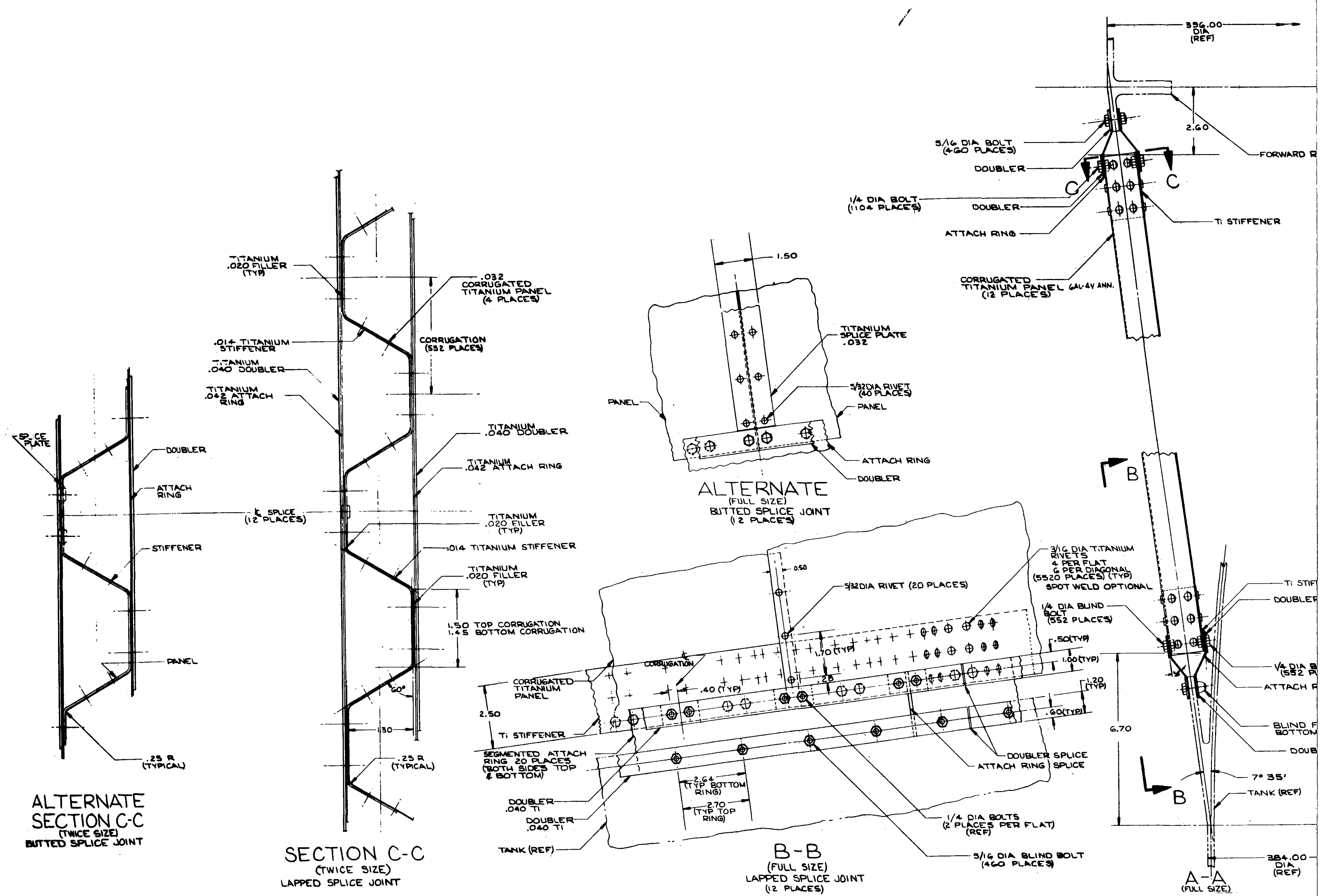

SPLICE PLATE
DOUBLER
ATTACH RING
℄ SPLICE (12 PLACES)
STIFFENER
PANEL
.25 R (TYPICAL)
ALTERNATE SECTION C-C
(TWICE SIZE)
BUTTED SPLICE JOINT
TITANIUM .020 FILLER (TYP)
.032 CORRUGATED TITANIUM PANEL (4 PLACES)
.014 TITANIUM STIFFENER
TITANIUM .040 DOUBLER
TITANIUM .042 ATTACH RING
CORRUGATION (552 PLACES)
TITANIUM .040 DOUBLER
TITANIUM .042 ATTACH RING
TITANIUM .020 FILLER (TYP)
.014 TITANIUM STIFFENER
TITANIUM .020 FILLER (TYP)
1.50 TOP CORRUGATION
1.45 BOTTOM CORRUGATION
60°
1.30
.25 R (TYPICAL)
SECTION C-C
(TWICE SIZE)
LAPPED SPLICE JOINT
1.50
TITANIUM SPLICE PLATE .032
5/32 DIA RIVET (40 PLACES)
PANEL
PANEL
ATTACH RING
DOUBLER
ALTERNATE
(FULL SIZE)
BUTTED SPLICE JOINT
(12 PLACES)
.50
5/32 DIA RIVET (20 PLACES)
3/16 DIA TITANIUM RIVETS
4 PER FLAT
6 PER DIAGONAL
(5520 PLACES) (TYP)
SPOT WELD OPTIONAL
1.70 (TYP)
.28
℄ CORRUGATION
.40 (TYP)
CORRUGATED TITANIUM PANEL
2.50
Ti STIFFENER
SEGMENTED ATTACH RING 20 PLACES (BOTH SIDES TOP & BOTTOM)
DOUBLER .040 Ti
DOUBLER .040 Ti
TANK (REF)
2.64 (TYP BOTTOM RING)
2.70 (TYP TOP RING)
.50 (TYP)
1.00 (TYP)
1.20 (TYP)
.60 (TYP)
DOUBLER SPLICE
ATTACH RING SPLICE
1/4 DIA BOLTS (2 PLACES PER FLAT) (REF)
5/16 DIA BLIND BOLT (460 PLACES)
B-B
(FULL SIZE)
LAPPED SPLICE JOINT
(12 PLACES)
396.00 DIA (REF)
2.60
FORWARD R
5/16 DIA BOLT (460 PLACES)
DOUBLER
C
C
1/4 DIA BOLT (1104 PLACES)
DOUBLER
Ti STIFFENER
ATTACH RING
CORRUGATED TITANIUM PANEL 6Al-4V ANN. (12 PLACES)
B
B
1/4 DIA BLIND BOLT (552 PLACES)
Ti STIF
DOUBLER
ATTACH R
BLIND F BOTTOM
DOUB
6.70
7° 35'
TANK (REF)
384.00 DIA (REF)
A-A
(FULL SIZE)

2

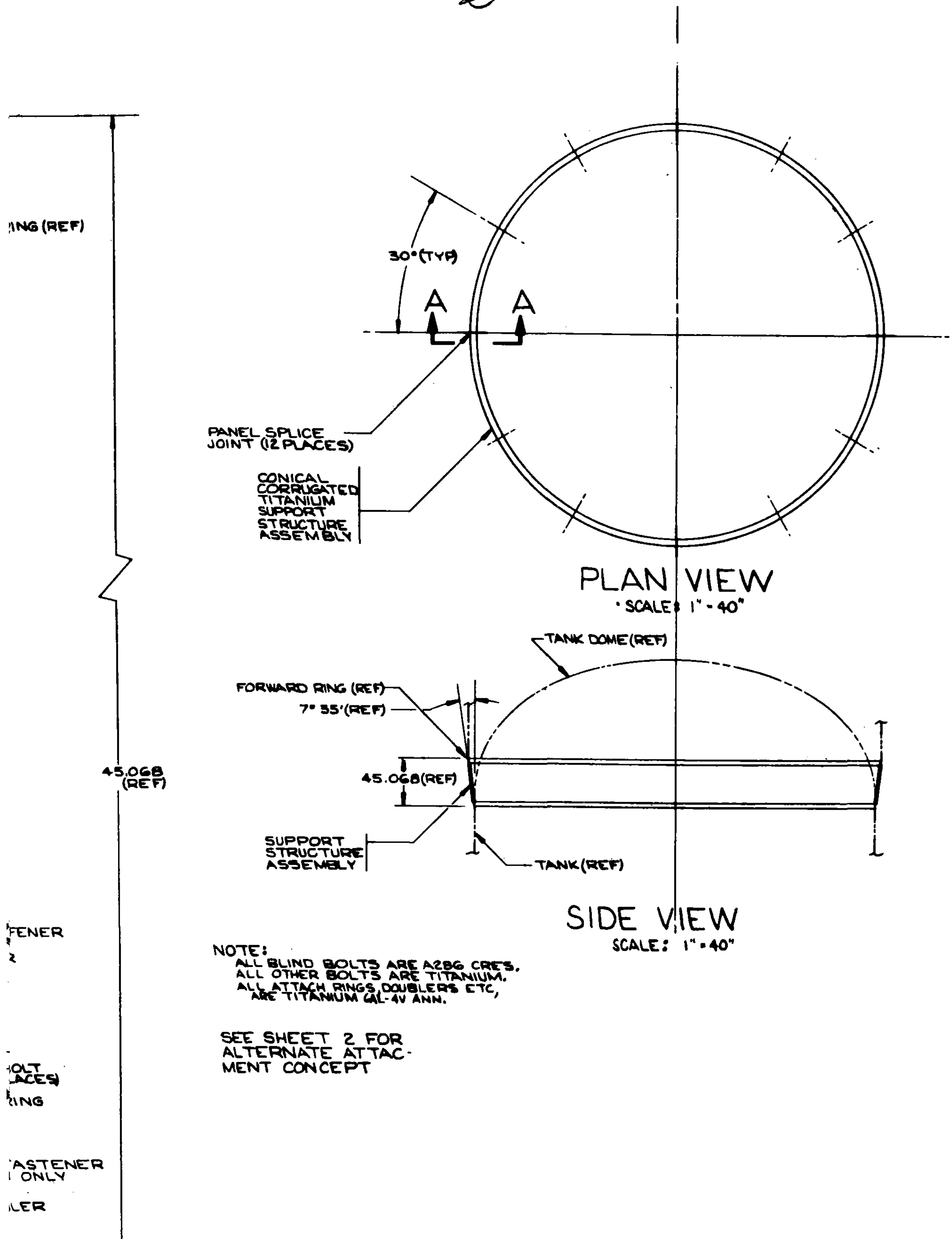

Figure 19: CORRUGATED TITANIUM CRYOGENIC TANK SUPPORT
Dwg No. SK 11-043081
Sht 1 of 2

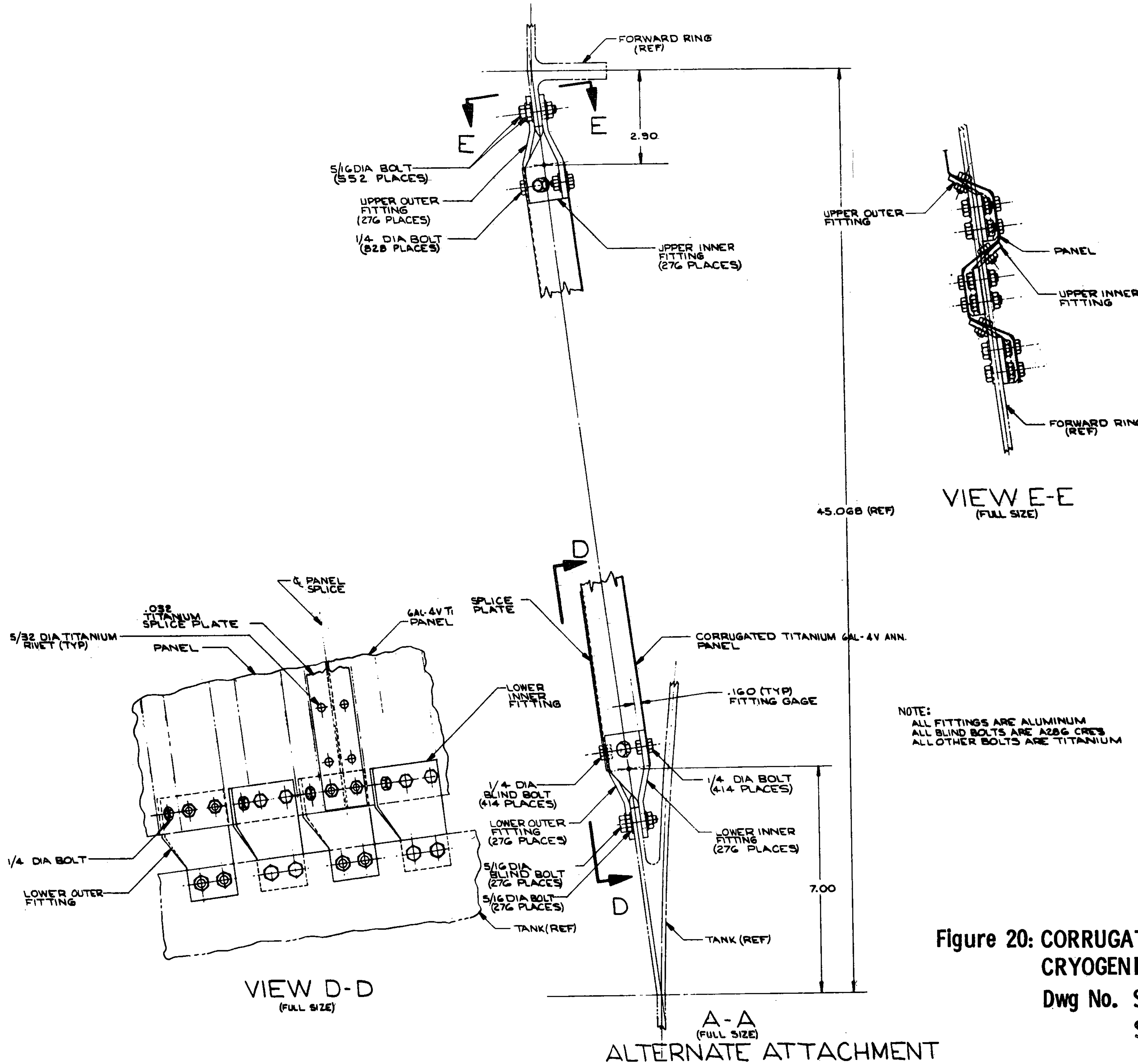

Figure 20: CORRUGATED TITANIUM CRYOGENIC TANK SUPPORT
Dwg No. SK 11-043081
Sht 2 of 2

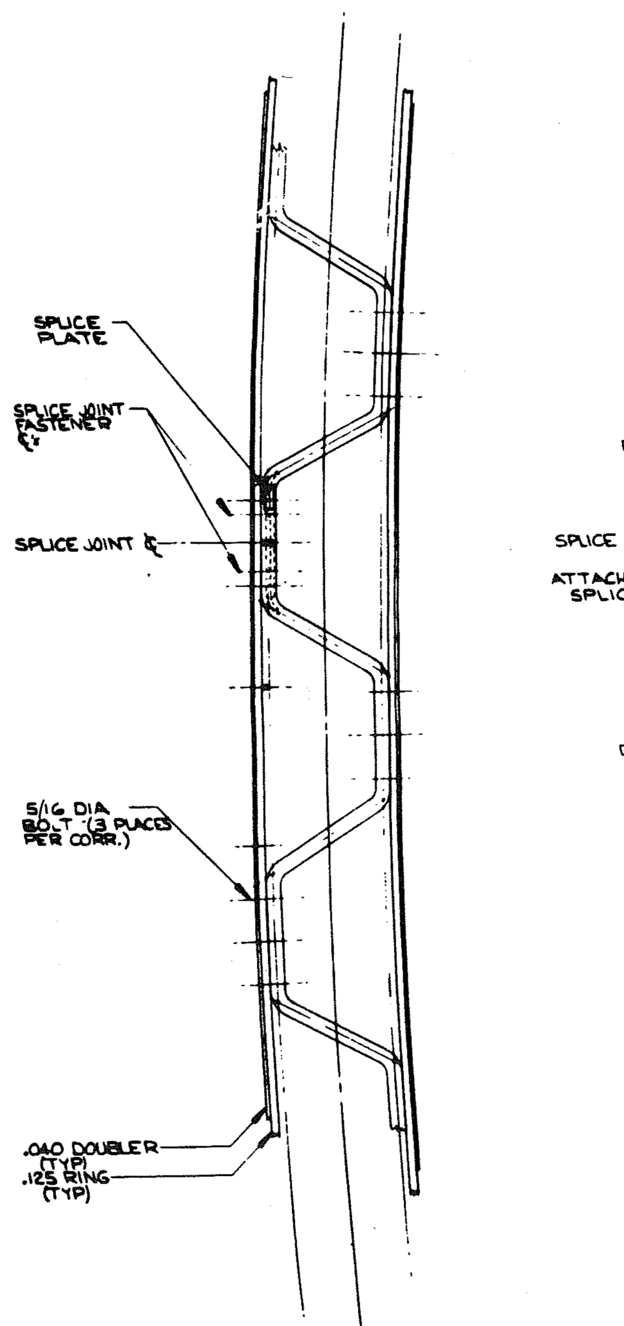

ALTERNATE VIEW C-C
(FULL SIZE)
BUTTED SPLICE JOINT
(NO FILLERS REQD)

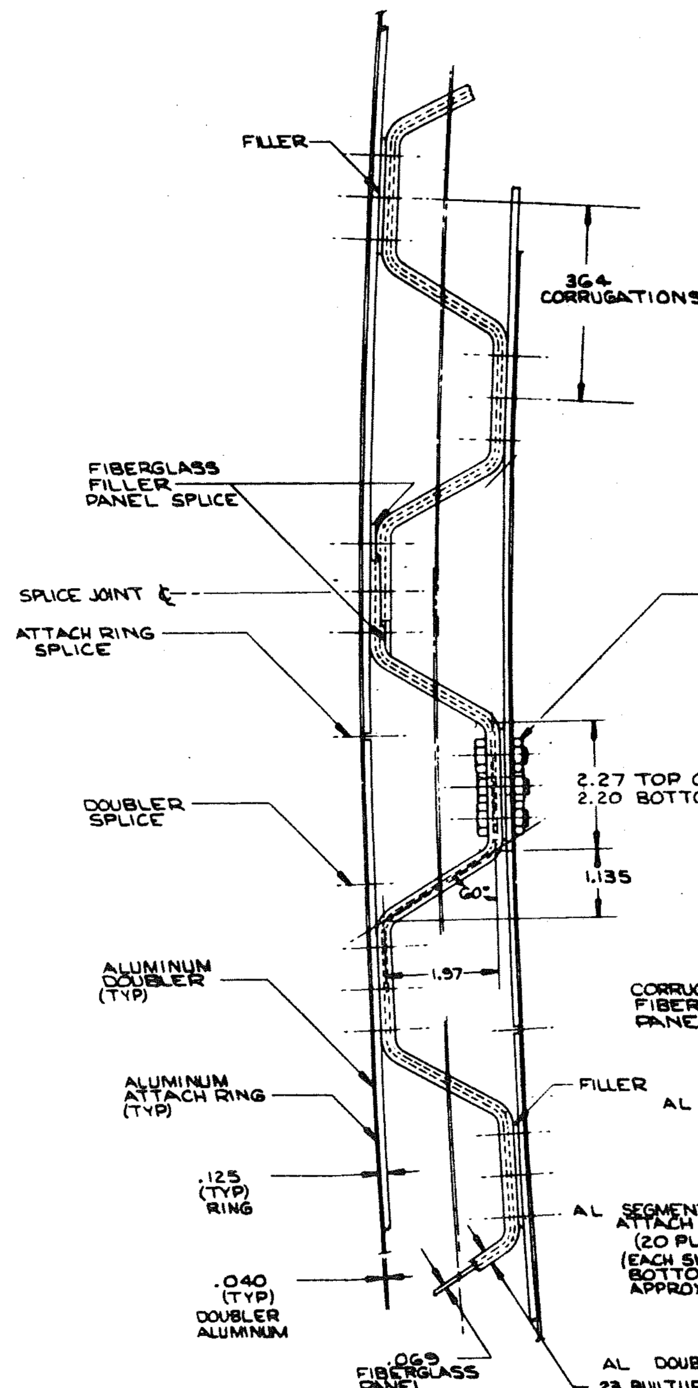

VIEW C-C
(FULL SIZE)
LAPPED SPLICE JOINT

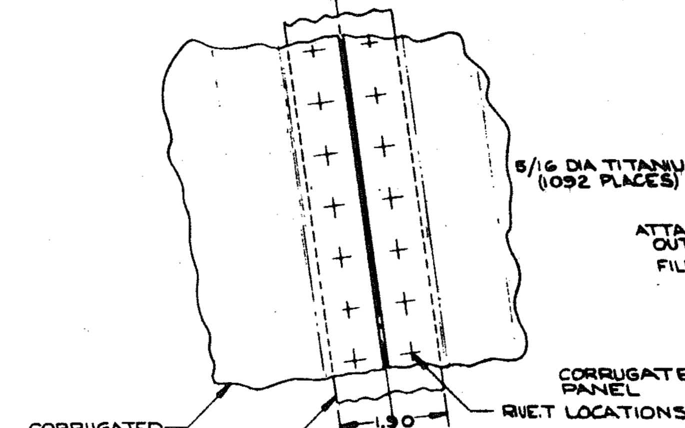

ALTERNATE
BUTTED SPLICE JOINT

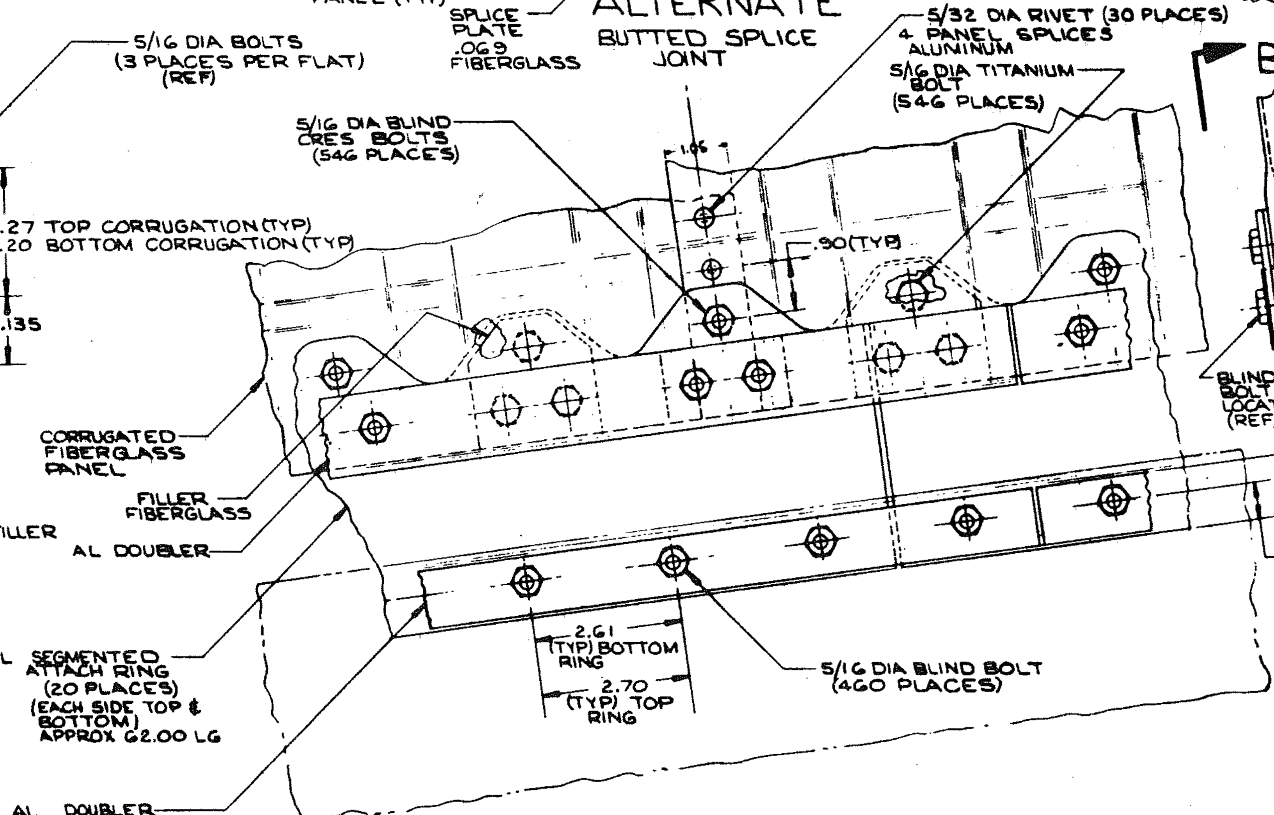

VIEW B-B
(FULL SIZE)
LAPPED SPLICE JOINT

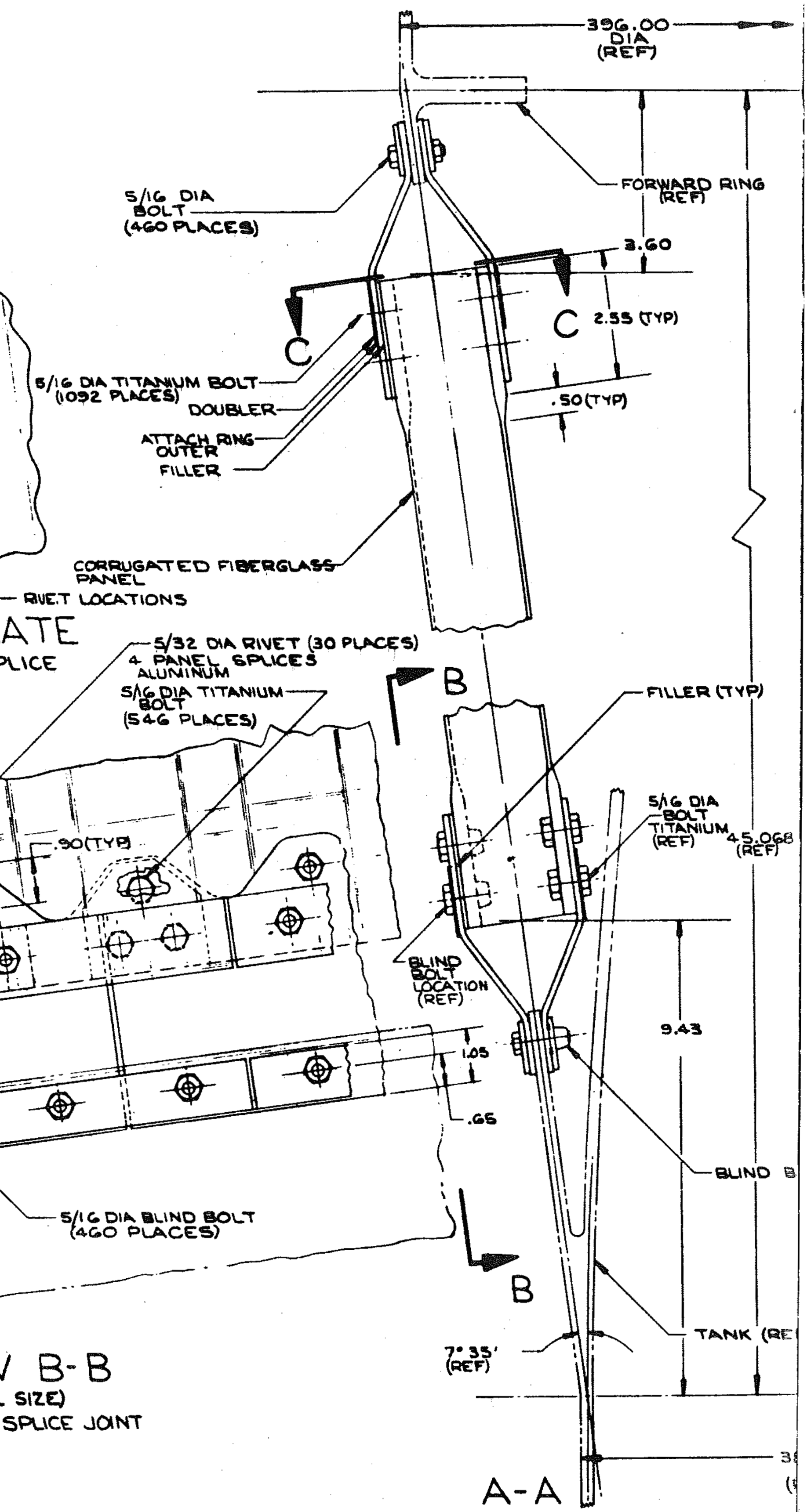

A-A
(FULL SIZE)

2

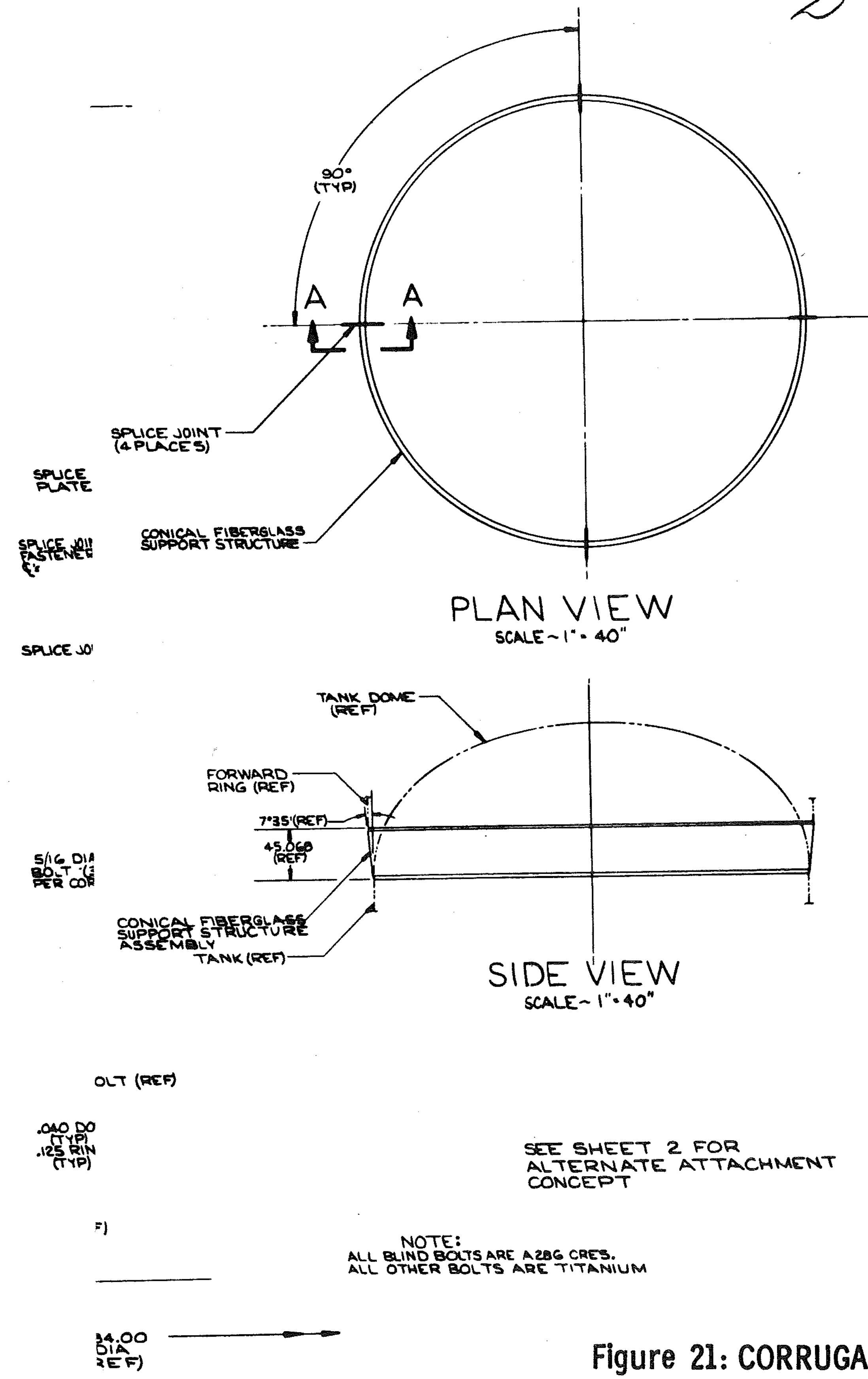

Figure 21: CORRUGATED FIBERGLASS CRYOGENIC TANK SUPPORT
Dwg No. SK 11-043080
Sht 1 of 2

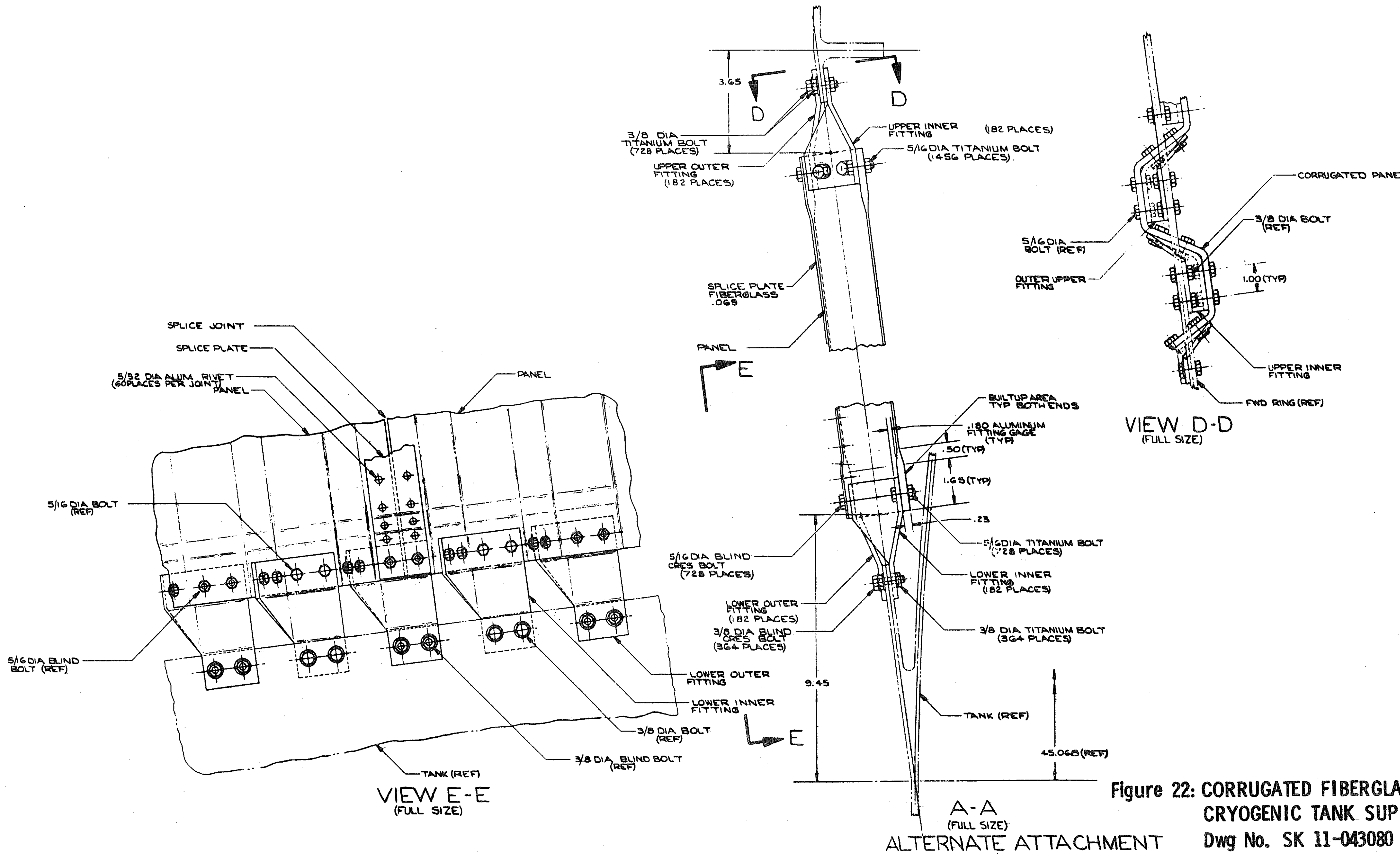

Figure 22: CORRUGATED FIBERGLASS CRYOGENIC TANK SUPPO
Dwg No. SK 11-043080
Sht 2 of 2

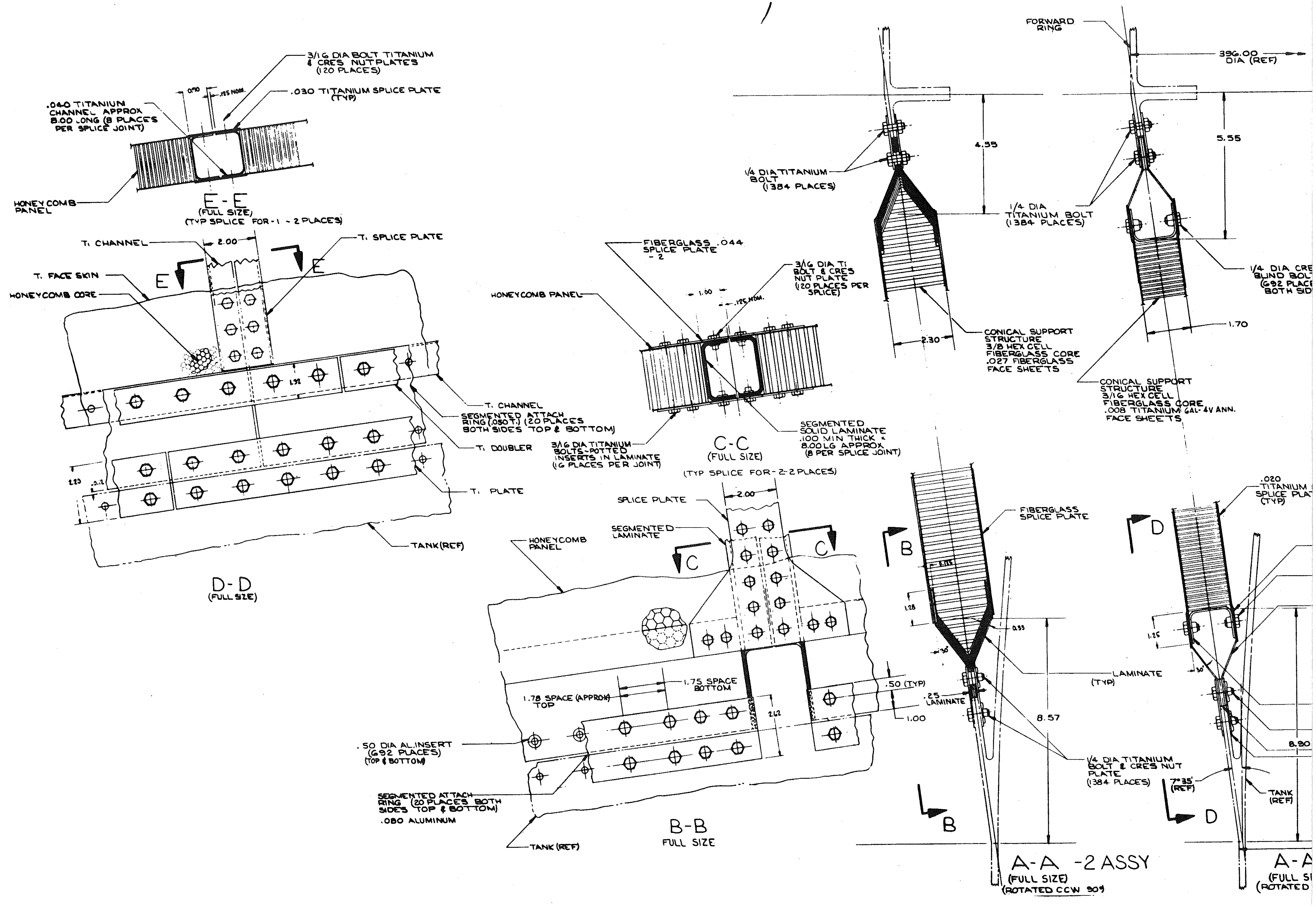
3/16 DIA BOLT TITANIUM & CRES NUTPLATES (120 PLACES)
.030 TITANIUM SPLICE PLATE (TYP)
.040 TITANIUM CHANNEL APPROX 8.00 LONG (8 PLACES PER SPLICE JOINT)
HONEYCOMB PANEL
E-E
(FULL SIZE)
(TYP SPLICE FOR -1 - 2 PLACES)
Ti CHANNEL
2.00
Ti SPLICE PLATE
Ti FACE SKIN
HONEYCOMB CORE
E
Ti CHANNEL
SEGMENTED ATTACH RING (.050 T.) (20 PLACES BOTH SIDES TOP & BOTTOM)
Ti DOUBLER
Ti PLATE
TANK (REF)
D-D
(FULL SIZE)
FIBERGLASS .044 SPLICE PLATE -2
3/16 DIA Ti BOLT & CRES NUT PLATE (120 PLACES PER SPLICE)
HONEYCOMB PANEL
1.00
.125 NOM.
SEGMENTED SOLID LAMINATE .100 MIN THICK x 8.00 LG APPROX (8 PER SPLICE JOINT)
3/16 DIA TITANIUM BOLTS-POTTED INSERTS IN LAMINATE (16 PLACES PER JOINT)
C-C
(FULL SIZE)
(TYP SPLICE FOR -2 - 2 PLACES)
SPLICE PLATE
SEGMENTED LAMINATE
HONEYCOMB PANEL
C
1.75 SPACE BOTTOM
1.78 SPACE (APPROX) TOP
.50 (TYP)
.25 LAMINATE
1.00
2.62
.50 DIA AL. INSERT (692 PLACES) (TOP & BOTTOM)
SEGMENTED ATTACH RING (20 PLACES BOTH SIDES TOP & BOTTOM) .080 ALUMINUM
TANK (REF)
B-B
FULL SIZE
FORWARD RING
396.00 DIA (REF)
1/4 DIA TITANIUM BOLT (1384 PLACES)
4.55
5.55
1/4 DIA TITANIUM BOLT (1384 PLACES)
1/4 DIA CRE BLIND BOL (692 PLACE BOTH SID
2.30
1.70
CONICAL SUPPORT STRUCTURE 3/8 HEX CELL FIBERGLASS CORE .027 FIBERGLASS FACE SHEETS
CONICAL SUPPORT STRUCTURE 3/16 HEX CELL FIBERGLASS CORE .008 TITANIUM 6AL-4V ANN. FACE SHEETS
FIBERGLASS SPLICE PLATE
.020 TITANIUM SPLICE PLA (TYP)
B
D
1.28
0.33
1.25
30°
LAMINATE (TYP)
8.57
8.90
1/4 DIA TITANIUM BOLT & CRES NUT PLATE (1384 PLACES)
7°35' (REF)
TANK (REF)
A-A -2 ASSY
(FULL SIZE)
(ROTATED CCW 90°)
A-A
(FULL SI
(ROTATED

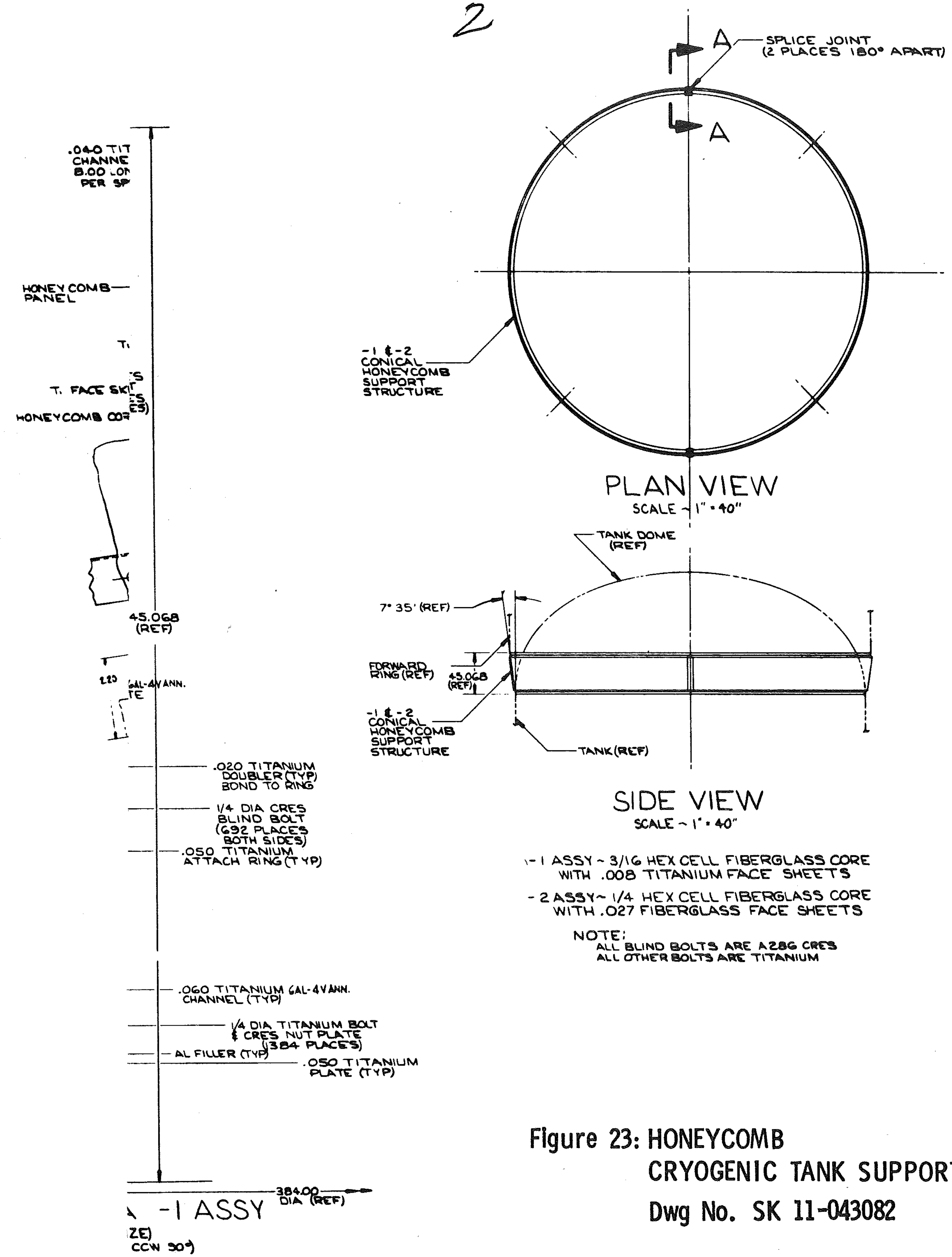

Figure 23: HONEYCOMB CRYOGENIC TANK SUPPORT Dwg No. SK 11-043082

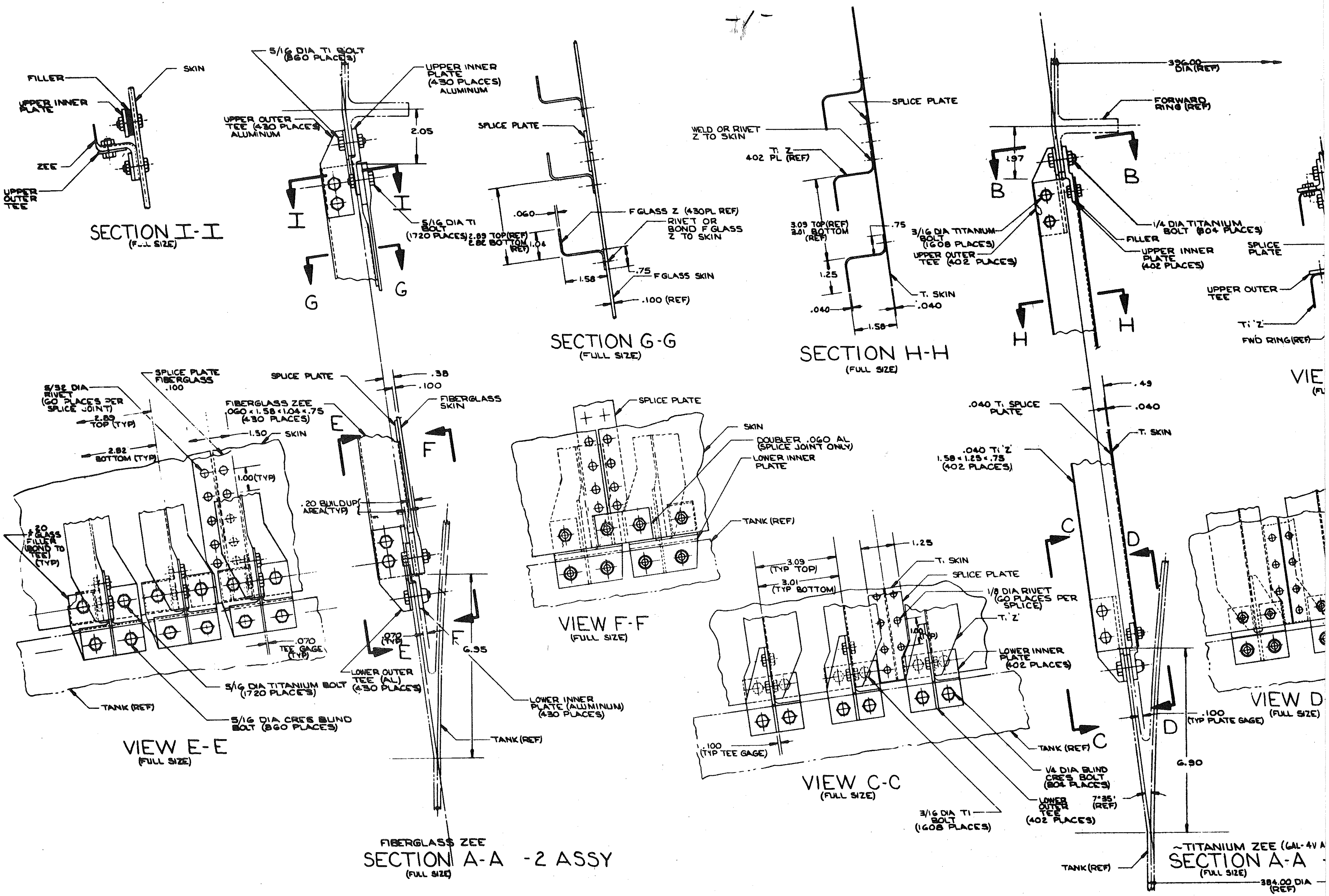

FILLER
SKIN
UPPER INNER PLATE
ZEE
UPPER OUTER TEE
SECTION I-I
(FULL SIZE)
5/16 DIA TI BOLT (860 PLACES)
UPPER INNER PLATE (430 PLACES) ALUMINUM
UPPER OUTER TEE (430 PLACES) ALUMINUM
2.05
5/16 DIA TI BOLT (1720 PLACES)
I
G
SPLICE PLATE
.060
F GLASS Z (430PL REF)
RIVET OR BOND F GLASS Z TO SKIN
2.89 TOP(REF)
2.82 BOTTOM (REF)
1.04
.75
1.58
F GLASS SKIN
.100 (REF)
SECTION G-G
(FULL SIZE)
SPLICE PLATE
WELD OR RIVET Z TO SKIN
Ti Z
402 PL (REF)
3.09 TOP(REF)
3.01 BOTTOM (REF)
.75
1.25
.040
1.58
T. SKIN
.040
SECTION H-H
(FULL SIZE)
396.00 DIA (REF)
FORWARD RING (REF)
1.97
B
3/16 DIA TITANIUM BOLT (1608 PLACES)
UPPER OUTER TEE (402 PLACES)
1/4 DIA TITANIUM BOLT (804 PLACES)
FILLER
UPPER INNER PLATE (402 PLACES)
H
SPLICE PLATE
UPPER OUTER TEE
Ti 'Z'
FWD RING(REF)
VIE
5/32 DIA RIVET (60 PLACES PER SPLICE JOINT)
SPLICE PLATE FIBERGLASS .100
2.89 TOP (TYP)
1.50
SKIN
2.82 BOTTOM (TYP)
1.00(TYP)
.20 F GLASS FILLER (BOND TO TEE) (TYP)
.070 TEE GAGE (TYP)
5/16 DIA TITANIUM BOLT (1720 PLACES)
TANK (REF)
5/16 DIA CRES BLIND BOLT (860 PLACES)
VIEW E-E
(FULL SIZE)
SPLICE PLATE
.38
.100
FIBERGLASS ZEE .060 x 1.58 x 1.04 x .75 (430 PLACES)
FIBERGLASS SKIN
E
F
.20 BUILDUP AREA(TYP)
.070 (TYP)
LOWER OUTER TEE (AL) (430 PLACES)
6.95
LOWER INNER PLATE (ALUMINUM) (430 PLACES)
TANK(REF)
FIBERGLASS ZEE
SECTION A-A -2 ASSY
(FULL SIZE)
SPLICE PLATE
SKIN
DOUBLER .060 AL (SPLICE JOINT ONLY)
LOWER INNER PLATE
TANK (REF)
VIEW F-F
(FULL SIZE)
.49
.040 Ti SPLICE PLATE
.040
T. SKIN
.040 Ti 'Z' 1.58 x 1.25 x .75 (402 PLACES)
C
D
3.09 (TYP TOP)
3.01 (TYP BOTTOM)
1.25
T. SKIN
SPLICE PLATE
1/8 DIA RIVET (60 PLACES PER SPLICE)
T. 'Z'
1.00 (TYP)
LOWER INNER PLATE (402 PLACES)
TANK (REF)
.100 (TYP TEE GAGE)
VIEW C-C
(FULL SIZE)
1/4 DIA BLIND CRES BOLT (804 PLACES)
3/16 DIA TI BOLT (1608 PLACES)
LOWER OUTER TEE (402 PLACES)
7°35' (REF)
.100 (TYP PLATE GAGE)
6.90
VIEW D
(FULL SIZE)
TANK(REF)
~TITANIUM ZEE (6AL-4V A
SECTION A-A
(FULL SIZE)
384.00 DIA (REF)

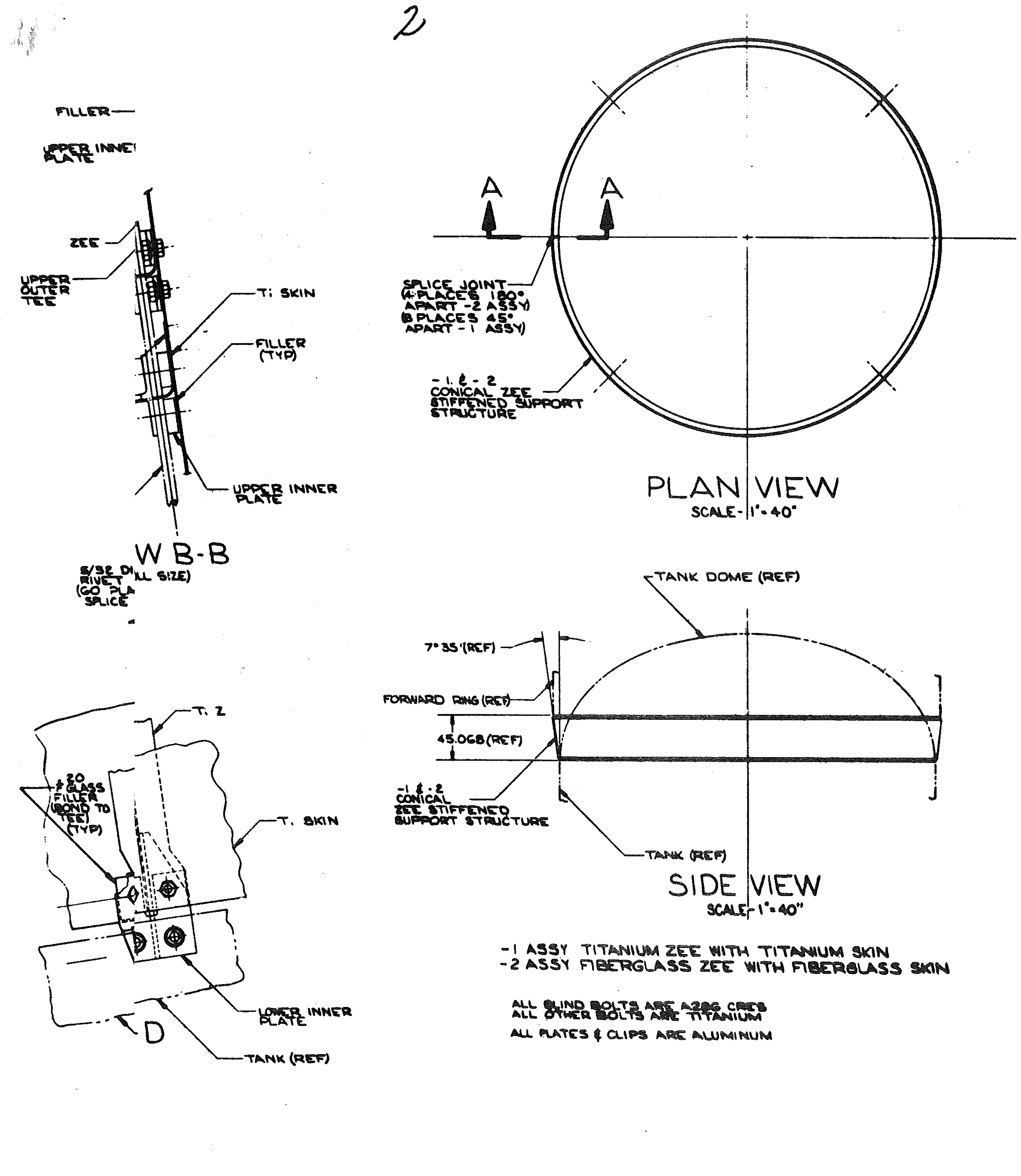

-1 ASSY

Figure 24: ZEE STIFFENED CRYOGENIC TANK SUPPORT Dwg No. SK 11-043084

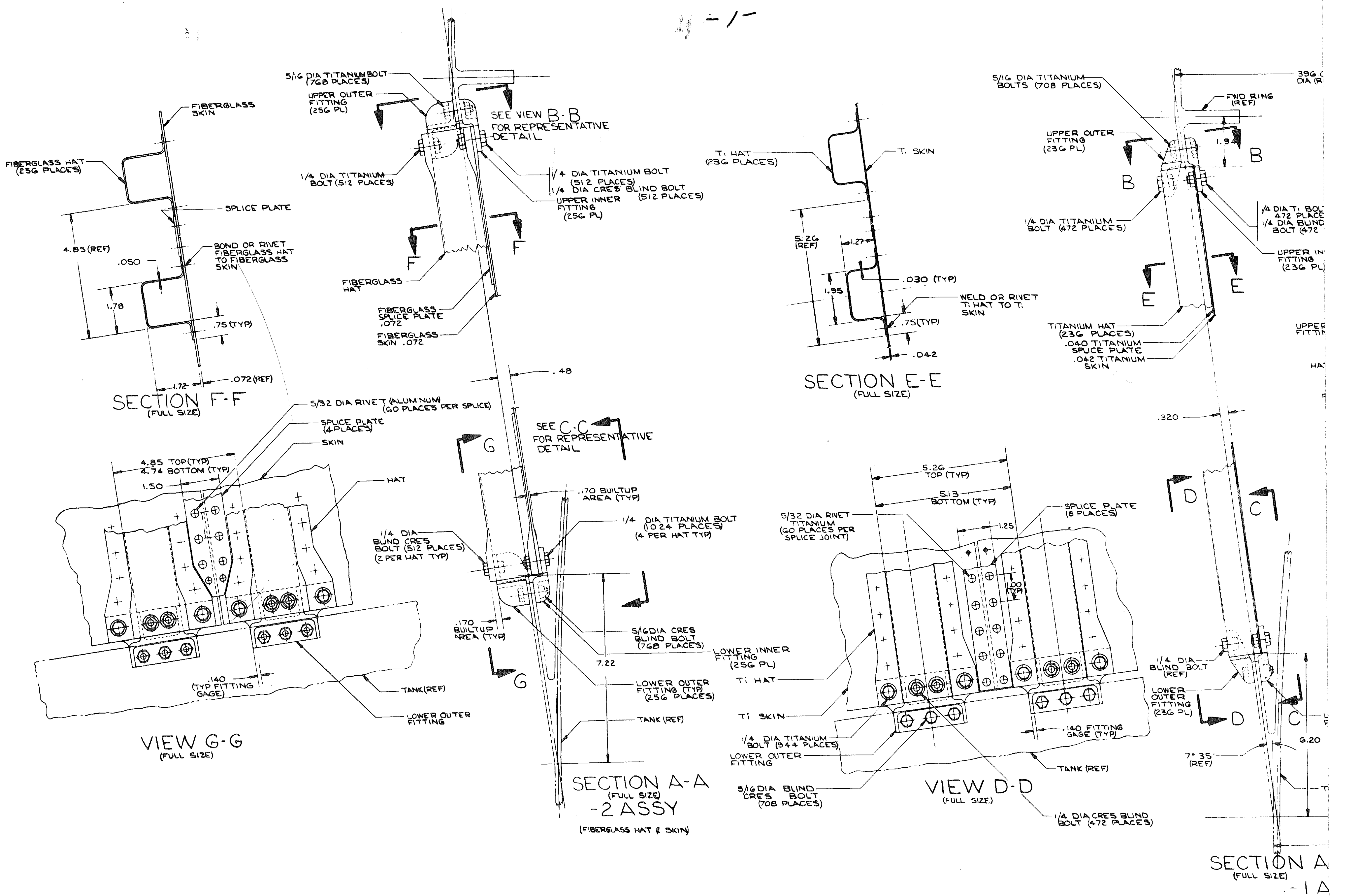
-1-
FIBERGLASS SKIN
FIBERGLASS HAT (256 PLACES)
SPLICE PLATE
4.85 (REF)
.050
BOND OR RIVET FIBERGLASS HAT TO FIBERGLASS SKIN
1.78
.75 (TYP)
1.72
.072 (REF)
SECTION F-F
(FULL SIZE)
5/16 DIA TITANIUM BOLT (768 PLACES)
UPPER OUTER FITTING (256 PL)
SEE VIEW B-B FOR REPRESENTATIVE DETAIL
1/4 DIA TITANIUM BOLT (512 PLACES)
1/4 DIA TITANIUM BOLT (512 PLACES)
1/4 DIA CRES BLIND BOLT (512 PLACES)
UPPER INNER FITTING (256 PL)
FIBERGLASS HAT
FIBERGLASS SPLICE PLATE .072
FIBERGLASS SKIN .072
.48
5/32 DIA RIVET (ALUMINUM) (60 PLACES PER SPLICE)
SPLICE PLATE (4 PLACES)
SKIN
HAT
4.85 TOP (TYP)
4.74 BOTTOM (TYP)
1.50
.140 (TYP FITTING GAGE)
TANK (REF)
LOWER OUTER FITTING
VIEW G-G
(FULL SIZE)
SEE C-C FOR REPRESENTATIVE DETAIL
.170 BUILTUP AREA (TYP)
1/4 DIA TITANIUM BOLT (1024 PLACES) (4 PER HAT TYP)
1/4 DIA BLIND CRES BOLT (512 PLACES) (2 PER HAT TYP)
.170 BUILTUP AREA (TYP)
5/16 DIA CRES BLIND BOLT (768 PLACES)
LOWER INNER FITTING (256 PL)
7.22
LOWER OUTER FITTING (TYP) (256 PLACES)
TANK (REF)
SECTION A-A
(FULL SIZE)
-2 ASSY
(FIBERGLASS HAT & SKIN)
Ti HAT (236 PLACES)
Ti SKIN
5.26 (REF)
1.27
1.95
.030 (TYP)
WELD OR RIVET Ti HAT TO Ti SKIN
.75 (TYP)
.042
SECTION E-E
(FULL SIZE)
5.26 TOP (TYP)
5.13 BOTTOM (TYP)
1.25
5/32 DIA RIVET TITANIUM (60 PLACES PER SPLICE JOINT)
SPLICE PLATE (8 PLACES)
1.00 (TYP)
Ti HAT
Ti SKIN
1/4 DIA TITANIUM BOLT (944 PLACES)
LOWER OUTER FITTING
5/16 DIA BLIND CRES BOLT (708 PLACES)
.140 FITTING GAGE (TYP)
TANK (REF)
VIEW D-D
(FULL SIZE)
1/4 DIA CRES BLIND BOLT (472 PLACES)
5/16 DIA TITANIUM BOLTS (708 PLACES)
UPPER OUTER FITTING (236 PL)
FWD RING (REF)
1.94
1/4 DIA TITANIUM BOLT (472 PLACES)
1/4 DIA Ti BOL 472 PLACE
1/4 DIA BLIND BOLT (472
UPPER IN FITTING (236 PL)
TITANIUM HAT (236 PLACES)
.040 TITANIUM SPLICE PLATE
.042 TITANIUM SKIN
.320
1/4 DIA BLIND BOLT (REF)
LOWER OUTER FITTING (236 PL)
7° 35' (REF)
6.20
SECTION A
(FULL SIZE)
-1 A

-2-

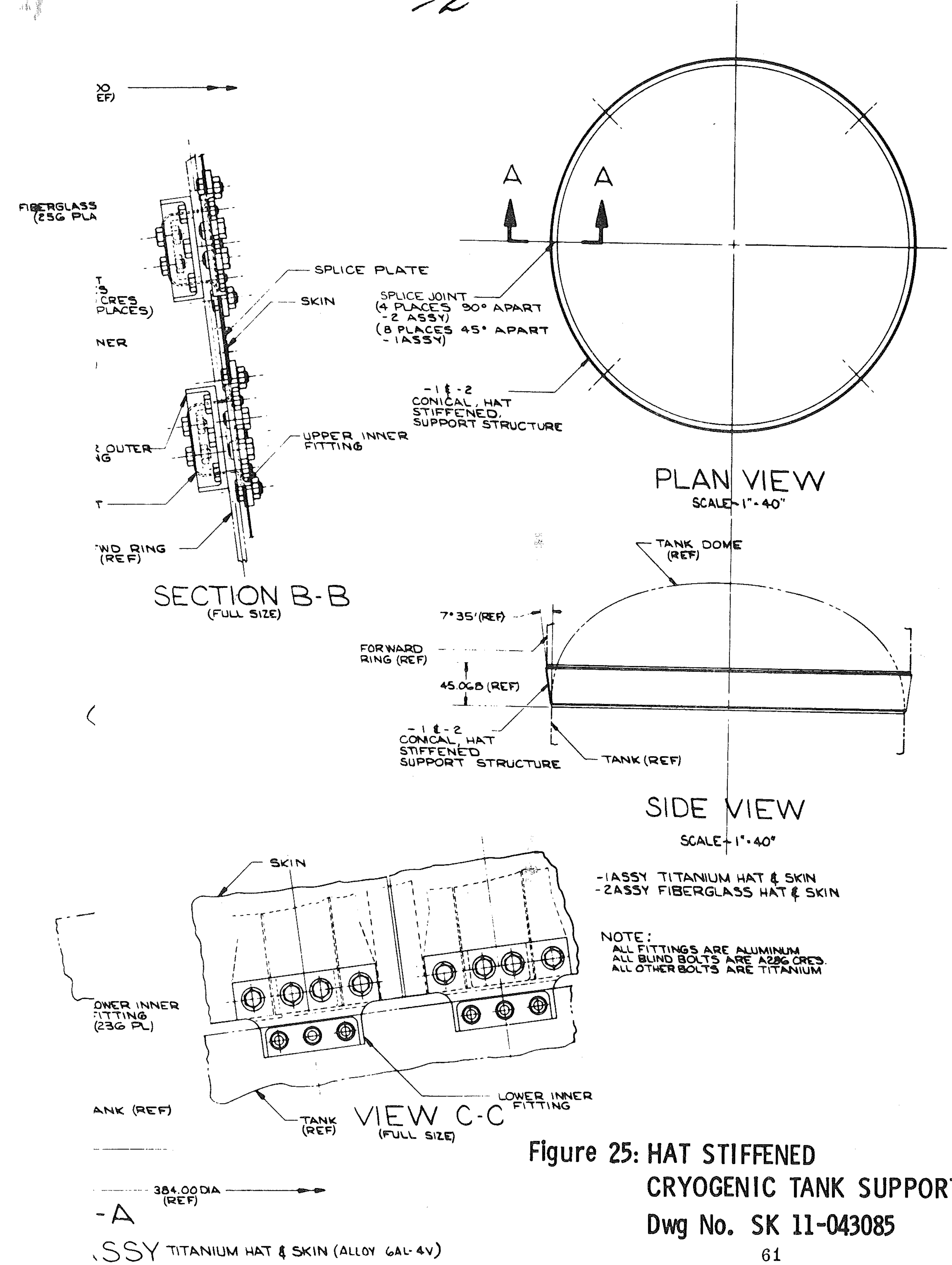

Figure 25: HAT STIFFENED CRYOGENIC TANK SUPPORT
Dwg No. SK 11-043085

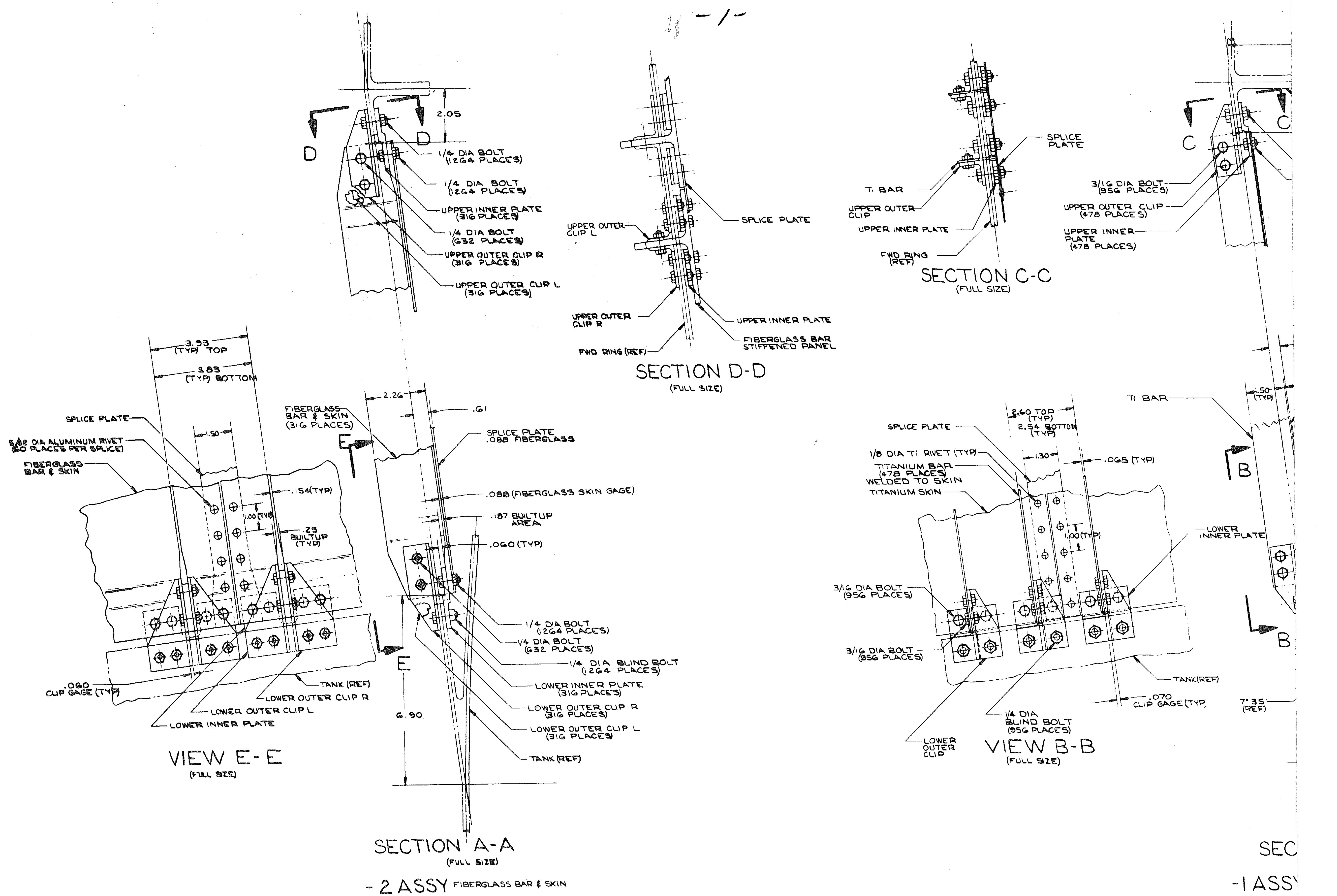
-1-
2.05
D
D
1/4 DIA BOLT (1264 PLACES)
1/4 DIA BOLT (1264 PLACES)
UPPER INNER PLATE (316 PLACES)
1/4 DIA BOLT (632 PLACES)
UPPER OUTER CLIP R (316 PLACES)
UPPER OUTER CLIP L (316 PLACES)
UPPER OUTER CLIP L
SPLICE PLATE
UPPER OUTER CLIP R
UPPER INNER PLATE
FWD RING (REF)
FIBERGLASS BAR STIFFENED PANEL
SECTION D-D
(FULL SIZE)
SPLICE PLATE
Ti BAR
UPPER OUTER CLIP
UPPER INNER PLATE
FWD RING (REF)
SECTION C-C
(FULL SIZE)
C
C
3/16 DIA BOLT (956 PLACES)
UPPER OUTER CLIP (478 PLACES)
UPPER INNER PLATE (478 PLACES)
3.93 (TYP) TOP
3.83 (TYP) BOTTOM
SPLICE PLATE
5/32 DIA ALUMINUM RIVET (60 PLACES PER SPLICE)
FIBERGLASS BAR & SKIN
1.50
.154 (TYP)
1.00 (TYP)
.25 BUILTUP (TYP)
.060 CLIP GAGE (TYP)
TANK (REF)
LOWER OUTER CLIP R
LOWER OUTER CLIP L
LOWER INNER PLATE
VIEW E-E
(FULL SIZE)
2.26
.61
FIBERGLASS BAR & SKIN (316 PLACES)
E
SPLICE PLATE .088 FIBERGLASS
.088 (FIBERGLASS SKIN GAGE)
.187 BUILTUP AREA
.060 (TYP)
1/4 DIA BOLT (1264 PLACES)
1/4 DIA BOLT (632 PLACES)
1/4 DIA BLIND BOLT (1264 PLACES)
LOWER INNER PLATE (316 PLACES)
LOWER OUTER CLIP R (316 PLACES)
LOWER OUTER CLIP L (316 PLACES)
E
6.90
TANK (REF)
SECTION A-A
(FULL SIZE)
-2 ASSY FIBERGLASS BAR & SKIN
Ti BAR
SPLICE PLATE
2.60 TOP (TYP)
2.54 BOTTOM (TYP)
1/8 DIA Ti RIVET (TYP)
TITANIUM BAR (478 PLACES) WELDED TO SKIN
TITANIUM SKIN
1.30
.065 (TYP)
1.00 (TYP)
LOWER INNER PLATE
1.50 (TYP)
B
B
3/16 DIA BOLT (956 PLACES)
3/16 DIA BOLT (956 PLACES)
TANK (REF)
.070 CLIP GAGE (TYP)
1/4 DIA BLIND BOLT (956 PLACES)
LOWER OUTER CLIP
VIEW B-B
(FULL SIZE)
7.35 (REF)
SEC
-1 ASSY

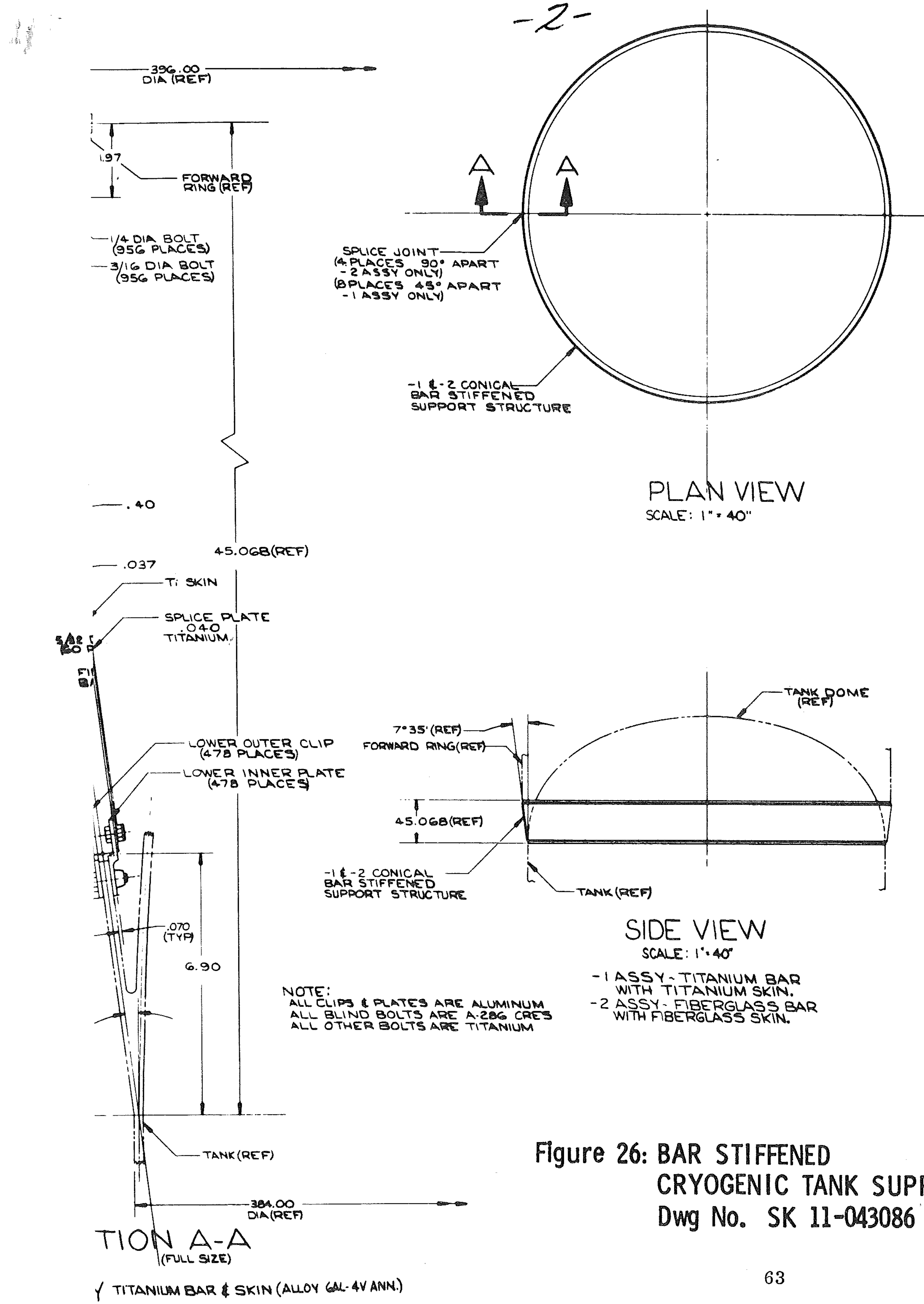

Figure 26: BAR STIFFENED CRYOGENIC TANK SUPPORT Dwg No. SK 11-043086

with Young's modulus, E, and coefficient of expansion α , were used for preliminary evaluations of material and material combinations under thermal gradients. The approach is illustrated in Figure 27. The ordinate is the stress in an element at -423°F. The abscissa is the stress in an element at 70°F. An initial temperature of 70°F was assumed for both elements. The values of thermal stress were determined by the equations:

$$\sigma_{T_c} = - \frac{E_c \left[\alpha_c \; \Delta T_c - \alpha_h \; \Delta T_h \right]}{\dfrac{E_c \; A_c}{E_h \; A_h} + 1}$$

$$\sigma_{T_h} = - \frac{E_h \left[\alpha_h \; \Delta T_h - \alpha_c \; \Delta T_c \right]}{\dfrac{E_h \; A_h}{E_c \; A_c} + 1}$$

where T_h and T_c represent temperatures of hot and cold members respectively.

Various values of the ratio A_c/A_h were calculated and plotted so that the stresses at any area ratio could be read for both hot and cold members.

From this figure, the materials and combinations of material which alleviated the effects of thermal gradients could be determined. It is important to note that not only the magnitude of the thermal stress was important, but also the slope of the line for the designated materials. For this study the adjoining members, i.e., the cone support and tank "y" ring were assumed to be at opposite temperature extremes. Selecting the most critical condition for the cone, where $A_c/A_h = \infty$, it can be seen that the titanium cone would incur significantly higher stresses than the fiberglass cone. The maximum thermal hoop compression stresses that could be generated for this condition were - 12,000 psi in the fiberglass cone and - 68,000 psi in the titanium cone. This comparison showed the superiority of the fiberglass for reducing thermal stresses due to lower modulus of elasticity. The stresses produced in the fiberglass under the most severe conditions were small and the designs had adequate capacity, whereas in the

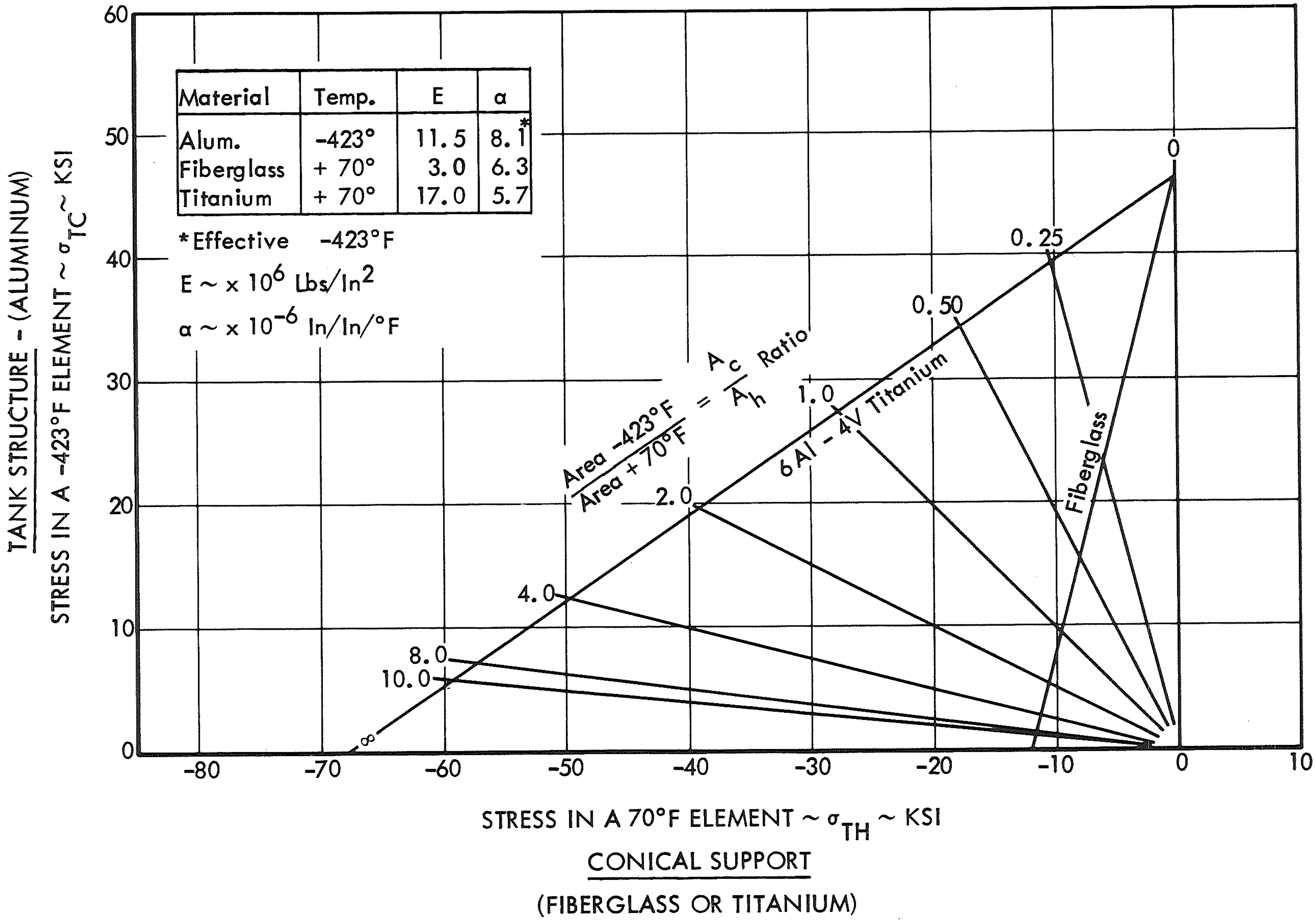

Figure 27: MAXIMUM POSSIBLE THERMAL HOOP STRESSES

titanium, the stresses were significant, indicating a possible need for translating joint designs.

Preliminary results showed a slight weight advantage for fiberglass in most of the cone configurations. Incorporation of a translating joint in the titanium cone would only have made this design heavier; therefore, the study effort to develop this type of design was considered unwarranted.

In actual applications the temperature extremes would probably not exist for long and any deflections resulting from thermal gradients would tend to reduce thermal stresses.

3.5.1 Manufacturing Feasibility

SK 11-043081 - Corrugated Titanium (Figures 19 and 20)

Forming of the corrugations would be difficult because the corrugation shape is tapered. The job could probably be accomplished best in heated, matched metal forming dies; however, development would be necessary. Heated forming (1200°F) of titanium would require application of a protective finish to avoid surface oxidation with the attendant cleaning problems. The number of formed cone segments would be a function of sheet width availability and forming technique. Segment joints would be used to provide circumferential "pay-off" for matching with the tank "y" ring.

Forming of the "y" shaped tank attach rings would take some development. An approach would be to make matched metal forming dies with the required curvature. This would permit fabrication of only relatively short lengths, therefore, a great quantity of parts would be necessary. Stretch forming is a candidate process, and except for die costs, would be relatively inexpensive. Roll forming to shape and curvature on Yoder Rolls is also a possibility.

Figure 20 shows forged attach plates instead of formed rings. The plates would require fabrication of two sets of forging dies (for right and left hand parts). The dies would be expensive to develop; however, the great quantity of parts would offset the cost.

Corrugation shape was designed so that the same attach plates could be used at top and bottom of the cone.

SK 11-043080 - Corrugated Fiberglass (Figures 21 and 22)

Fiberglass tooling for laminating corrugated sections would be complex due to the varying corrugation width. However, once the tool was perfected, the layup and curing of laminates would be routine. Producing build-ups at the ends of corrugations would require recesses in the tool and it would be difficult to control build-up thickness without a post cure grinding operation involving hand work.

Splice joints between segments could be simplified by using bonds with only a few rivets to hold the parts in place and to apply bonding pressure. Doublers could also be bonded to cone attachment rings to minimize the number of detail parts and to aid in positioning while drilling bolt holes. Comments regarding forming of metallic "y" attach rings and forged plates for the titanium structure apply to the fiberglass structure as well.

It was assumed in both titanium and fiberglass corrugation designs that inside "y" attachment ring segments would be bolted to the cone prior to installation on the tank. This approach would ease fit-up and the cone could then be attached to the tank using temporary fasteners. The outer attach ring segments would be added to complete the installation. Blind fasteners would be used due to limited access. In the case of forged attach plate designs, only the inner plates would be assembled to the cone prior to installation. The outer plates would be added with blind fasteners as in the case of the attach ring segments.

SK 11-043082 - Honeycomb Sandwich, Titanium Face Skins (Figure 23)

Assembly of prefabricated details by standard metalbond techniques could be accomplished with no unusual problems. Titanium skin splices would be made as material width and length dictated by lapping and adhesive bonding. The two-segment design was considered feasible in terms of tooling, curing facilities, and handling; however, scrappage of an assembly due to bonding defects or lay-up errors would be expensive because of the materials and labor involved.

Core forming does not constitute a manufacturing problem. Forming of edge attachment channels would be difficult and would require special processes such as heated, matched die forming or roll forming. Splice joint channels would be made by standard metal forming processes. The segmented "y" attach rings would present fabrication problems similar to those of the corrugated cones.

SK 11-043082 - Honeycomb Sandwich, Fiberglass Face Skins (Figure 23)

The configuration of the edge attachment laminate will cause manufacturing complications which could result in a part of questionable reliability if layup and cure of the entire assembly is made in one operation. An alternate approach would be to prefabricate laminate edge members and bond these to the core/skin assembly. This approach would necessitate additional tooling and bonding steps. Edge splice channels would be produced and installed in this manner. The outer face skin would be laminated and cured as a separate part to assure flatness. This part would be bonded to the outer surface of the core as the final process.

Assembly of panels for honeycomb sandwich designs could be accomplished separately from the tank, with the segment splice joints providing circumferential "pay-off" for fitting to the tank "y" ring. The sandwich cones are expected to be rigid and easy to handle. Also, the butt joint configuration lends itself to positioning with tank and stage structure rings better than the other configurations utilizing lap joints because the part can be rested on the attachment ring. Shim stock could be used for minor fit up discrepancies. The inner splice plate could be riveted to the small end of the cone to act as a guide during assembly.

SK 11-043084 - Zee Stiffened Titanium (Figure 24)

This part did not present any unusual fabrication problems. Sheet could be formed to the required shapes using standard metal forming methods. Machined end fittings were numerous which would result in high costs. The part would be flexible and present problems in handling and assembly.

SK 11-043084 - Zee Stiffened Fiberglass (Figure 24)

This was a good design for laminated structure. Tooling and layup of the zees would be standard procedure. The reinforcements at the ends of the zees could be built into the original layup or bonded on as a secondary step. The reinforcement at edges of the skin would be produced at the time of molding and curing. A male mold would be used. Aluminum end fittings would require extensive machining and the assemblies would be flexible and difficult to handle in large sections.

SK 11-043085 - Hat Stiffened Titanium (Figure 25)

This part could be produced using standard fabrication techniques. Hat sections could be cold formed to the required configuration. End attach fittings would require extensive milling and therefore, be costly. This part would be flexible like the zee stiffened structure.

SK 11-0430-85 - Hat Stiffened Fiberglass (Figure 25)

This design would present no unusual manufacturing problems. Comments regarding end fittings and laminate end buildups made for the zee stiffened skin are applicable.

SK 11-043086 - Bar Stiffened Titanium (Figure 26)

Welding of bars to the skin would present major manufacturing problems. EB welding from the face skin side would be possible; however, "Out of Vacuum" EB welding is mostly experimental and, if vacuum chamber welding was used, part size would be limited due to the conical shape. A great number of welding setups would be necessary due to the numerous bars, therefore labor costs would be high. Parts distortion is one of the major problems in EB welding of thin gages and it is possible that a hot sizing operation after welding this configuration would be necessary. Curved dies would be required for this operation. Current manufacturing development efforts for constructing stiffened titanium panels are being directed towards diffusion bonding. This approach also requires expensive heated, matched dies, but the distortion problem is eliminated. End fittings for the bar stiffened cone would require extensive machining.

SK 11-043086 - Bar Stiffened Fiberglass (Figure 26)

Fabrication of this concept as configured, i.e., with integral bar stiffeners, would present problems. No satisfactory tooling approach was devised during the manufacturing analysis. An apparent method of fabrication would be to bond prefabricated stiffeners to a prefabricated skin. Alignment and perpendicularity of stiffeners would be difficult to maintain and this problem would be compounded if numerous stiffeners were bonded at one time in an effort to reduce labor costs and oven time. Reinforcements on the ends of stiffeners and skins would be produced as described for zee construction. Fabrication of end attach fittings would involve extensive machining. Assembly of all three stiffened skin concepts would probably be accomplished on the tank "y" ring, with the edge splice joints made as the assembly progressed. This approach would ensure that the cone fit the tank.

3.6 STRUCTURAL CONCEPT WEIGHTS

Figures 28, 29 and 30 present weight breakdowns for the various methods of construction studied. Figure 31 is a summarization of total and elemental weights for all concepts and Figure 32 identifies the elements as percentages of cone weight. The data showed that titanium corrugated construction yielded the least cone weight with fiberglass honeycomb sandwich the second lightest, although approximately 100 pounds heavier. Fiberglass corrugated construction, using the forged fittings, was the third lightest. The stiffened skin concepts represented the heaviest structure.

Consideration of attachment details had a marked effect on total cone weight as evidenced by comparing Figure 17 with Figure 31. The initial weight evaluation, which considered only the basic panel construction, indicated that corrugated titanium and fiberglass construction were the least weight, with titanium and fiberglass honeycomb sandwich a close second. When finalized designs were considered, the attachments and end stiffening increased the weight of the fiberglass corrugated and titanium honeycomb sandwich designs to less competitive positions. Edge attachments particularly penalized honeycomb sandwich construction.

BASIC CORRUGATION MATERIAL	TITANIUM			FIBERGLASS		
NO. OF PANEL SPLICES	12			4		
TYPE OF PANEL SPLICES	Lap	Butt		Lap	Butt	
TYPE OF ATTACHMENT - PANELS TO SUPT. RING	Segmented Rings		Forged Fittings	Segmented Rings		Forged Fittings
ITEM/WEIGHT (LB)						
BASIC CORRUGATIONS	(306.0)	(306.0)	(306.0)	(235.0)	(235.0)	(235.0)
PANEL END STIFFENING	(18.6)	(18.6)	--	(93.0)	(93.0)	(93.0)
PANEL SPLICE	(3.7)+	(3.9)	(3.9)	(8.1)+	(1.3)	(1.3)
PANEL END FITTINGS, DOUBLERS & FAST.	(180.5)	(180.5)	(141.6)	(433.6)	(433.6)	(255.8)
Upper Ring Segments	53.3		--	170.5		--
Lower Ring Segments	51.9		--	166.8		--
Doublers	31.0		--	25.6		--
Forged Fittings	--		72.7	--		158.0
Titanium Fasteners	20.6		53.7	37.8		49.2
Steel Lockbolts	23.7		15.2	32.9		48.6
ATTACHMENT - END FITTINGS TO SUPT. RING	(66.9)	(66.9)	(77.8)	(52.3)	(52.3)	(73.1)
Titanium Fasteners	15.9		59.7	17.6		54.3
Steel Lockbolts	13.9		18.1	15.0		18.8
Doubler Plates	37.1		--	19.7		--
"Y-RING" Δ WT.**				(+54.8)	(+54.8)	(+54.8)
TOTAL BASIC ASSEMBLY	575.7	575.9	529.3	876.8	870.0	713.0
Δ WT. TO ALL STEEL FASTENERS	13.5	13.5	42.0	20.2	20.2	38.2
TOTAL ASSY. WT. WITH STEEL FASTENERS	589.2*	589.4	571.3	897.0*	890.2	751.2

This weight assumes optional spot welding of panel end stiffeners. If these stiffeners are riveted to corrugations assy., the weight would increase from 10 to 19 pounds, dependent on rivet type.
Titanium Corrugated Cone assumed to be baseline. Positive and Negative ΔWts. relate to this design.
These weights include corrugation fillers (2.3 Lb. for Titanium & 7.2 Lb. for Fiberglass).

Figure 28: WEIGHT SUMMARY- CORRUGATED PANEL SUPPORT STRUCTURE

BASIC SKIN MATERIAL	TITANIUM		FIBERGLASS	
TYPE OF CORE	HEX CELL FIBERGLASS			
CELL SIZE - IN.	3/16		3/8	
PANEL END FTG.	SEGMENTED TI. RING		LAMINATED FIB. FTG.	
NUMBER OF PANEL SPLICES	2		2	
ITEM/WEIGHT LB.				
BASIC HONEYCOMB PANEL	291.4		262.3	
Skin - Outer		52.8		67.5
Skin - Inner		52.4		66.6
Core		147.8		109.7
Adhesive (10 mil.)		38.4		18.5*
PANEL SPLICE	8.0		9.7	
Splice Plates		1.2		0.8
Edge Members		3.2		4.8
Fasteners		3.6		3.8
Inserts		--		.3
PANEL END STIFFENING & ATTACH.	386.1		306.7	
Laminated Ftgs.		--		221.2
Channel End Stiffeners		93.4		--
Segmented Attach. Rings		153.8		--
Attach. Ring Doublers		15.4		--
Support Attachment Plates		82.9		85.5
Attachment Plate Fillers		40.6		--
FASTENERS	101.2		67.7	
Panel - Steel Lockbolts		33.5		--
Supt. Ftg. - Titanium		67.7		67.7
"Y-RING" ΔWT.	-26.9		-14.1	
TOTAL BASELINE ASSEMBLY	759.8		632.3	
ΔWT. ASSUMING 15 MIL. ADHESIVE	+19.2		+9.2	
TOTAL (WITH 15 MIL. ADHESIVE)	779.0		641.5	

*Adhesive used only on one side

Figure 29: WEIGHT SUMMARY - HONEYCOMB PANEL SUPPORT STRUCTURE

STIFFENER TYPE	HAT		ZEE		BAR	
PANEL ATTACHMENT	Milled Fittings					
NO. OF PANEL SPLICES	8	4	8	4	8	4
BASIC PANEL MATERIAL	Ti.	Fib.	Ti.	Fib.	Ti.	Fib.
ITEM WEIGHT - LB.						
BASIC PANEL	(551.6)	(397.2)	(608.0)	(474.0)	(544.6)	(500.7)
Skin	309.3	203.6	288.0	282.9	266.5	247.6
Stiffeners	237.5	189.6	315.0	183.9	278.1	253.1
Rivets*	4.8	4.0	5.0	7.2	--	--
PANEL END STIFFENING	--	(95.1)	--	(71.4)	--	(46.1)
Skin		24.6		22.1		25.0
Stiffeners		70.5		49.3		21.1
PANEL SPLICE PENALTY	(1.7)	(1.3)	(2.7)	(1.8)	(2.9)	(1.6)
PANEL END FITTINGS	(141.2)	(163.7)	(101.2)	(82.4)	(72.0)	(82.2)
Inner	61.2	66.5	51.5	34.6	38.6	31.6
Outer	80.0	97.2	41.9	36.6	33.4	50.6
Fillers	--	--	7.8	11.2	--	--
FASTENERS	(107.4)	(128.4)	(74.5)	(173.8)	(85.0)	(137.7)
Panel - Titanium	38.9	48.3	36.0	114.8	42.8	81.9
Panel - Steel	18.2	24.0	--	--	--	--
Supt. Ftg. - Titanium	25.0	27.7	18.6	30.7	20.6	28.6
Supt. Ftg. - Steel	25.3	28.4	19.9	28.3	21.6	27.2
"Y -RING" Δ WT.	(+3.1)	(+35.2)	(+24.8)	(+22.3)	(+26.9)	(+26.9)
TOTAL BASIC ASSEMBLY	805.0	820.9	811.2	825.7	731.4	795.2
Δ WT. TO ALL STL. FASTENERS	23.6	28.1	20.2	53.8	23.5	40.9
TOTAL (WITH STL. FASTENERS)	828.6	849.0	831.4	879.5	754.9	836.1

*These weights can be removed if optional bonded or spot weld stiffeners used.

Figure 30: WEIGHT SUMMARY - STIFFENED PANEL SUPPORT STRUCTURE

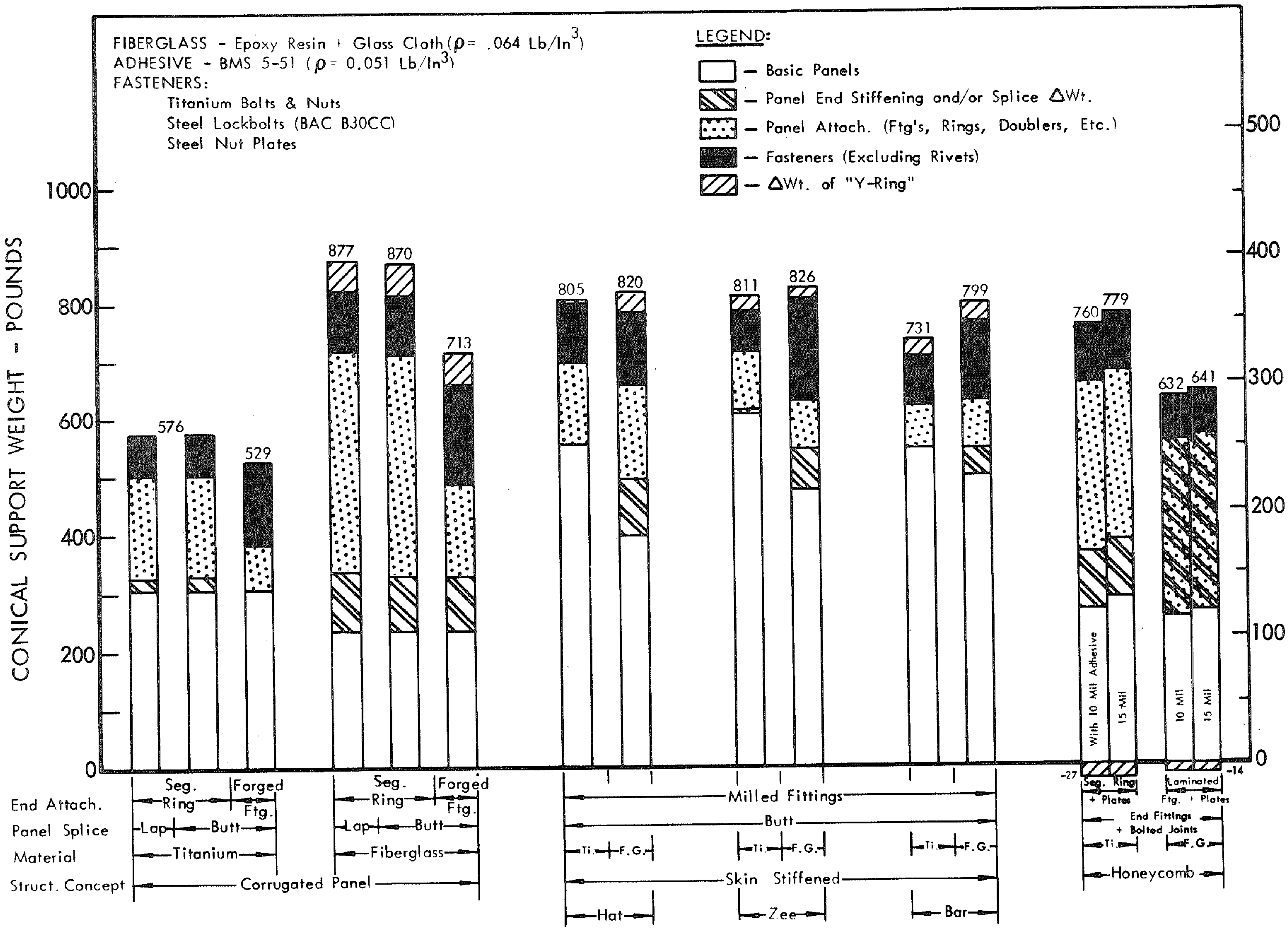

Figure 31: WEIGHT BREAKDOWN
CONICAL SUPPORT SYSTEMS - CRYOGENIC TANK SUPPORT

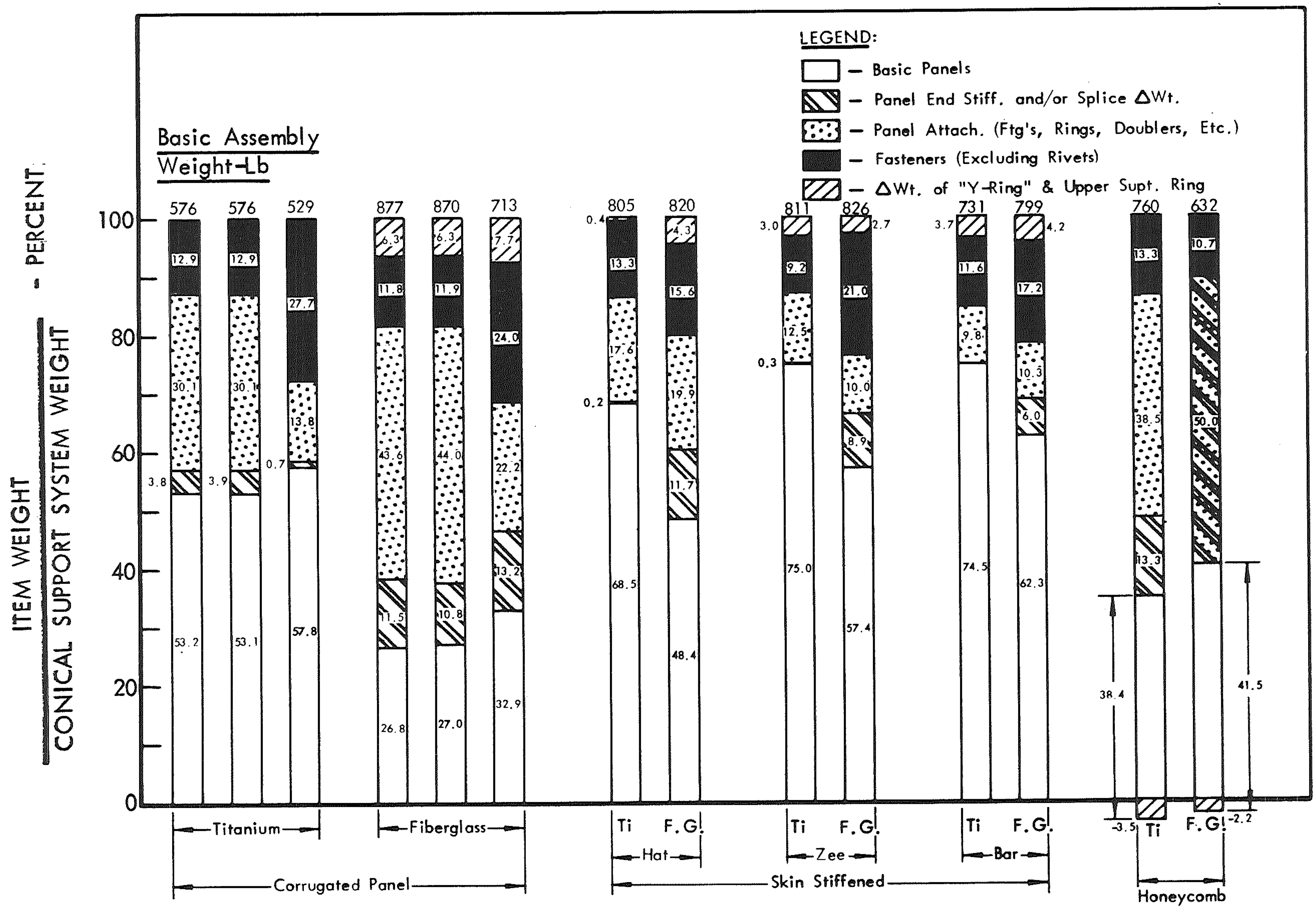

Figure 32: WEIGHT BREAKDOWN BY PERCENT
CONICAL SUPPORT SYSTEMS - CRYOGENIC TANK SUPPORT

Thermally induced strains were not accounted for in the titanium designs. It has been shown that thermal stresses were relatively high for titanium; thus the addition of an alleviating device (translating joint) could increase weight significantly. The corrugated titanium design could be the one exception in that it has the capability to expand and contract. Fiberglass thermal stresses were shown to be within the capacity of the material, therefore, translating designs were unnecessary and cone weights are realistic.

Weight comparisons alone could not be used to justify selection of a particular tank support structure since support heat leak greatly affected payload weight through boil-off losses. The scope of this contract did not allow a mission oriented parametric study to identify the relative importance of support weight and heat leak; however, it was possible to make comparisons based on certain assumptions.

It was assumed that support heat leak was essentially one-dimensional, (i.e., there was sufficient insulation of the proper design to thermally isolate the support), and therefore, the concepts could be compared in terms of hydrogen boil-off weight as well as structural weight. This simplified approach did not account for tank growth to compensate for boil-off losses or the alternate of operating the vessel at higher pressures; however, both of these approaches would increase inert weight and tend to degrade the higher heat leak supports and enhance those with lower heat leak.

A second assumption was that the cone was sufficiently long to produce temperatures of $37^{o}R$ and $535^{o}R$ at cold and warm ends respectively under steady state conditions.

The total mission time was assumed to be 256 days, with the first 23 days allotted to nonvented pressure rise from top-off to operating pressure.

Heat flow was calculated using the length of cone between attachments to aluminum tank and support ring. This length varied depending upon end attachment design. No attempt was made to analyze heat flow across contact resistances such as bolted joints. The splice joint members contributed very little to total heat flow, thus the number of joints could be altered for manufacturing reasons with only slight thermal effect.

The results of the heat flow analysis are presented in Figure 33. Conical support structural weights were added to hydrogen boil-off losses for weight totals. Fiberglass honeycomb sandwich provided the least total weight by a significant margin. The best titanium design was also honeycomb sandwich, however, the total weight was over 240% greater. Corrugated fiberglass construction was the second best approach but was 128% heavier than fiberglass honeycomb.

3.7 SUBSCALE CONICAL SUPPORT DESIGN

The final effort in Phase I was the preparation of a conical support detail design. The support was designed to fit a 105-inch diameter tank and tapered to approximately 117-inches at the large end. This part was intended primarily for thermal performance tests. The cross section shape, thickness and material gages were the same as the 32 ft. counterpart as was the cone length. This was done in an effort to produce the same heat leak per inch of cone circumference in the subscale test article as in the full scale part. Fiberglass honeycomb sandwich with fiberglass face skins was shown to be the most promising concept in the study; therefore, the subscale cone utilized these materials. Figures 34 and 35 are drawings of the part.

A four segment design was adopted rather than the two segments used in the full size cone of Figure 23. This was done to simplify tool fabrication and handling as well as to reduce the amount of materials committed to a single cure cycle. The increase in full size cone heat flow due to the extra joints was shown (in Figure 33) to be minor. Changes to reduce fabrication costs included (1) the substitution of NAS 501 stainless steel bolts for titanium and A286 bolts, (2) elimination of nut plates along one side of each segment joint, and (3) the substitution of Volan A finish for 901 finish on the "S" glass cloth used to fabricate laminate face skins and edge members. The Volan finish results in a laminate with lower strength, typically 9% lower in compression and 27.6% in tension (Owens-Corning Fiberglas Corporation data) however the properties were more than adequate for the design.

	Configuration	Weight (Lb)	Heat Flow (Btu/Hr.)*	H_2 Boiloff Wt.** (Lb)	Σ Weight (Lb)	Heat Flow Ratio Opposite Mat'l Counter-Part	Splice Joint % of Total Cone Heat Flow
Fiberglass	Honeycomb	632	16.5	476	1108		0.43
	Corrugated-Butt Joints + "Y" Ring Attach.	870	26.7	771	1641		0.46
	Corrugated-Lap Joint "Y" Attach Rings	877	26.7	771	1648		0.24
	Corrugated-Butt Joints + Forged Plates	713	24.6	710	1423		0.46
	Hat Stiffened	821	32.6	940	1761		0.27
	Zee Stiffened	826	40.7	1175	2001		0.29
	Bar Stiffened	795	43.7	1260	2055		0.24
Titanium	Honeycomb	760	66.9	1930	2690	4.1/1	1.28
	Corrugated-Butt Joints + "Y" Ring Attach	576	161.5	4660	5236	6.1/1	1.22
	Corrugated-Lap Joints "Y" Ring Attach	576	160.2	4630	5206	6.0/1	0.41
	Corrugated-Butt Joints Forged Plates	529	161.5	4660	5189	6.6/1	1.22
	Hat Stiffened	805	286.3	8270	9075	8.8/1	0.45
	Zee Stiffened	811	343.3	9910	10721	8.4/1	0.38
	Bar Stiffened	731	296.4	8560	9291	6.8/1	0.45

Mean Thermal Conductivity

Titanium = 0.24 $\frac{\text{Btu-In}}{\text{In}^2\ \text{Hr.}\ ^\circ\text{R}}$

Fiberglass = 0.013 "

** 5600 Hour Mission

Figure 33: HEAT FLOW ANALYSIS RESULTS

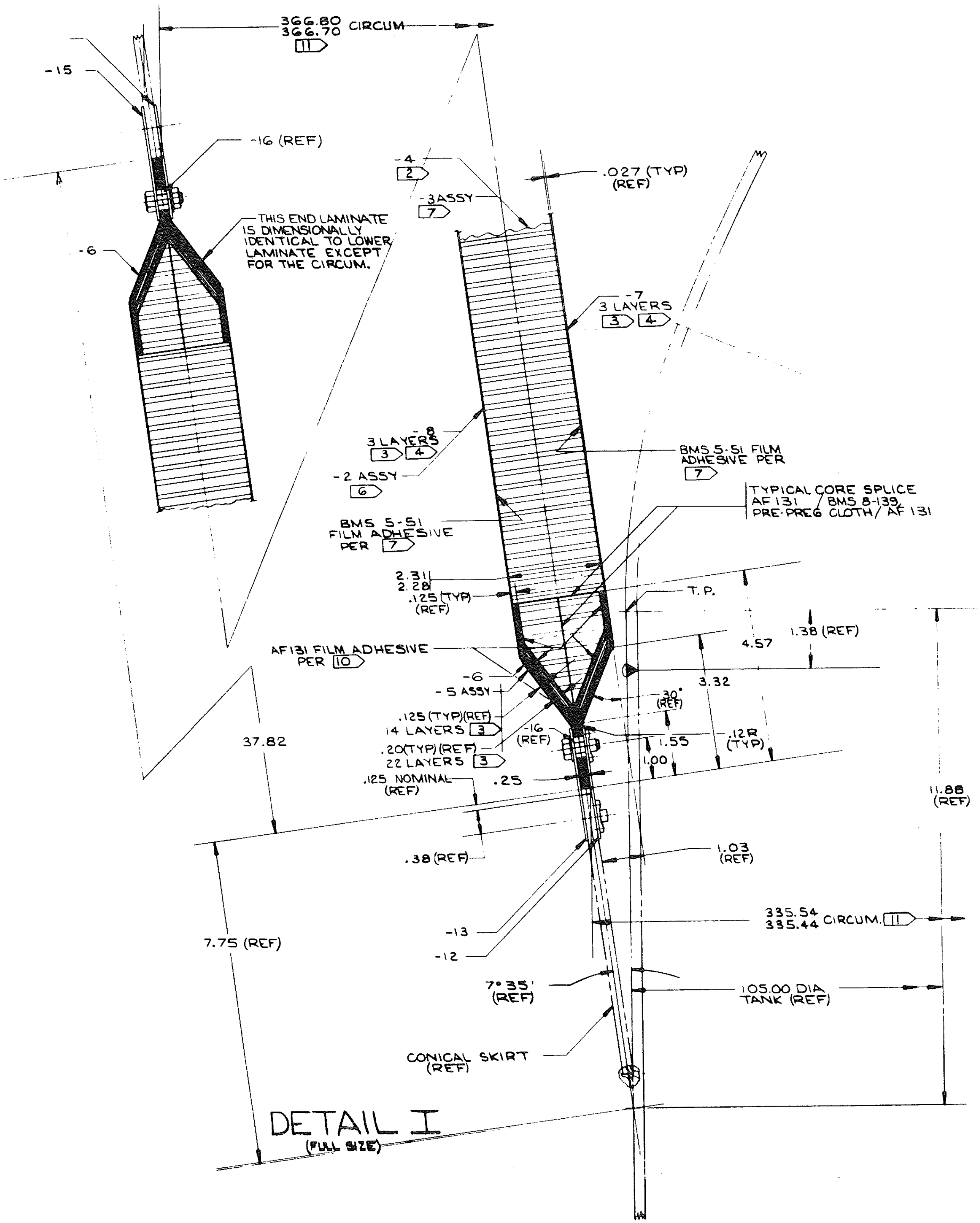

366.80
366.70 CIRCUM
11
-15
-16 (REF)
THIS END LAMINATE IS DIMENSIONALLY IDENTICAL TO LOWER LAMINATE EXCEPT FOR THE CIRCUM.
-6
-4
2
-3ASSY
7
.027 (TYP)
(REF)
-7
3 LAYERS
3 4
-8
3 LAYERS
3 4
-2 ASSY
6
BMS 5-51 FILM ADHESIVE PER
7
TYPICAL CORE SPLICE
AF 131 / BMS 8-139
PRE-PREG CLOTH / AF 131
BMS 5-51
FILM ADHESIVE
PER 7
2.31
2.28
.125 (TYP)
(REF)
T.P.
1.38 (REF)
4.57
AF131 FILM ADHESIVE
PER 10
-6
-5 ASSY
3.32
30°
(REF)
.125 (TYP)(REF)
14 LAYERS 3
-16
(REF)
1.55
.12R
(TYP)
.20(TYP)(REF)
22 LAYERS 3
1.00
37.82
.125 NOMINAL
(REF)
.25
11.88
(REF)
.38 (REF)
1.03
(REF)
335.54
335.44 CIRCUM. 11
7.75 (REF)
-13
-12
7°35'
(REF)
105.00 DIA
TANK (REF)
CONICAL SKIRT
(REF)
DETAIL I
(FULL SIZE)

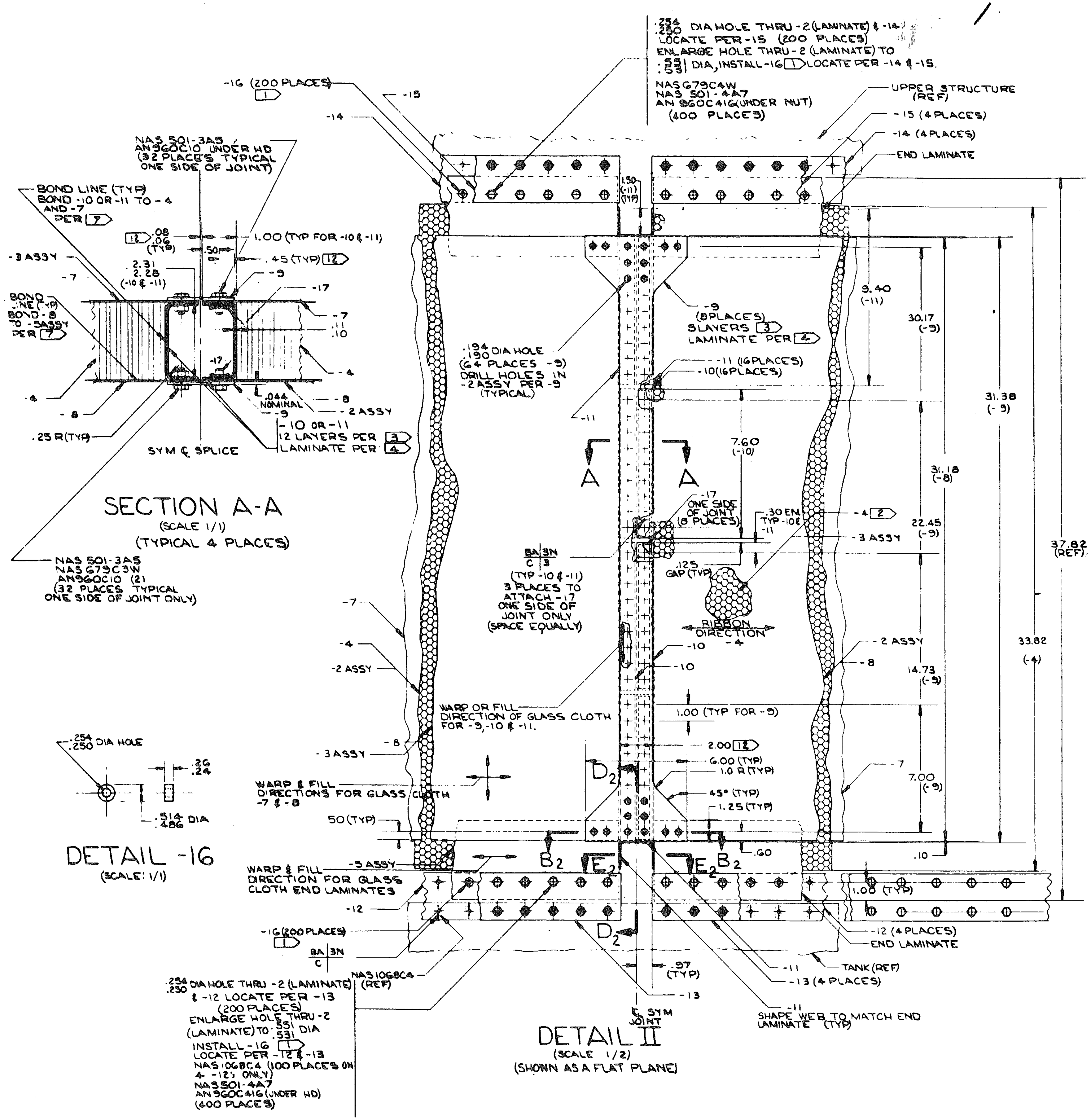

1. BOND -16 INSERT IN PLACE WITH BMS-5-25. (PER BAC 5010 TYPE 54 GRADE 1)
2. HRP 3/8-GF11-2.2LBS/FT³ HONEYCOMB. HEXCEL PRODUCTS INC. 2332 4TH ST. BERKELEY, CALIF.
3. STYLE 181,'S FIBERGLASS CLOTH WITH VOLAN A FINISH IN U.S. POLYMERIC E787 PREPREG FORM (.009 THICK REF)
4. LAMINATE BY POSITIVE PRESSURE MOLDING SUCH AS DESCRIBED IN BAC 5456.
   1. MATERIALS PER 3
   2. PARTING AGENT PER SEC 3.4
   3. MISC. MATL PER SEC 3.5
   4. PREPARE MOLDING SURFACE PER SEC 4.2
   5. APPLY PARTING FILM PER SEC 4.3
   6. LAYUP PER DRAWING.
   7. VACUUM BAG & CURE AT 50 PSI ±5 AUTOCLAVE PRESSURE FOR 4 HRS AT 325° ±5° F.
   8. MACHINE FINISH PER SEC 4.9

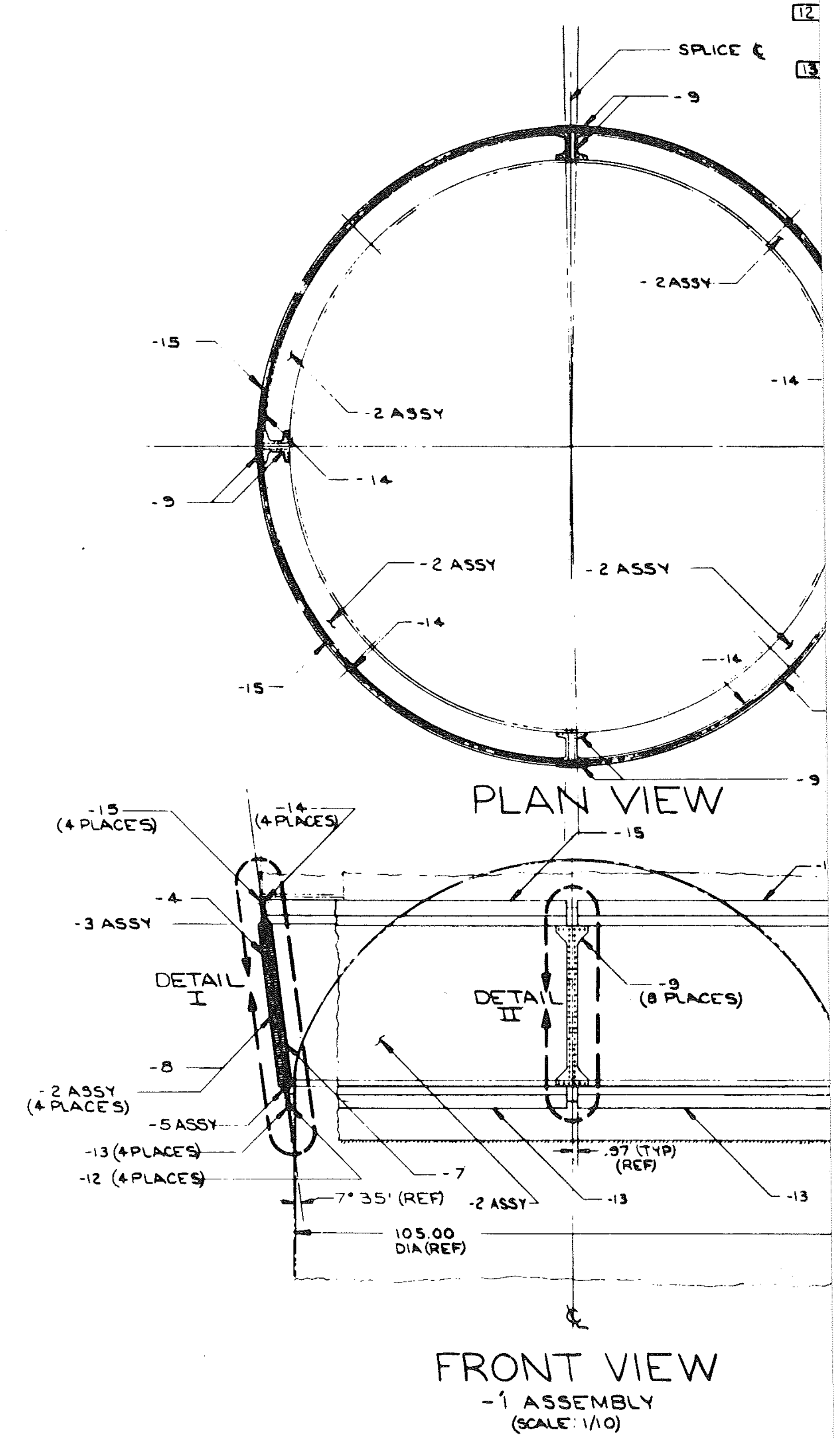

- BOND PER BAC 5514-551 WITH MODIFIED EPOXY BMS 5-51 TYPE 2 GRADE 10.(.010 FILM ADHESIVE) EXCEPT AS FOLLOWS: 1. CURE TIME ~ 90 MIN. 2. CURE PRESSURE ~ 15 PSI. 3. CURE TEMP-300° F. — 2 -
- CLEAN LAMINATED FIBERGLASS BEFORE BONDING AS FOLLOWS:
  1. WIPE WITH MEK
  2. SAND WITH 320 ABRASIVE PAPER TO REMOVE GLOSS.
  3. WIPE WITH MEK & AIR DRY.
- CORE SHALL BE HANDLED IN A MANNER TO AVOID CONTAMINATION. IF CORE BECOMES CONTAMINATED, CLEAN PER BAC 5529.
- LAMINATE BY POSITIVE PRESSURE MOLDING SUCH AS DESCRIBED IN BAC 5529 EXCEPT AS FOLLOWS.
  A. APPLY AF131 FILM ADHESIVE (.075 #/FT², .010 THICK) (3M Co) BETWEEN CORE AND PRE PREG.
  B. FINAL CURE AT 300° AT 45±5 PSI FOR 4 HOURS.
  C. MATL'S PER 3 & 2.

THE FIBERGLASS CLOTH REQUIRES A SPLICE ON ANY LAYUP IT SHOULD LAPPED 1.00". ADJACENT LAPS WILL BE STAGGERED TO PREVENT [illegible]ESSIVE BUILDUP.

- CONE TO BE ROUND WITHIN .25 ON THE DIAMETER AS MEASURED IN THE FREE STATE. (OR ON THE MOLD)
- JOINTS MAY BE ADJUSTED ON ASSY OF QUARTER PANELS (-2) TO MEET CIRCUMFERENTIAL TOLERANCES.
- ELASTIC STOP NUT CORP. UNION, NEW JERSEY

BON[illegible]
BON[illegible]
AND
P[illegible]

-3 ASSY

REVISIONS

SYM	LTR	DESCRIPTION	APPROVED
	A	REVISED DRAWING AS FOLLOWS: NAS 501 BOLTS REPLACED ALL UN-DEFINED [illegible] CHANGED [illegible] NUTS TO NAS 679 NUTS PROVIDED .125 GAP BETWEEN -2 & [illegible] ADDED SECTION [illegible] CHANGED -11 LENGTH FROM 10.84 TO [illegible] & SHORTENED TAPERED [illegible] FROM [illegible] TO 1.50 CHANGED 8 STYLE 181, [illegible] FIBERGLASS CLOTH IN [illegible] TO READ: STYLE 181, [illegible] FIBERGLASS CLOTH WITH VOLAN A FINISH IN [illegible] IN TABLE I CHANGED DIM 41.75 TO 41.28.	[illegible]
	B	REVISED SHEET 1 AS FOLLOWS: [illegible] ADDED TO PICTURE CORE SPLICE METHOD IN DETAIL [illegible]. ADDED TIME TEMP & PRESSURE TO 7 CHANGED 325° TEMP TO 300° & 50 PSI TO 45±5 PSI IN 10 CHANGED -11 DIM 9.14 TO 9.40 DELETED [illegible] [illegible] REVISED SEGMENT RING & LAMINATE HOLE CALLOUT TO SHOW PROPER DRILLING SEQUENCE. REVISED SHEET 2 AS FOLLOWS: CHANGED -12 -13 -14 & -15 (8 EACH REQD) TO (4 EACH REQD). PARTS LENGTHS, TABLE I, [illegible] & PICTURE CHANGED ACCORDINGLY	

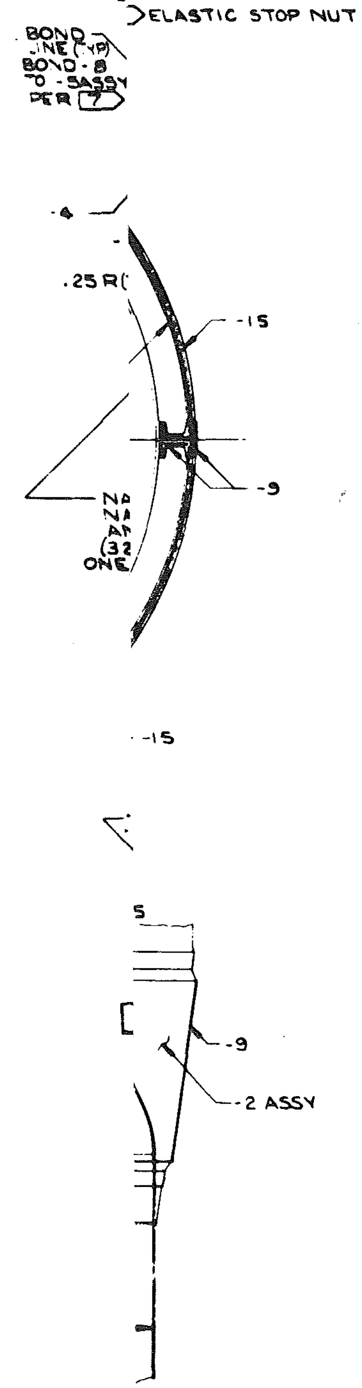

-5	-3	-2	-1	QTY REQD	PART OR IDENTIFYING NUMBER	NOMENCLATURE	ZONE	MATERIAL AND SPECIFICATION	HT-TR	FINISH	STAGE	
			✓	32	NAS43DD3-156A	SPACER						
			✓	400	NAS679C4W	NUT						A
			✓	288	NAS679C3W	NUT						A
			-12	100	NAS1068C4	NUTPLATE						
			✓	800	NAS 501-4A7	BOLT						A
			✓	512	NAS 501-3A5	BOLT						A
			✓	32	NAS 501-3A26	BOLT						A
			✓	800	AN960C416	WASHER						
			✓	900	AN960C10	WASHER						
		✓		8	-17	NUT-GANG CHANNEL		MAKE FROM NGJ1-02-J8 13				
		✓		400	-16 1	INSERT		2024-T4 AL RD BAR PER QQ-A-225/6 .50 x .25 x .25				
			✓	4	-15	SEGMENTED RING UPPER OUTER		2024-T3 AL SHT PER QQ-A-250 .080 x 2.8 x 91.0			R	B
			✓	4	-14	SEGMENTED RING UPPER INNER					R	B
			✓	4	-13	SEGMENTED RING LOWER OUTER					R	B
			✓	4	-12	SEGMENTED RING LOWER INNER		2024-T3 AL SHT PER QQ-A-250 .080 x 2.8 x 91.0			R	B
	✓			4	-11	SPLICE CHANNEL		3 4 8				
	✓			4	-10	SPLICE CHANNEL		3 4 8				
			✓	8	-9	SPLICE PLATE		3 4			R	
		✓		1	-8	SKIN - OUTER		3 4 8				
	✓			1	-7	SKIN & BUILDUP - INNER		3 4 8				
✓				1	-6	BUILDUP - OUTER		3				
-		✓		1	-5	LAMINATE ASSY		10				
	✓			1	-4	CORE		2 9				
✓	-			1	-3	CORE ASSY		7				
		-	✓	4	-2	PANEL ASSY		7			R	
			-	-	-1	SUPPORT STRUCTURE ASSEMBLY		—	—	—	—	

RELEASE

Figure 34: SUBSCALE CONICAL SUPPORT STRUCTURE DESIGN

Dwg. SK 11-043090 Sheet 1 of 2

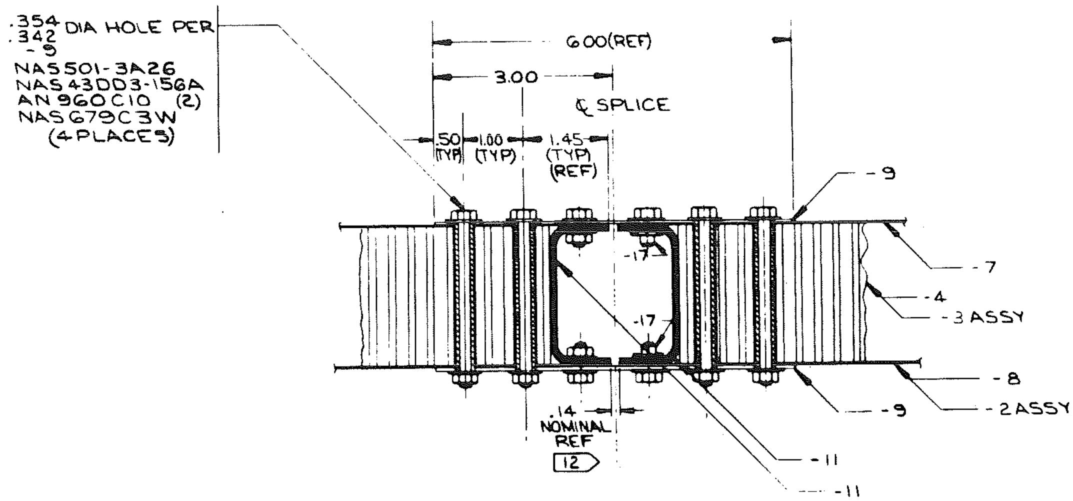

SECTION B-B
(SCALE 1/1)
(TYPICAL)

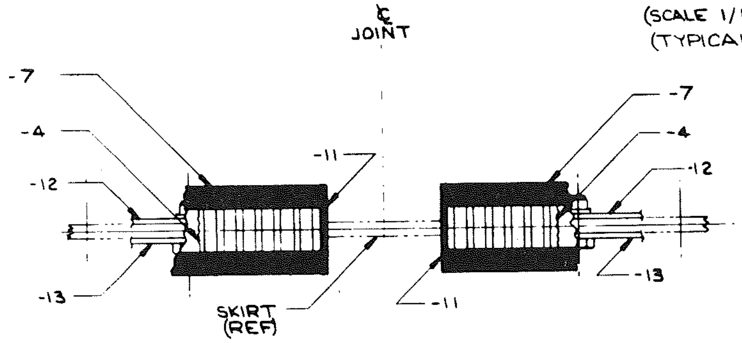

SECTION E-E
(SCALE 1/1)

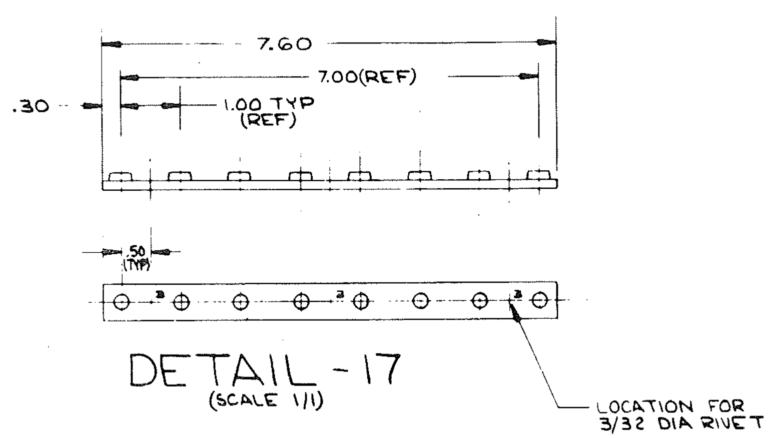

DETAIL-17
(SCALE 1/1)

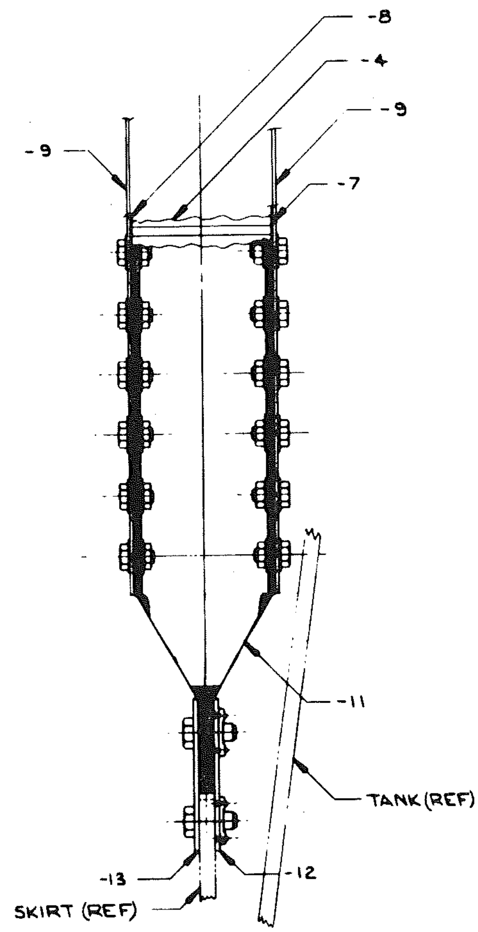

SECTION D-D
(SCALE 1/1)

		REVISIONS	
ARE	LTR	DESCRIPTION	APPROVE
	A	SEE SHEET 1	
	B	SEE SHEET 1 6-29-69	

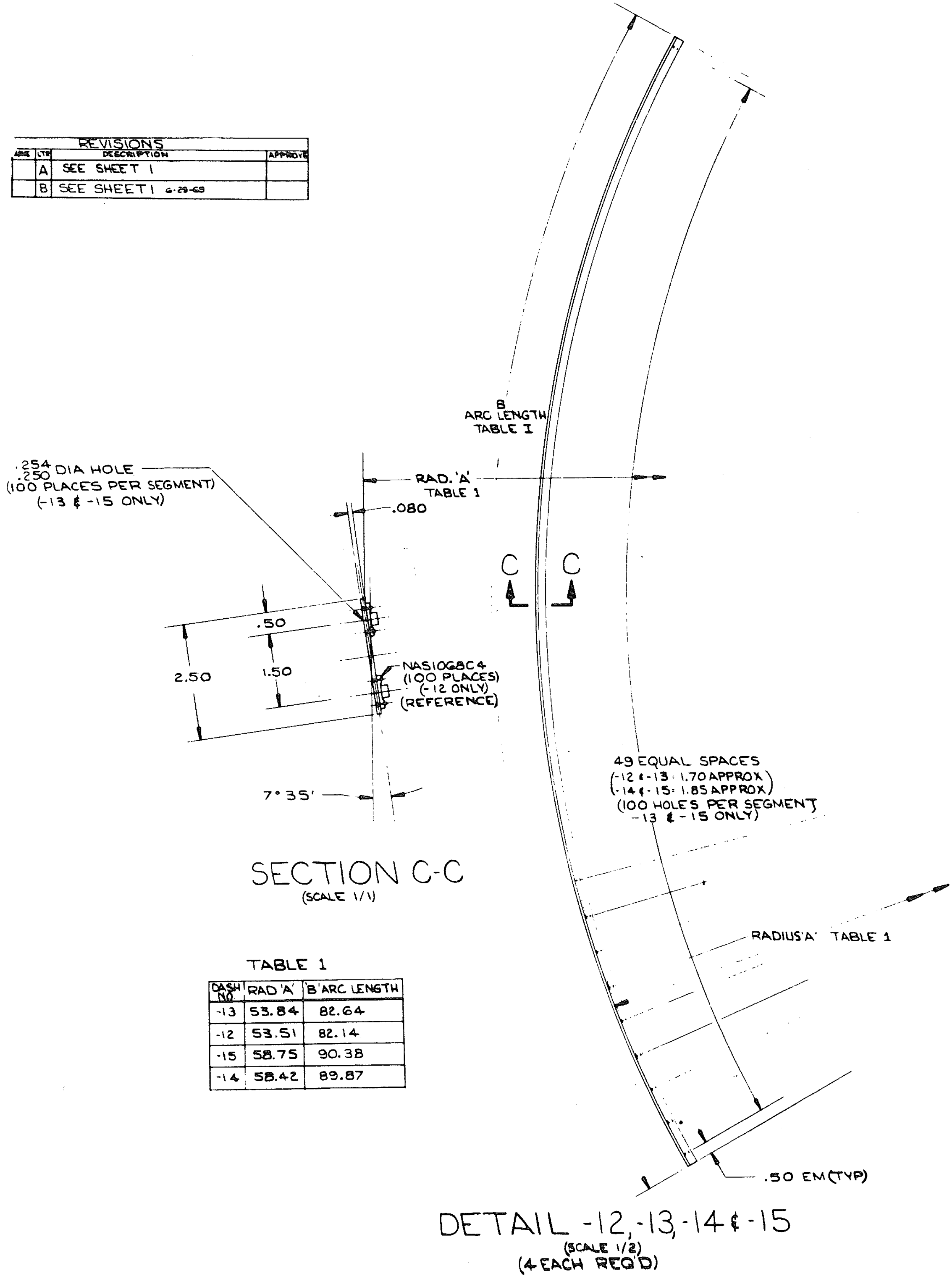

TABLE 1

DASH NO	RAD 'A'	'B' ARC LENGTH
-13	53.84	82.64
-12	53.51	82.14
-15	58.75	90.38
-14	58.42	89.87

Figure 35: SUBSCALE CONICAL SUPPORT STRUCTURE DESIGN
Dwg. SK 11-043090 Sheet 2 of 2

4.0 PHASE II - SUBSCALE CONICAL SUPPORT FABRICATION

4.1 MOLD TOOLING

The conical support was molded in quarter segments on a male tool constructed of high temperature fiberglass. A hydrocal plaster model representing the inner surface of the quarter segment was made first. The model, shown in Figure 36, was coated with Epocal "Release-All" followed by a moisture insensitive epoxy gel coat, U.S.G. 415-5T2. A layer of hydrocal plaster with reinforcing hair completed the reverse mold shown in Figure 37.

The reverse mold was used to form the high temperature fiberglass tool shown in Figure 38. Molding materials consisted of class cloth broadgoods and U.S.G. 503-29 resin with a U.S.G. 408-2d gel coat.

Fiberglass splice plates, shown in Figure 39, were cut from five ply sheet laminates which had been autoclave cured at 50 psi between aluminum caul plates. The fiberglass channel members, shown in this photograph, were twelve ply laminates, autoclave cured in the aluminum female tool shown in the background. The full length channels were then cut to appropriate lengths.

4.2 FABRICATION

Fabrication and assembly procedures employed in this program are outlined in the plan of Figure 40. Several efforts were initiated concurrently. These were; forming of honeycomb core, laminating of the outer skins, longitudinal splice plates and edge channels, and forming the tapered honeycomb edge pieces.

The four outer skins were laminated, bagged and autoclave cured 4 hours at $325^{\circ}F$ on the high temperature mold. These three ply laminates were so flexible however that they could have been molded flat.

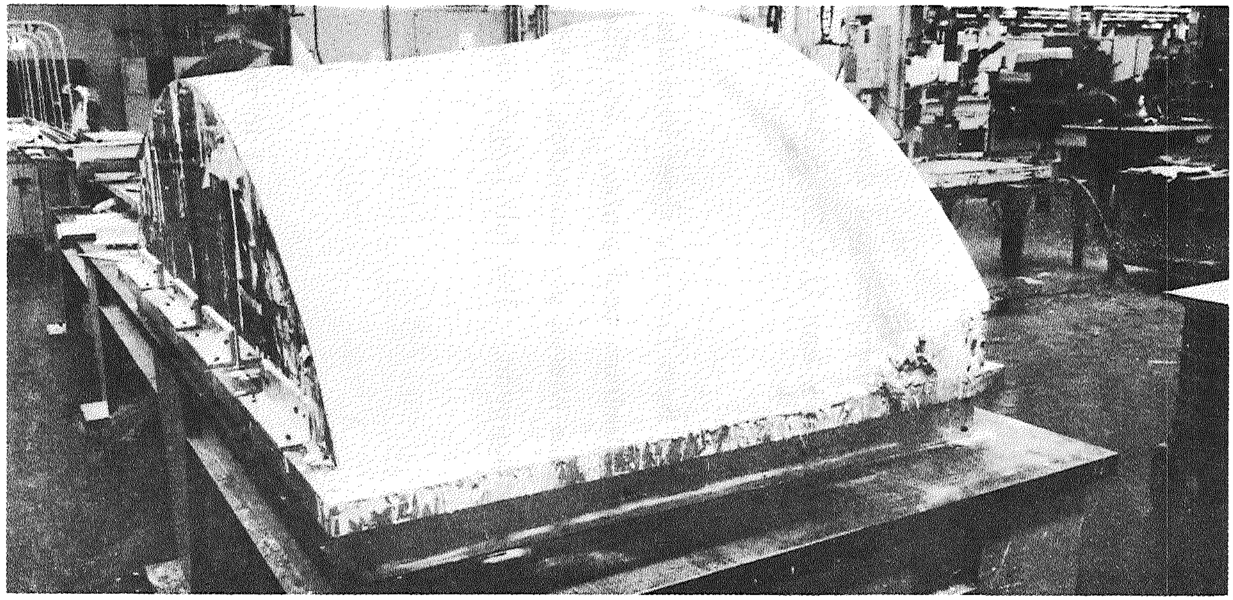

Figure 36: PLASTER MODEL

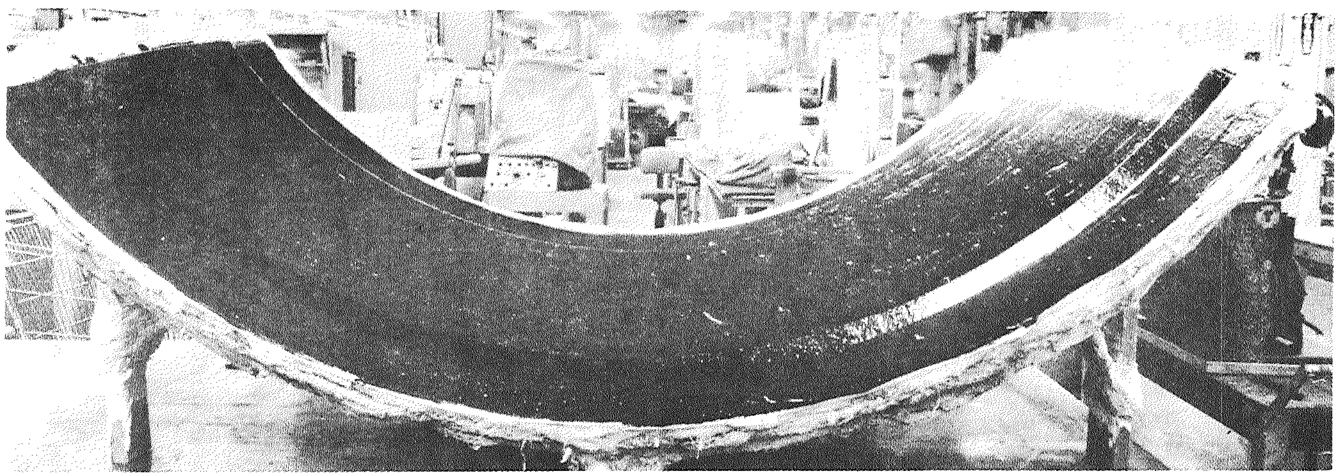

Figure 37: PLASTER REVERSE MOLD

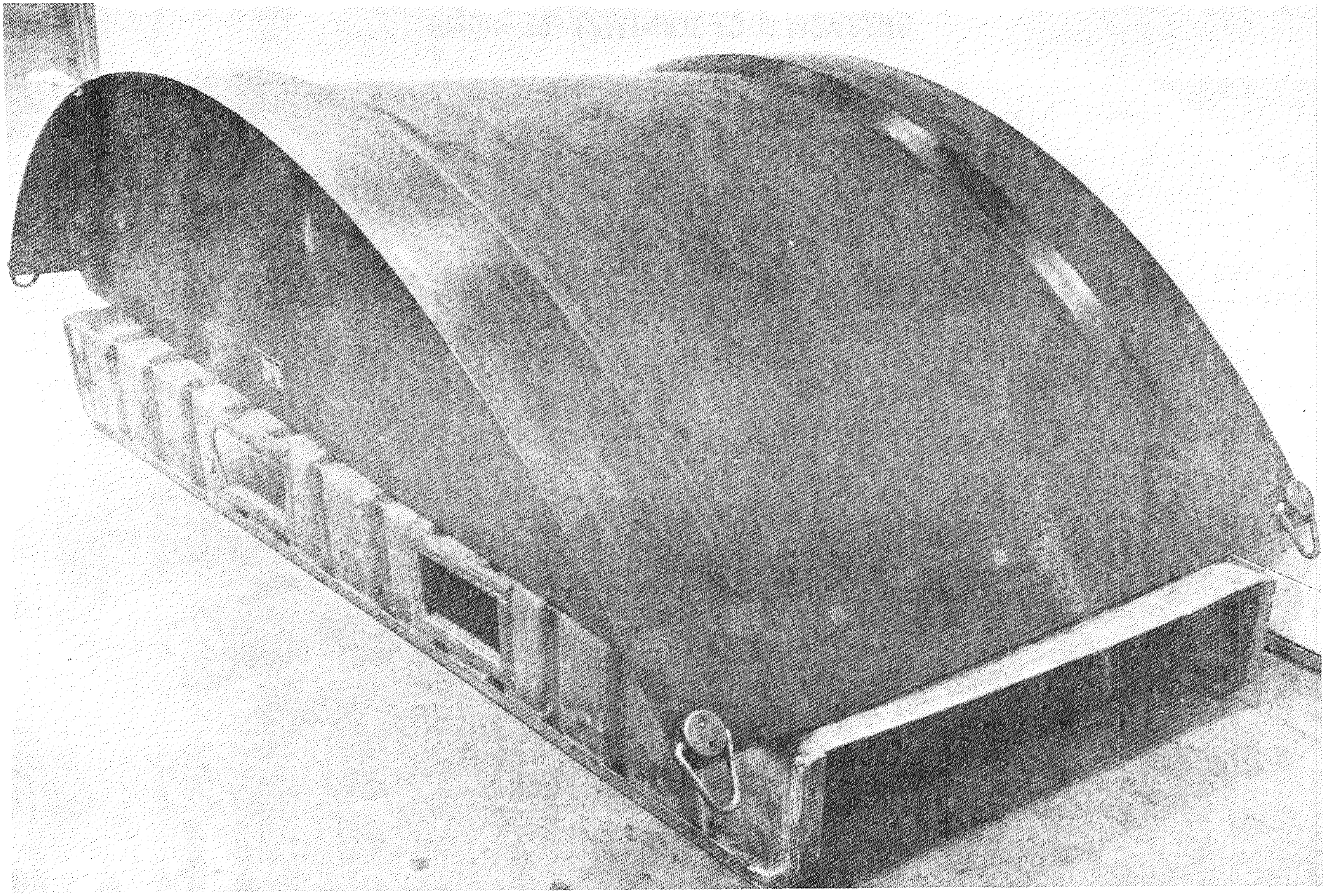

Figure 38: FIBERGLASS MOLD TOOL

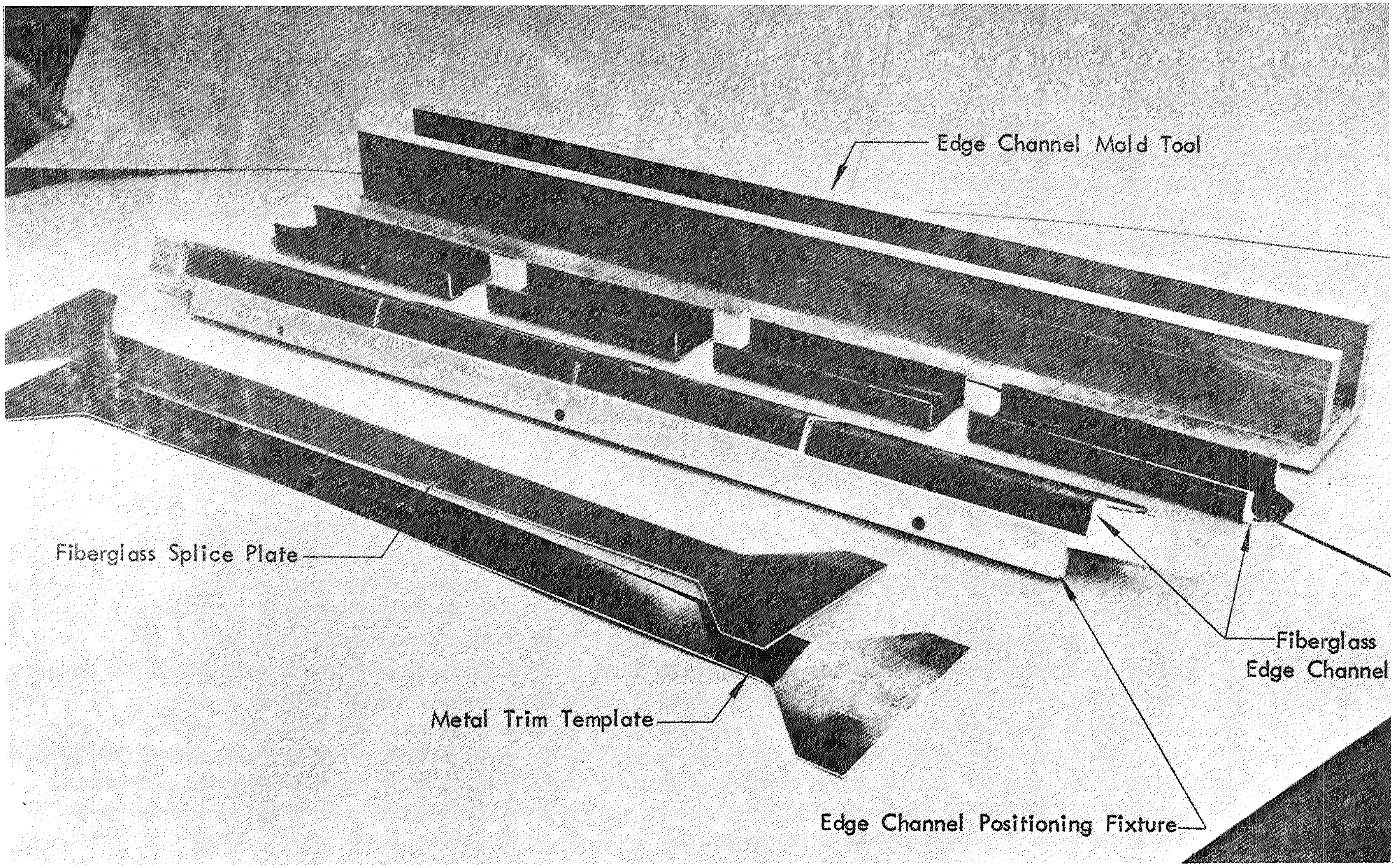

Figure 39: LAMINATE EDGE MEMBERS

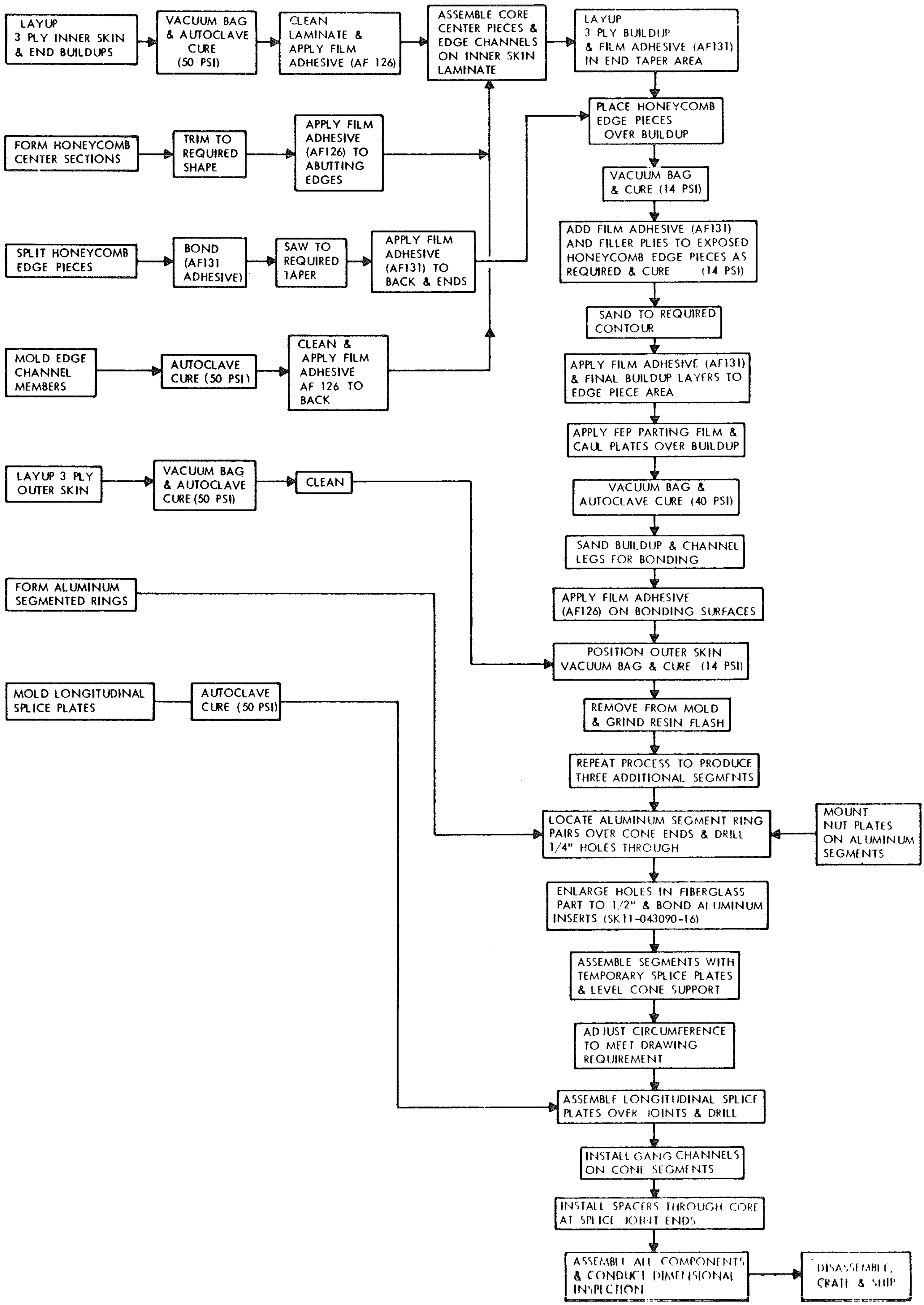

Figure 40: MANUFACTURING PLAN

Honeycomb core (Hexcel HRP) center sections and edge pieces were formed by placing them in a 600-675°F oven for 30 seconds and then in a 57" radius forming press for 15 seconds. The center sections were trimmed to shape and stored. The three stages of core edge piece preparation are shown in Figure 41. The formed sections were split on a band-saw, bonded together in the curved fixtures shown in Figure 42 and then tapered with a bandsaw in the fixture shown in Figure 43. The curvature was sprung out of the parts during the tapering operation to simplify the process; however, this resulted in a concave surface when they returned to their original contour.

Splitting and bonding were considered necessary to stabilize the edge pieces during subsequent bonding operations. The adhesive used was a layer of epoxy prepreg cloth (BMS8-139) sandwiched between two layers of AF131 film adhesive. The assembled parts were given a flash cure, 10 minutes at 450°F, which was sufficient to set the adhesive. Final cure was accomplished in subsequent bonding operations.

Fabrication of a quarter segment was initiated by molding the inner skin and end buildups as an integral assembly. The layer quantity and arrangement are shown below, and a photograph of the completed assembly is shown in Figure 44. The cure cycle was 4 hours at 325°F under 50 psi pressure.

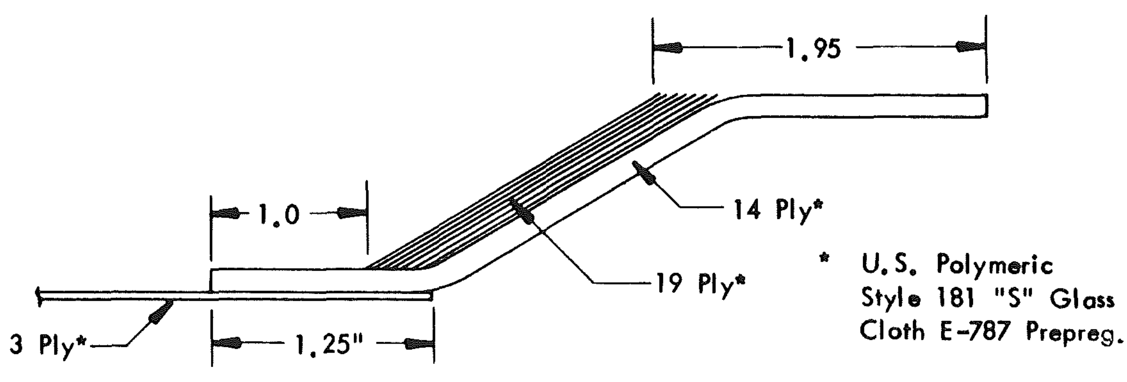

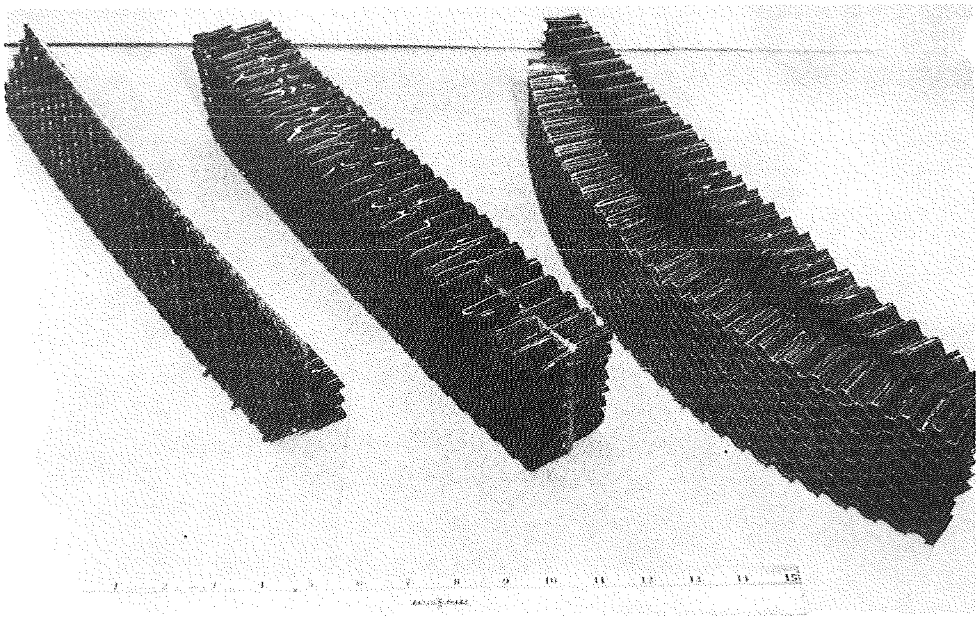

Figure 41: CORE EDGE PIECE PREPARATION

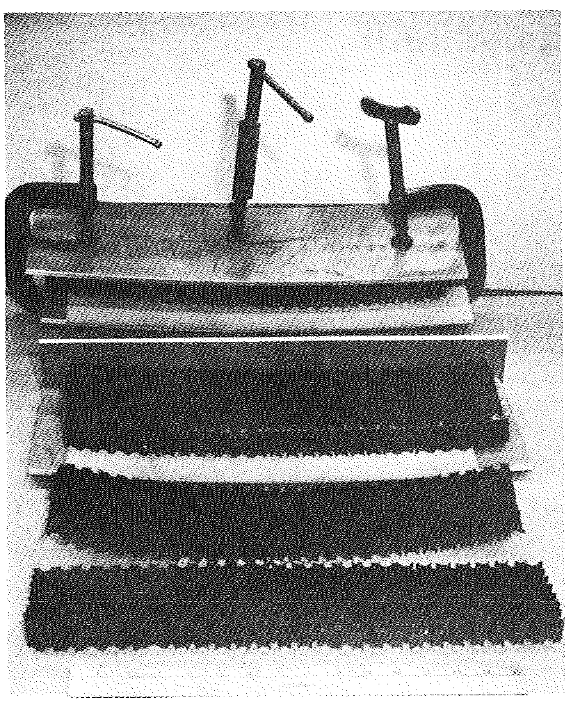

Figure 42:
CORE EDGE PIECE BONDING

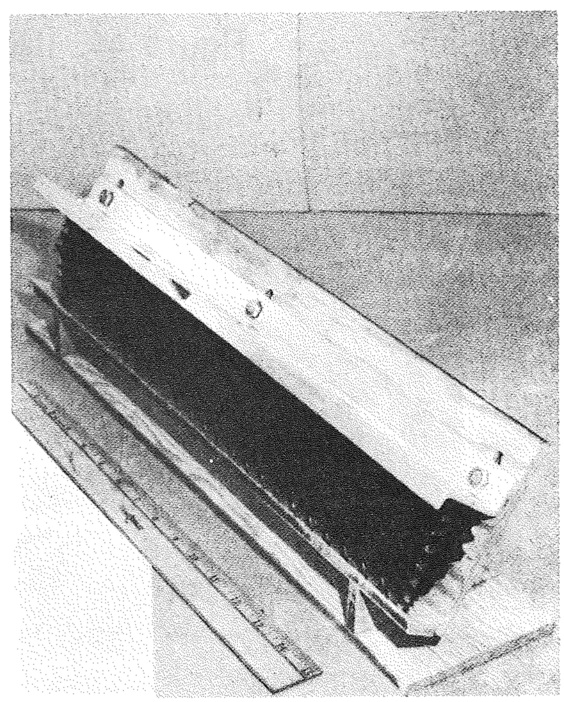

Figure 43:
CORE EDGE PIECE TRIM TOOLING

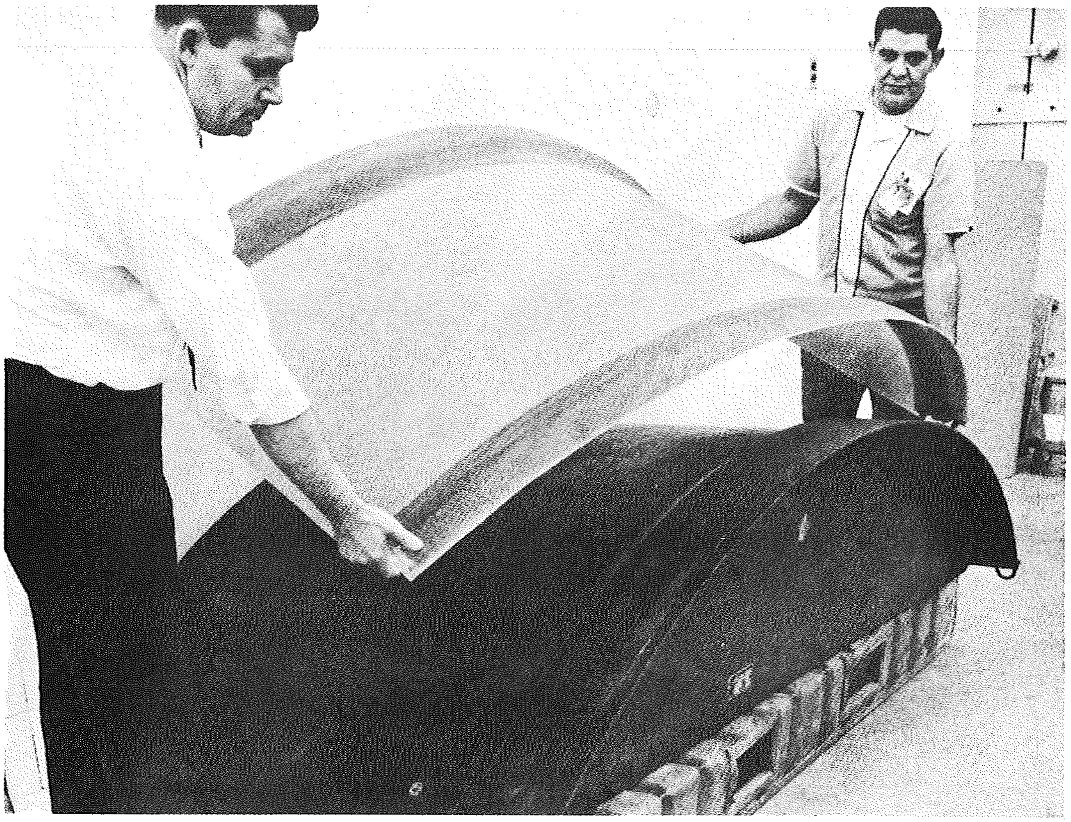

Figure 44: INNER SKIN LAMINATE

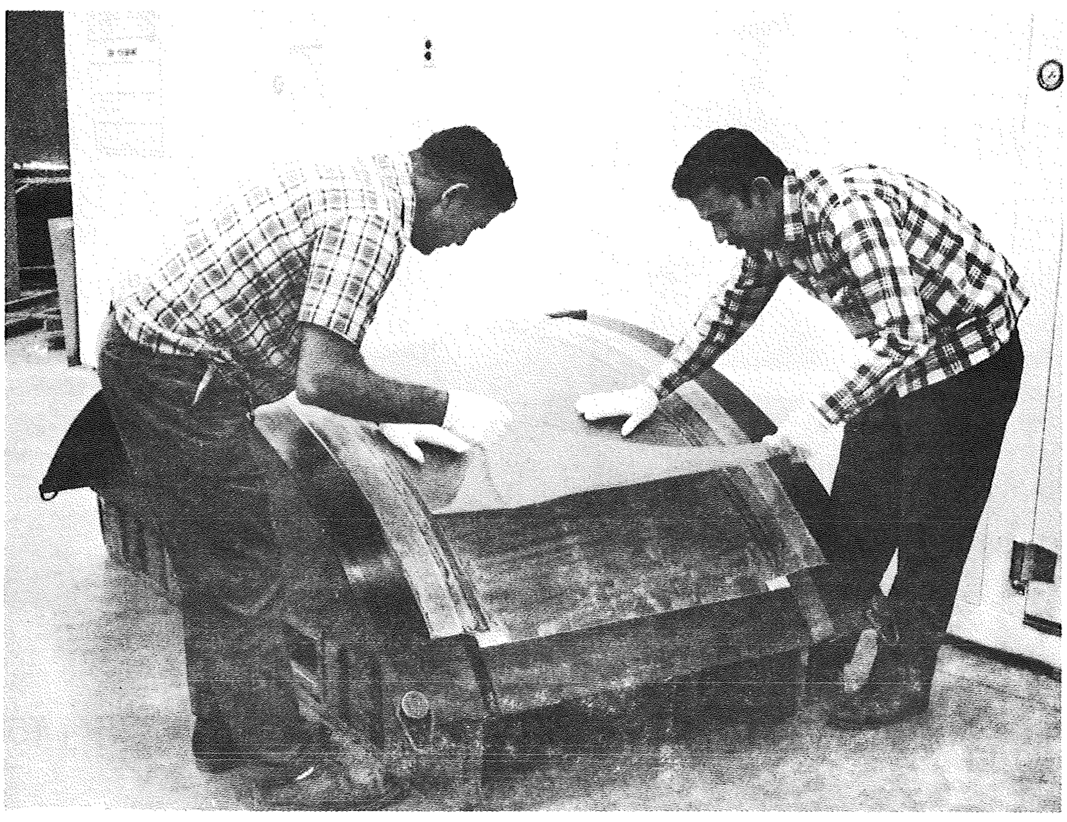

Figure 45: FILM ADHESIVE APPLICATION

After cure the 19 ply buildup was sanded flush with the 14 ply surface, then the entire skin was sanded to remove resin gloss and washed with Acetone or MEK. A layer of AF126 film adhesive was applied to the core bonding surface as shown in Figure 45. Edge channel members were mounted on aluminum locating tools, a layer of AF126 adhesive applied to the back of each channel, and the tool clamped to the mold shown in Figure 46. Figure 47 shows core center sections being placed. A strip of AF126 film adhesive was used for core butt bonds. The completed assembly was covered with a plastic film and mylar bands were used to draw the core sections against the adhesive. Irregularities along the core edges were removed by trimming as shown in Figure 48.

An additional three plies of prepreg glass cloth were used in the end taper areas to cushion and conform to the shape of the honeycomb edge pieces. AF131 adhesive film was used between these three layers and the cured laminate and the core. Core butt bonds were made with a glass cloth prepreg and AF131 film adhesive sandwich. The sketch below shows arrangement details and Figure 49 shows application of three glass cloth plys over the film adhesive.

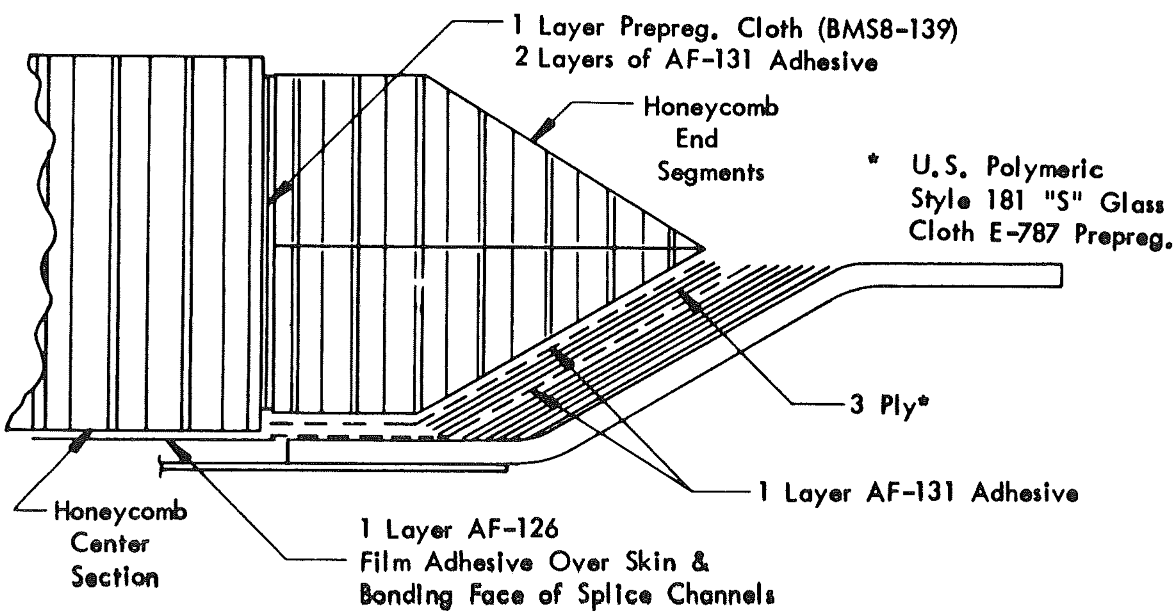

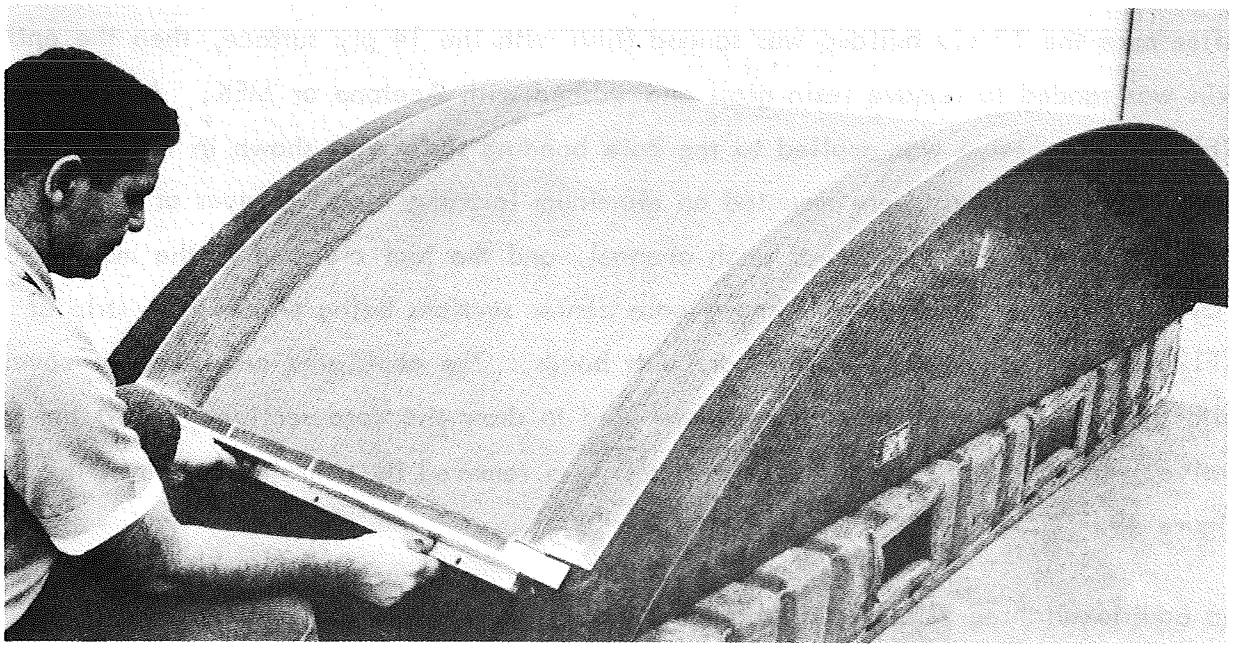

Figure 46: EDGE MEMBER PLACEMENT

Figure 47: CORE CENTER SECTION PLACEMENT

Figure 48: CORE TRIMMING

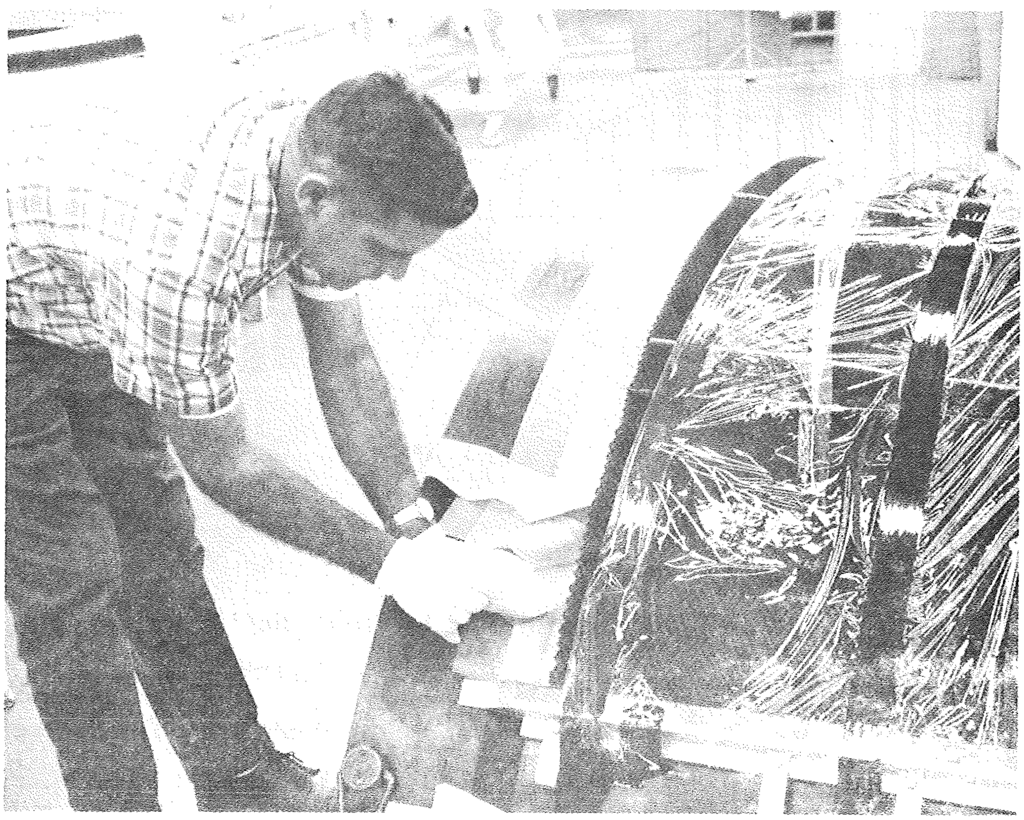

Figure 49: EDGE BUILDUP APPLICATION

Figure 50 is a photograph showing placement of the core edge pieces and the adhesive between abutting edges. Figure 51 illustrates the vacuum bagged assembly prior to cure. The cure cycle was 300°F for 90 minutes.

It was necessary to fill the concave areas on the edge pieces with additional plys prior to adding the required 14 and 22 ply buildups. AF131 adhesive was used between the fillers and the core, and the assembly was cured at 300°F for 90 minutes under vacuum pressure. After cure the surface was sanded to a smooth contour in preparation for adding the required buildups. The sketch below shows the filled area and the arrangement of plys and adhesive used to complete the edge laminate. The 14 and 22 ply buildups were applied and cured in one operation. Aluminum caul plates were used over the laminate to maintain the required contour and corner radii. The cure cycle was 4 hours at 300°F under 40 psi pressure.

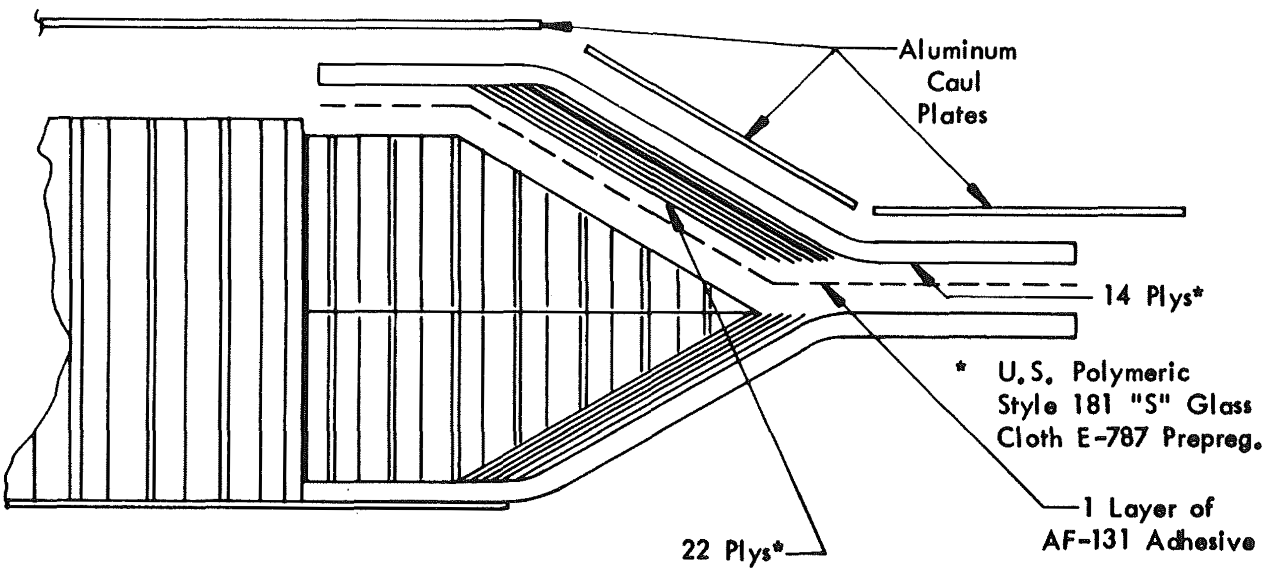

Bonding the outer skin to the assembly constituted the final step in molding the one quarter segment. The faying surface of the edge buildup and channel members, as well as the entire skin, was sanded to remove resin gloss then washed with Acetone

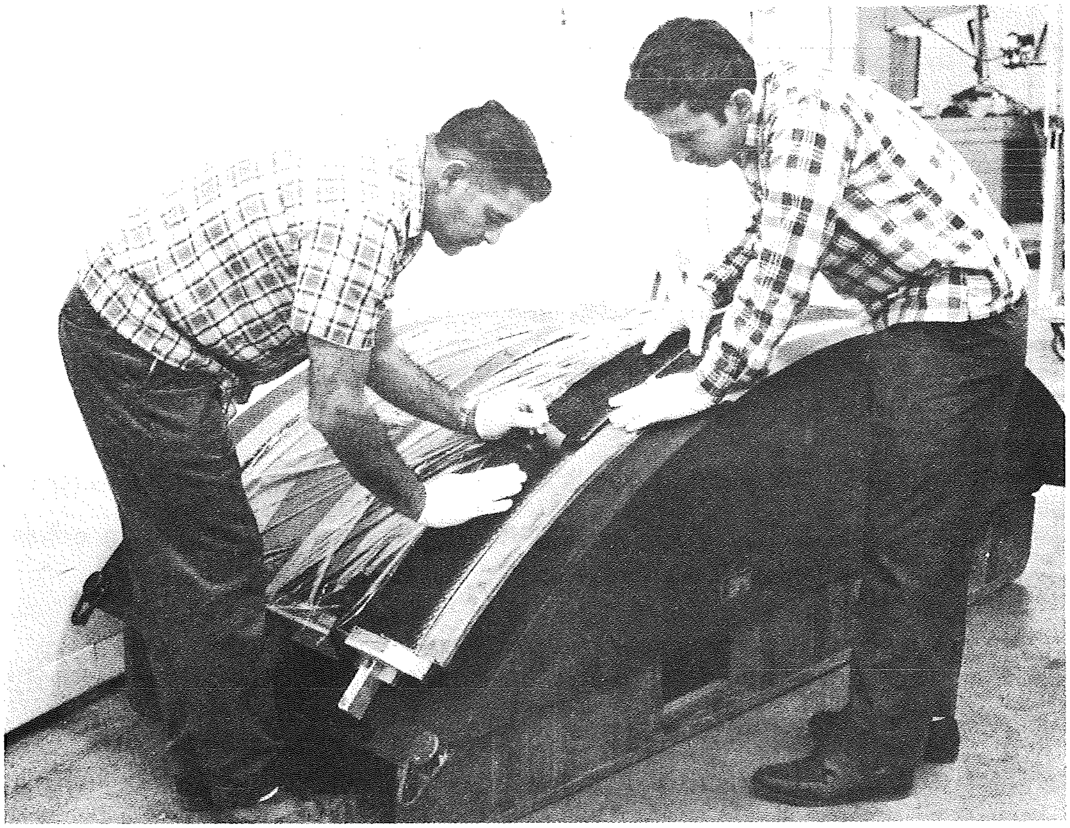

Figure 50: CORE EDGE PIECE PLACEMENT

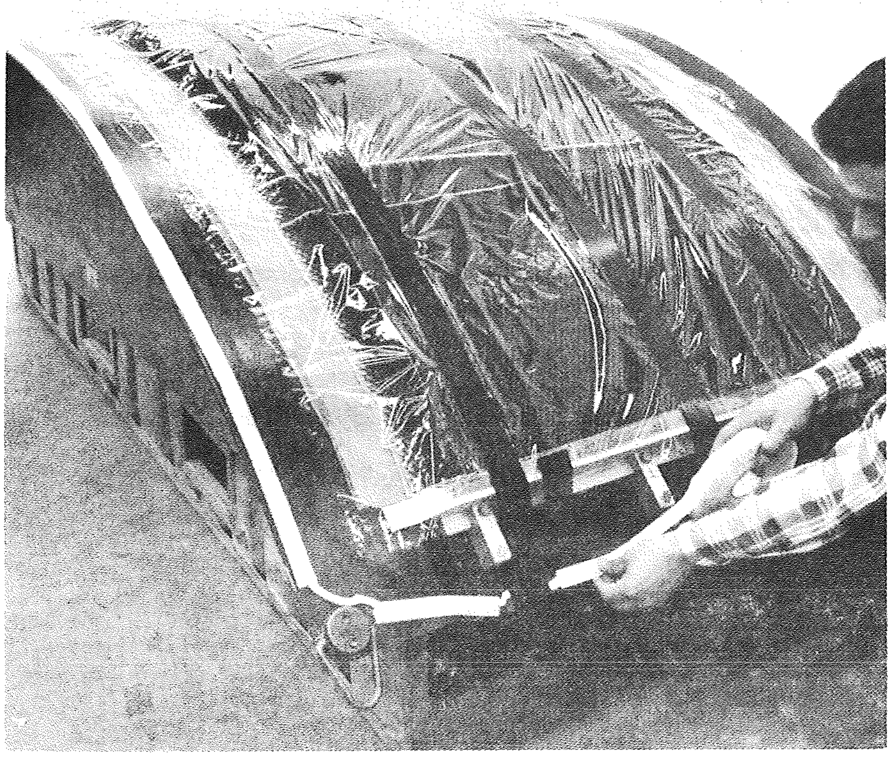

Figure 51: VACUUM BAG ASSEMBLY

or MEK. A layer of AF126 film adhesive was applied over the bonding surface and the precured outer skin placed over the adhesive. The assembly was vacuum bagged and cured for 90 minutes at 300°F. Figure 52 shows a completed segment after removal from the mold.

Aluminum segmented rings predrilled with undersize holes were located inside and outside of the 1/4" thick laminate edge and clamped in place. The holes were then drilled out to full size as shown in Figure 53. The segmented rings were coded to aid in subsequent assembly operations. The holes in the fiberglass laminate were enlarged to 1/2" and aluminum inserts bonded in place with an Epoxy-Amine paste adhesive (BMS5-25). Figure 54 shows this operation.

The four segments were assembled into the finished configuration and temporarily joined with aluminum bars across the longitudinal splice joints. Each segment was shimmed from the floor so that the narrow end of the cone was in a level plane. The circumference of the cone was adjusted to match the aluminum tank "Y" ring at MSFC, leaving allowance for the 1/8" gap shown on the design drawing. The adjustment capability was provided by the longitudinal splice joints. Fiberglass longitudinal splice plates were positioned over the joints and used as a template for drilling holes. The plates were then coded and removed to allow installation of gang channels. A pair of finished segments with splice plates installed are shown in Figure 55. One pair of fiberglass splice plates was left undrilled and aluminum plates were substituted for the final assembly. The fiberglass plates were intended to be drilled by MSFC when the cone was assembled on the tank, thus allowing payoff for dimensional discrepancies.

The conical support was assembled as a final check on fit up of the parts. Each joint, splice plate and segmented aluminum ring was coded to simplify future assembly. A photograph of the finished part is shown in Figure 56. The support was then disassembled, packaged and shipped to MSFC.

Two significant problem areas were encountered during fabrication. One was crushing of the honeycomb core during cure of the end buildups. The difficulty was experienced

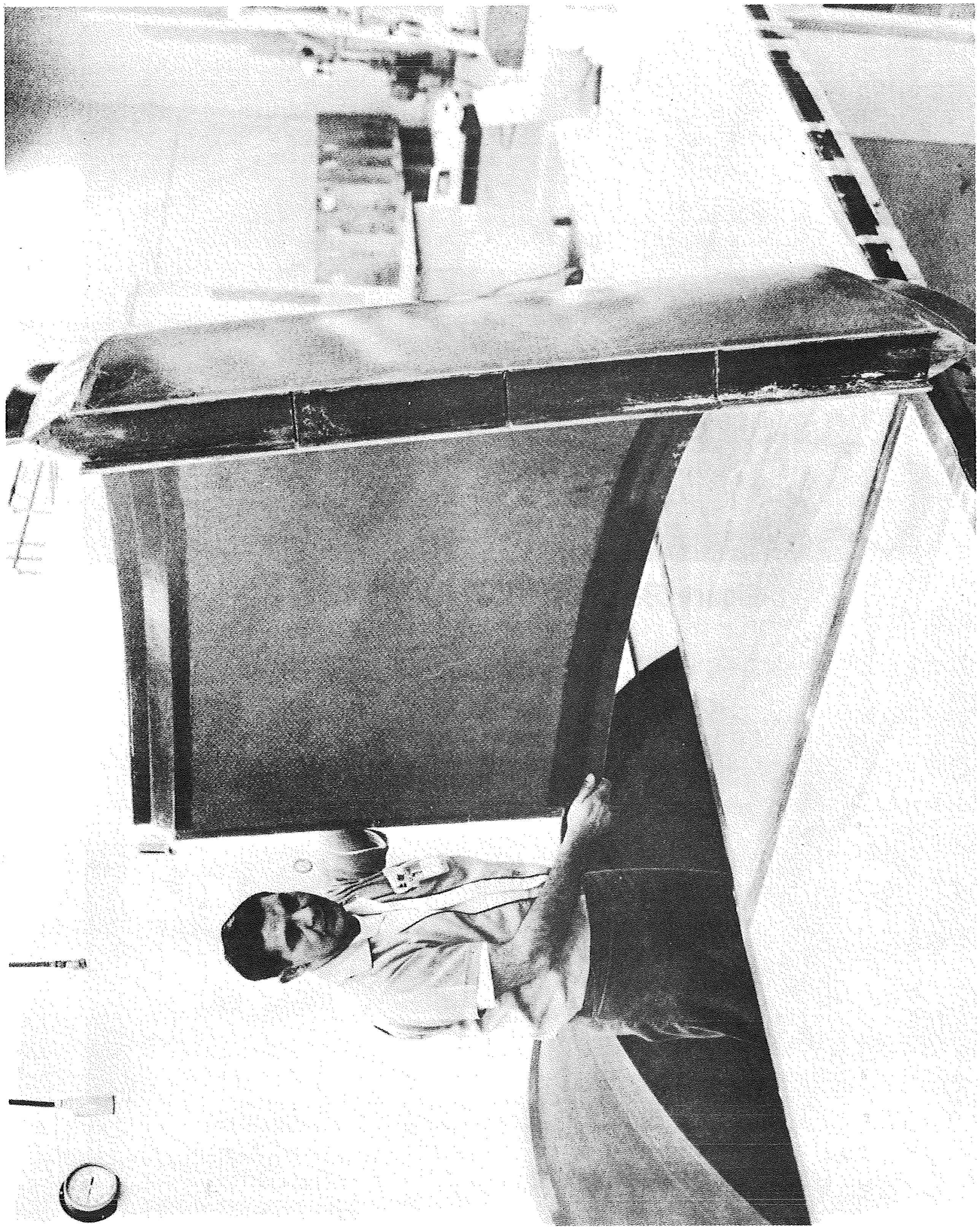

Figure 52: CONICAL SUPPORT QUARTER SEGMENT

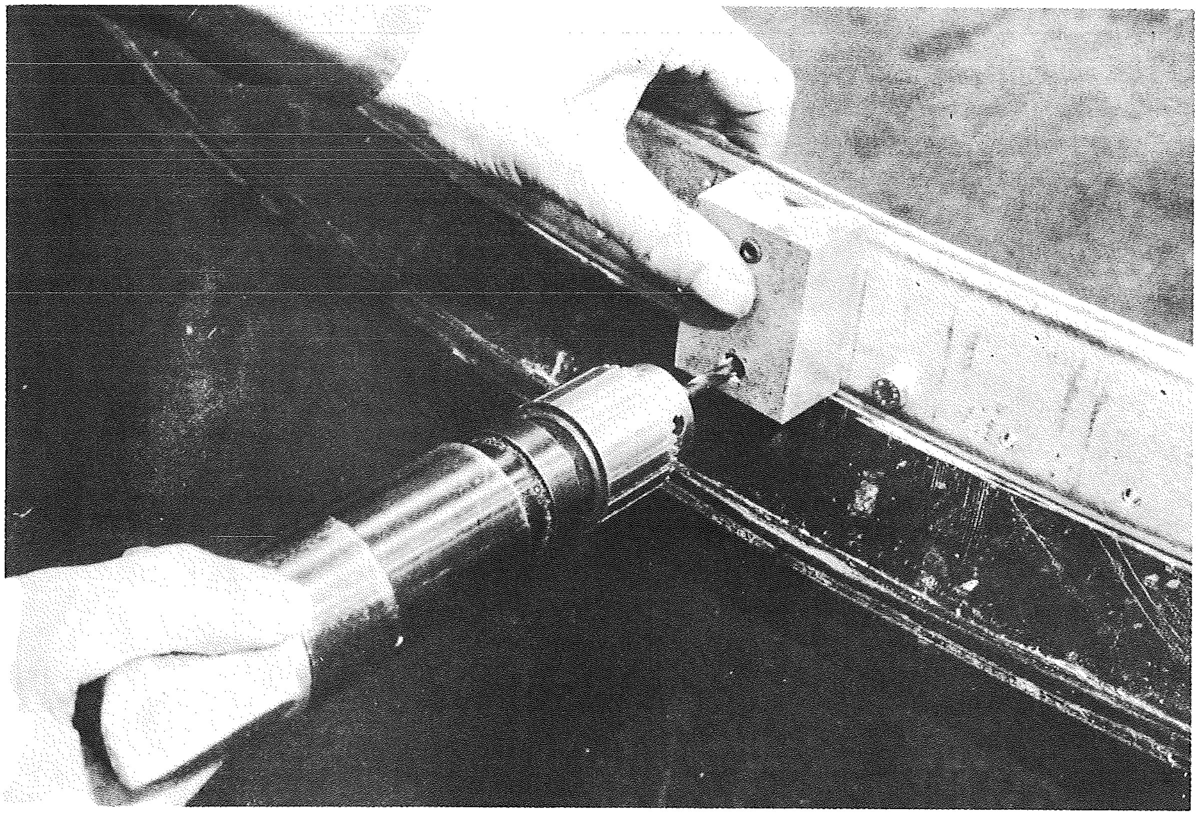

Figure 53: DRILLING OPERATION

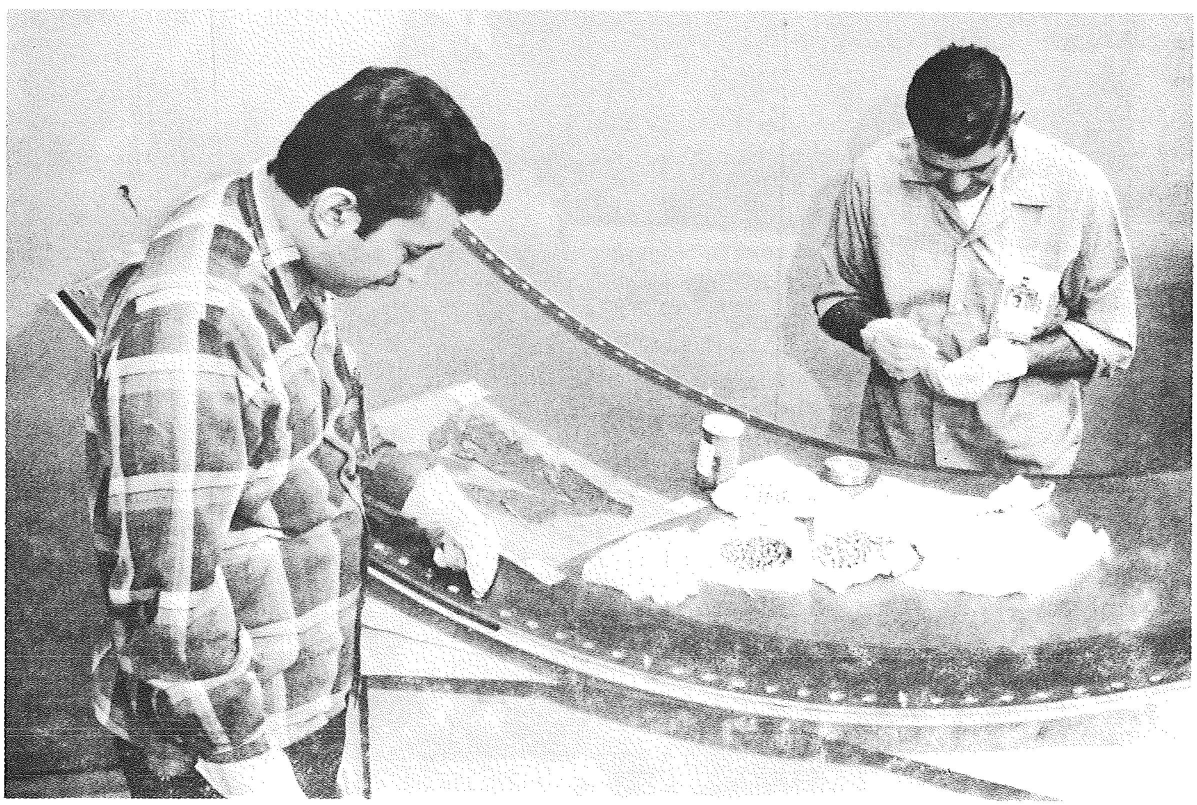

Figure 54: ALUMINUM INSERT INSTALLATION

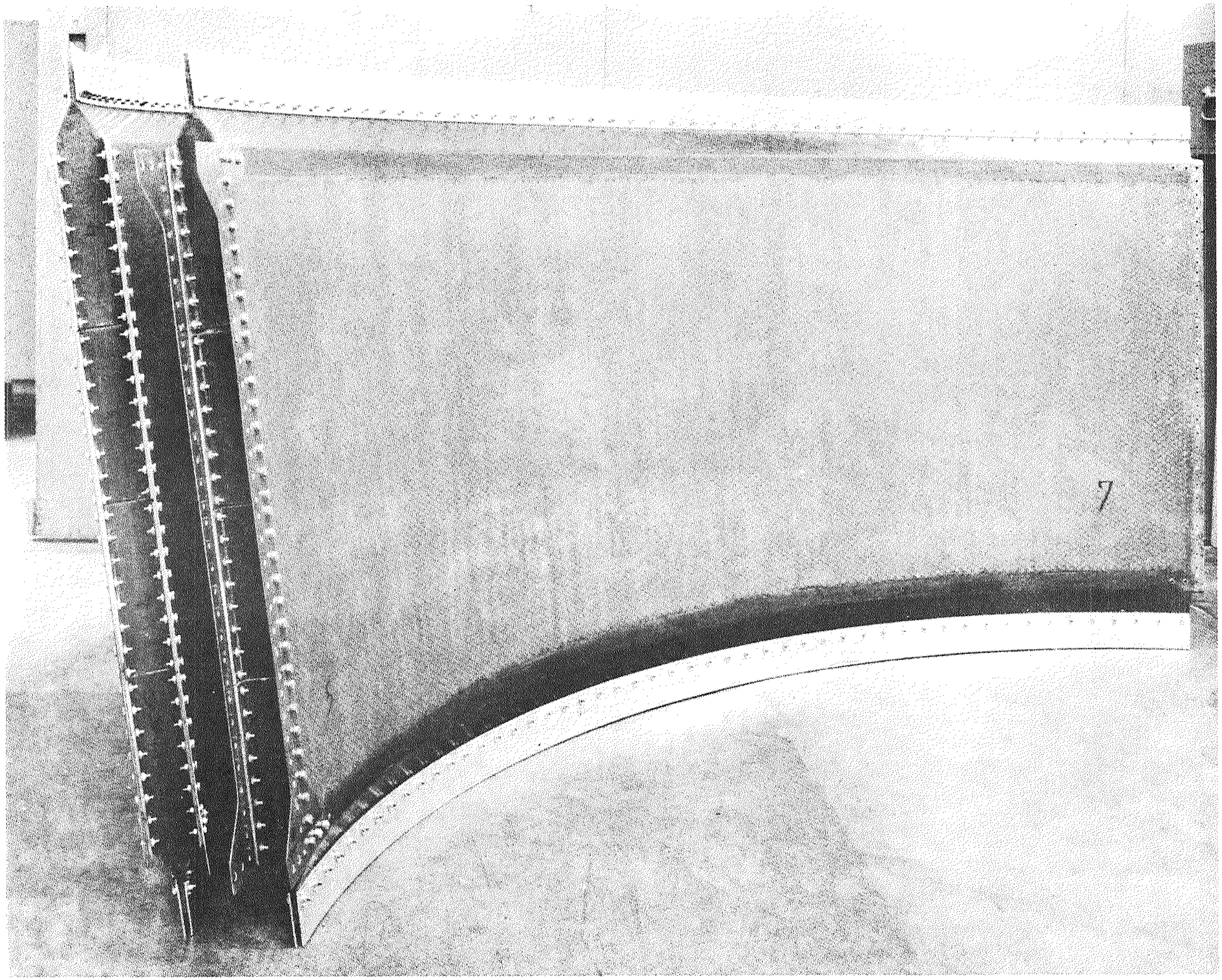

Figure 55: COMPLETED QUARTER SEGMENTS

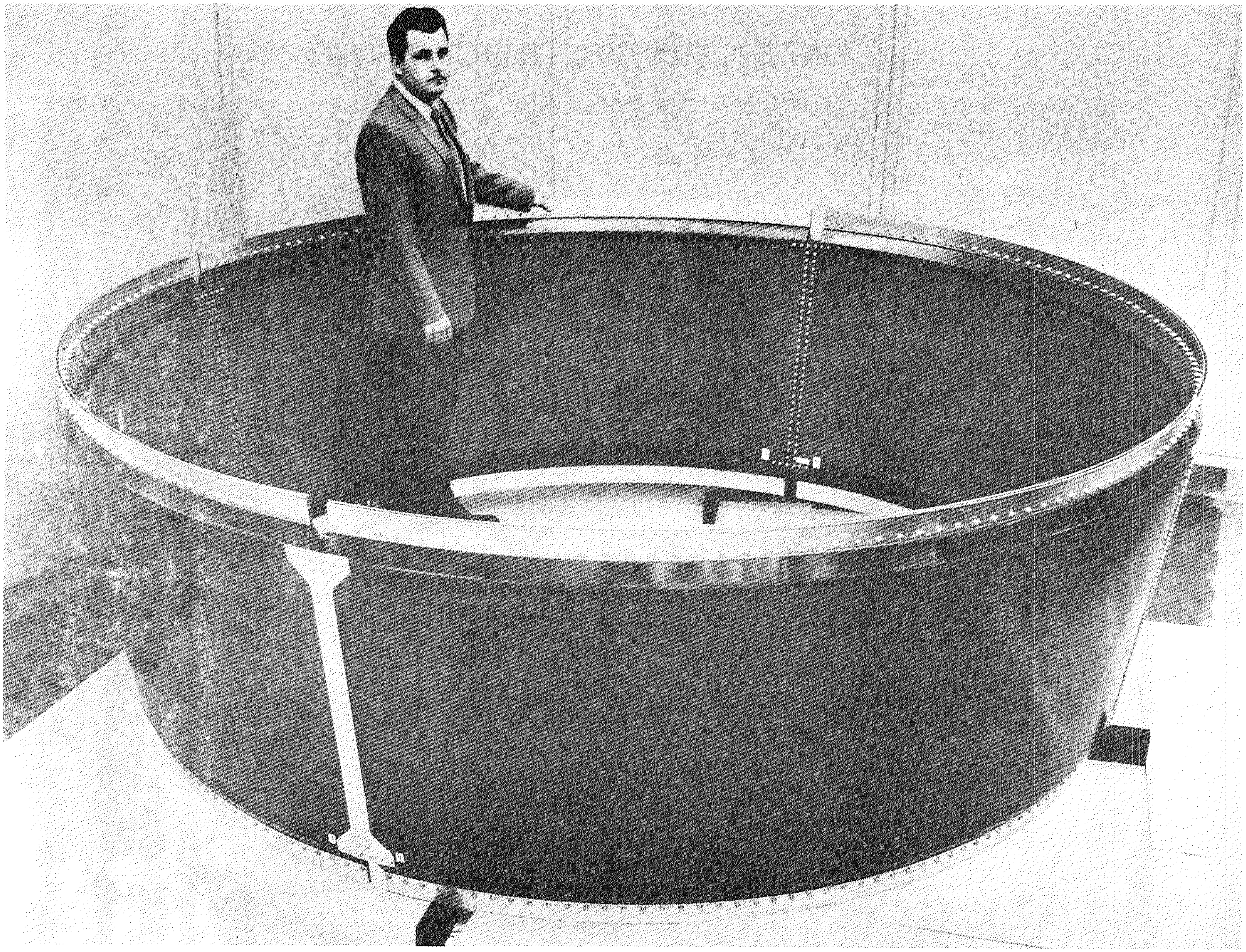

Figure 56: COMPLETED CONICAL SUPPORT

on the third and fourth segments. Crushing was extensive on the third segment although only 1/16" to 1/8" deep. Two isolated areas were evidenced on the fourth segment. At this stage the core was bonded to the inner skin and along the edges; however, the exposed face was unstabilized. An aluminum caul plate was used over the core to distribute the pressure. During the initial phase of the cure process, vacuum pressure may have been released prematurely allowing the caul plate to rise from the core surface and, subsequently, be forced down again as autoclave pressure was applied. If this occurred, an uneven distribution of pressure could have caused the crushing. Excessive heating during the forming process would have embrittled the HRP core thus contributing to the failure.

The second problem was one of dimensional control. Upon completion of the final curing process it was found that the quarter segments were sprung away from the mold and could not be returned with hand pressure. An arc of the design diameter was scribed on the floor and comparisons showed that each segment deviated from this line. When the ends of the segment were placed on the line the center was outside of the arc from 0.25 to 0.30 inches. The deviation was consistently in the center of the segment. The reason for the warpage is unknown, however a contributing factor could have been thermal expansion in conjunction with the use of precured laminates. Assuming the tank "Y" ring is round, the clamping forces applied to bring the conical support into alignment will produce a bending stress of approximately 2000 psi in each fiberglass segment, thus no detrimental effects are anticipated.

5.0 CONCLUSIONS AND RECOMMENDATIONS

5.1 PHASE I

The study results showed that fiberglass construction was the more weight-efficient design in all cases when both structural and boiloff weights were considered. This was due largely to the low thermal conductivity of the material. Fiberglass honeycomb sandwich construction was the best design approach considered.

An analysis to determine potential structural weight savings based on configuration cross section alone will not yield realistic results. The effect of edge members, reinforcements and fasteners can increase basic construction weight by more than 100% as evidenced for honeycomb sandwich and corrugated fiberglass support designs.

Stiffened skin designs were considered the most easily fabricated and the corrugated designs probably the most difficult. Honeycomb sandwich fabrication was essentially state-of-the-art; however, the integral, tapered edge attachment laminate added complexity.

Clearance between conical support and tank head was very limited. This was expected to cause problems in insulating the support and could reduce its thermal isolating effectiveness. Several alternatives were possible. These were: (1) lengthening the aluminum "y" ring with an attendant weight penalty, (2) relocation of the "y" ring to a more forward position on the tank head, or (3) lengthening the conical support to account for some loss of isolation capability at the cold end. It is recommended that a thorough stress and thermal analysis of this joint be conducted as insulation designs are developed. This will provide insight into the magnitude of the problem and identify advantages or disadvantages in some of the alternatives suggested.

Compression stability critical structure such as this conical support could be an ideal area of application for advanced filamentary composites of boron, carbon or hybrid mixtures including fiberglass. The high specific modulus of these materials might be utilized to increase the stiffness and provide competitive structural weights provided sufficient cryogenic physical and mechanical properties were available for a complete assessment. The cryogenic thermal conductivity and strength data currently available for these materials is very limited.

5.2 PHASE II

It can be concluded that fabrication of honeycomb sandwich structure with integral tapered laminate edge members is feasible, although somewhat laborious with the selected tooling and processing approaches. Data on the structural adequacy of this design is not available; however, structural tests may be conducted by NASA at a later date.

The manufacturing techniques employed in this program can be scaled directly to MNV size conical supports which gives confidence that an acceptable full size support could be built.

Construction of the honeycomb sandwich concept required the addition of several unplanned manufacturing steps. Collapse or lateral compaction of the core during bonding was anticipated due to the tapered edges. To avoid this problem, the core edge pieces were split and bonded together to add rigidity. A better approach would be to cut the taper on the outside of the core after bonding, thus eliminating the lateral force. This approach also would have produced a more even tapered surface, eliminating the need for filler plys.

It had been planned to cure the inner skin laminate, end buildups and bond the core to the skin all in one operation. Preliminary tests proved that this was impossible because the unstabilized core collapsed when the 45 psi laminating pressure was applied. It became necessary to laminate the inner skins and buildups in one operation and bond the core to this assembly in another step, thus permitting reduced core bonding pressure.

The conical segments contain some residual stress as evidenced by the reduction in curvature after removal from the mold. There was no major warpage across the parts because upper and lower corners of adjacent segments matched reasonably well when the support was assembled. In a large structure such as the MNV conical support it may be advisable to use a greater number of segments to minimize distortion in the event that residual molding stresses cannot be eliminated.

6.0 REFERENCES

1. Toth, L.W., et. al., "Program for the Evaluation of Structural Reinforced Plastic Materials at Cryogenic Temperatures", Contract NAS 8-11070 for NASA/MSFC, Goodyear Aerospace Corp., GER 12792, August 1966.

2. Bartlett, Donald H., "Nonmetallic Parts for Launch Vehicles and Spacecraft Structures", Contract NAS 8-18037 for NASA/MSFC, Boeing Document No. D2-114155-1, March 1968.

3. Seide, P., Weingarten, V.I., and Morgan, E.J., "Final Report on the Development of Design Criteria for Elastic Stability of Thin Shell Structures", Space Technology Laboratories, Inc, Report STL/TR-60-0000-19425, December 1960.

4. Block, D.L., "Buckling of Eccentrically Stiffened Orthotropic Cylinders Under Pure Bending", NASA TND-3351, March 1966.

5. Douglas Aircraft Co., "Design Concepts for Minimum Weight High Performance Supersonic Aircraft Structures", Vol. I ASD-TDR-63-871, September 1963, ASTIC 036226.

6. Gerard, George, and Becker, Herbert, Handbook of Structural Stability, Part I - "Buckling of Flat Plates", NACA TN 3781, July 1957.

7. Roark, R.J., "Formulas for Stress and Strain", 4th Edition, McGraw-Hill Book Company.

8. Peterson, James P., and Card, Michael F., "Investigation of the Buckling Strength of Corrugated Webs in Shear", NASA-TND-424, June 1960.

9. Apollo Program Office, "Structural Systems and Program Decisions", NASA SP-6008, pp. L1-L8, June 1966, ASTIC 036634.

10. Shanley, F.R., "Weight Strength Analysis of Aircraft Structures", Dover Publications Inc., Second Edition, 1960.

11. Koelle, "Handbook of Astronautics", Section 22, Structural Analysis by Hellebrand, E.A., McGraw-Hill Book Co., 1961.

12. Farrar, D.J., "The Design of Compression Structures for Minimum Weight", Journal of the Royal Aeronautical Society, November 1949.

13. Bleich, Friedrich, "Buckling Strength of Metal Structures".

14. Timoshenko and Gere, "Theory of Elastic Stability".

15. Anon., Composite Construction for Aircraft, Part III - "Design Procedures" MIL-HDBK 23, U.S. Dept. of Defense, Nov. 1961 (Revised Oct. 1962).

16. Peterson, J.P., and Anderson, J.K., "Structural Behavior and Buckling Strength of Honeycomb Sandwich Cylinders Subjected to Bending".

17. Bruhn, E.F., "Analysis and Design of Flight Vehicle Structures", Tri-State Offset Co., 1965.

18. Anon., Sandwich Construction for Aircraft, Part II - "Materials Properties and Design Criteria", MIL-HDBK-23, U.S. Dept. of Defense, 2nd Edition, 1955.

19. Weingarten, V.I., Morgan, E.J., and Seide, P., "Elastic Stability of Thin Walled Cylindrical and Conical Shells Under Axial Compression", AIAA Journal, Vol. 3, No. 3, March 1965.